AD-A195 473 DEEP WATER MASS CIRCULATION IN THE ALBORAN BASIN: MEASUREMENTS - AUGUST 1... (U) SACLANT ASW RESEARCH CENTRE LA SPEZIA (ITALY) P PISTEK FEB 88 1/2

UNCLASSIFIED SACLANTCEN-SR-196 F/G 8/3 NL

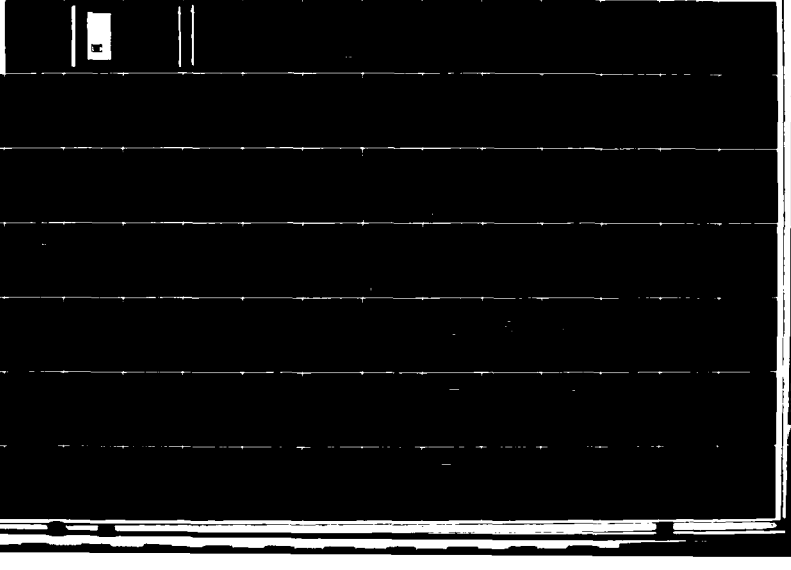

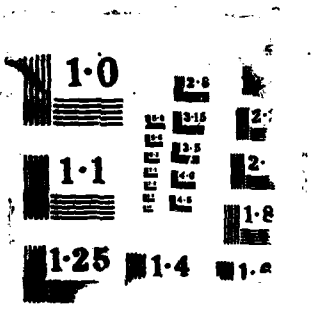
1·0
1·1
1·25
1·4
1·8

(4)

SACLANT
RESEARC
MEMORAN

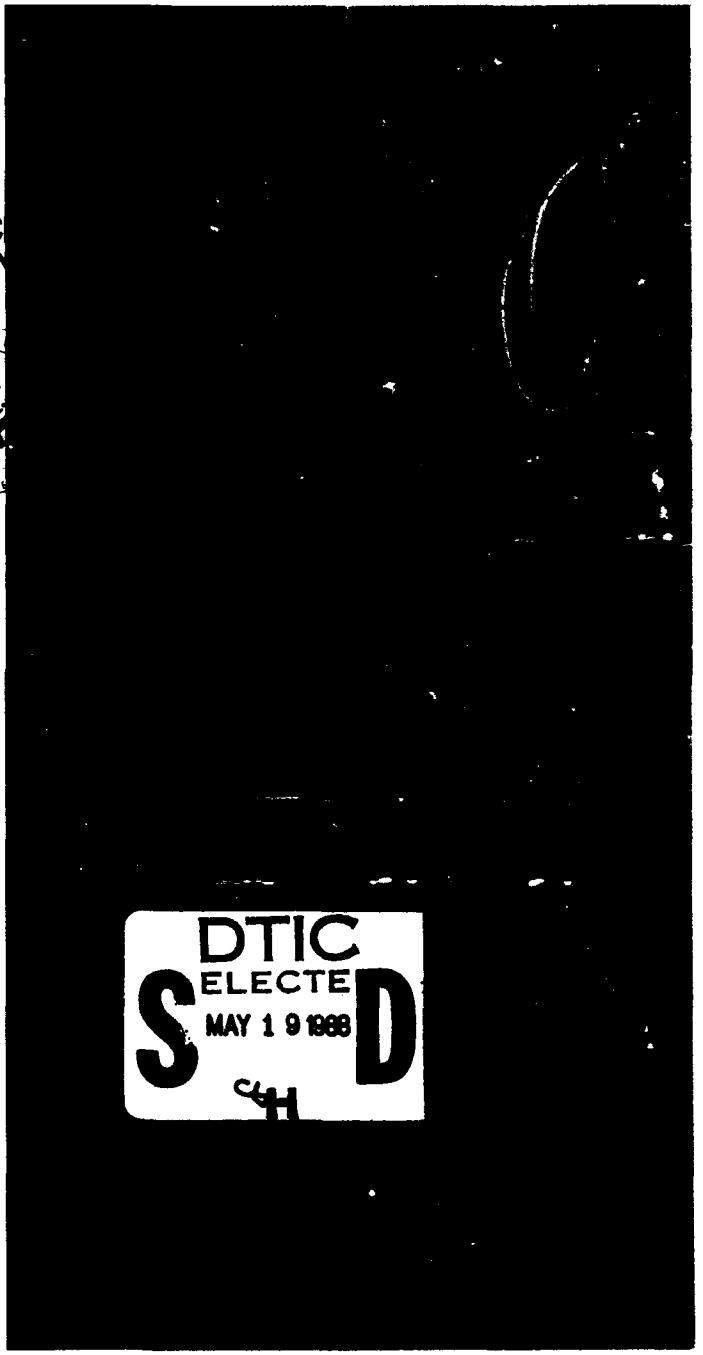

This document is released to a NATO Government at the direction of SACLANT ASW Research Centre subject to the following conditions:

- The recipient NATO Government agrees to use its best endeavours to ensure that the information herein disclosed, whether or not it bears a security classification, is not dealt with in any manner (a) contrary to the intent of the provisions of the Charter of the Centre, or (b) prejudicial to the rights of the owner thereof to obtain patent, copyright, or other like statutory protection therefor.

- If the technical information was originally released to the Centre by a NATO Government subject to restrictions clearly marked on this document the recipient NATO Government agrees to use its best endeavours to abide by the terms of the restrictions so imposed by the releasing Government.

Page count for SM-196
(excluding covers)

Pages	Total
i–vi	*6*
1–33	33
❶1–❶120	120
	159

SACLANT ASW Research Centre
Viale San Bartolomeo 400
19026 San Bartolomeo (SP), Italy

tel: 0187 540 111
telex: 271148 SACENT I

NORTH ATLANTIC TREATY ORGANIZATION

Initial Distribution for SM-196

Ministries of Defence	
JSPHQ Belgium	2
DND Canada	10
CHOD Denmark	8
MOD France	8
MOD Germany	15
MOD Greece	11
MOD Italy	10
MOD Netherlands	12
CHOD Norway	10
MOD Portugal	2
MOD Spain	2
MOD Turkey	5
MOD UK	20
SECDEF US	68
NATO Authorities	
Defence Planning Committee	3
NAMILCOM	2
SACLANT	3
SACLANTREPEUR	1
CINCWESTLANT/ COMOCEANLANT	1
COMSTRIKFLTANT	1
CINCIBERLANT	1
CINCEASTLANT	1
COMSUBACLANT	1
COMMAIREASTLANT	1
SACEUR	2
CINCNORTH	1
CINCSOUTH	1
COMNAVSOUTH	1
COMSTRIKFORSOUTH	1
COMEDCENT	1
COMMARAIRMED	1
CINCHAN	3
SCNR for SACLANTCEN	
SCNR Belgium	1
SCNR Canada	1
SCNR Denmark	1
SCNR Germany	1
SCNR Greece	1
SCNR Italy	1
SCNR Netherlands	1
SCNR Norway	1
SCNR Portugal	1
SCNR Turkey	1
SCNR UK	1
SCNR US	2
SECGEN Rep. SCNR	1
NAMILCOM Rep. SCNR	1
National Liaison Officers	
NLO Canada	1
NLO Denmark	1
NLO Germany	1
NLO Italy	1
NLO UK	1
NLO US	1
NLR to SACLANT	
NLR Belgium	1
NLR Canada	1
NLR Denmark	1
NLR Germany	1
NLR Greece	1
NLR Italy	1
NLR Netherlands	1
NLR Norway	1
NLR Portugal	1
NLR Turkey	1
NLR UK	1
Total external distribution	241
SACLANTCEN Library	10
Stock	29
Total number of copies	280

SACLANTCEN SM-196

Deep water mass circulation in the Alboran Basin: Measurements – August to November '83

ALBORAN III

P. Pistek

The content of this document pertains to work performed under Project 04 of the SACLANTCEN Programme of Work. The document has been approved for release by The Director, SACLANTCEN.

Issued by:
Underwater Research Division

R. Thiele
Division Chief

Deep water mass circulation in the Alboran Basin: Measurements – August to November '83

ALBORAN III

P. Pistek

Abstract: The circulation of the deep water mass in the western Alboran Sea is studied. Interaction between the three different water masses, the Atlantic, the Levantine and the Deep Western Mediterranean water, causes complicated flow patterns in the deep water circulation of the western Alboran Sea.

Floats and current meters deployed in the northern and the central western Alboran displayed slow and variable current speed. Floats deployed on the Moroccan continental slope moved swiftly along the slope towards Gibraltar with accelerating speed, and then passed through the Strait of Gibraltar into the Atlantic. Upward bending of isolines across the Moroccan continental slope extended from Gibraltar to 3°20'W, and were strongest in the western Alboran Sea. Deep Western Mediterranean water was observed at a depth of less than 300 m near the sill, indicating the passage of this water from the Mediterranean to the Atlantic. Levantine water mass was concentrated in the central Alboran, turning southward near latitude 4°40'W, but not crossing the Moroccan continental slope, and partly continued along longitude 36°10' towards Gibraltar.

Three floats were deployed in the western Mediterranean at a depth of 60 m to investigate the upper layer circulation. Their tracks did not show the existence of anticyclonic gyre in agreement with the satellite infrared images of the sea surface temperature. This 'anomalous' behaviour was visible in the satellite infrared images for the period of at least 6 weeks.

Keywords: Alboran basin o anticyclonic gyre o Atlantic o circulation o geostrophic current o Levantine o Mediterranean o modelling o moroccan continental slope o remote sensing o sound propagation o Spanish continental slope o Strait of Gibraltar o upwelling

intentionally blank page

Preface

The SACLANTCEN Applied Oceanography Group made two cruises in 1980, three cruises in the winter of 1982, and two cruises in the summer-fall of 1983 within the Alboran Sea. This strategically important area has a complicated and variable oceanographic structure with strong frontal zones, as well as eddies and jets. All these features must be considered in determining the variability of sound propagation and the purpose of the cruises was to obtain oceanographic data which would help in the description and understanding of them; ultimately the data were to be used in the numerical modelling of Alboran Sea circulation.

Earlier oceanographic measurements, satellite infrared imagery and numerical modelling of the circulation were utilised to design and modify the experiments. Very useful in this respect was the newly developed shipborne automatic picture transmission system (Wannamaker, 1983) installed on the SACLANTCEN R/V *Maria Paolina G* giving in-situ knowledge of the sea-surface temperature.

The three sets of cruises performed were:

(a) Preparatory cruises in 1980 – Alboran I;
(b) Cruises in the winter period of 1982 – Alboran II;
(c) Cruises in the summer period of 1983 – Alboran III.

The results of the 1980 preparatory cruises were described in by Pistek in (1984). Results of the 1982 measurements were described by Pistek in (1985). This present report treats the results of Alboran III, the purpose of which was to investigate the deep Alboran Sea circulation in the summer and compare it with that in the winter. Also, there was to be an investigation of the circulation in the western Alboran Sea using a combination of Lagrangian and Eulerian techniques.

In design, the experiment was a repetition of the 1982 measurements (Pistek, 1985): Swallow-type floats were deployed and acoustically tracked from the moored autonomous listening stations and eight current meters were moored on the four moorings to supplement the float measurements. An additional autonomous listening station was built and the floats were improved, including a transmission every 80 h of depth information. The Italian R/V *Magnaghi* helped in collection of CTD data between the two cruises performed by *Maria Paolina G*.

Contents

1. Introduction

The Mediterranean is an area where evaporation greatly exceeds precipitation and river runoff. The only connection with the outside ocean is through the Strait of Gibraltar. To achieve a mass balance, a net flow from the Atlantic is required. A salt balance given the observed salinities in the Atlantic and the Mediterranean, requires a net inflow (resulting from the difference between the surface inflow and the bottom outflow) with a magnitude about one-twentieth the magnitude of the inflow. This problem was treated by Defant (1961) and Deacon (1971), and Lacombe (1961) and Lacombe et al. (1964) arrived at a value for the fluxes about 30% smaller than the figures given by Bethoux (1980), whose 1.68 Sv (53×10^{12} m^3/year) for inflow and 1.60 Sv (50.5×10^{12} m^3/year) for outflow were obtained by considering all of the budgets for the Mediterranean. Neither of these estimates can be regarded as definitive.

As the circulation in the Alboran Sea is in the vicinity of the Strait of Gibraltar it is strongly influenced by these exchange fluxes. This influence is clearly visible for the inflow of the Atlantic water into the Alboran Sea, but the importance of dynamics in the Strait of Gibraltar for the deep Alboran Sea circulation has only recently been indicated in the published results of measurements by Lacombe and Richez (1982) and some theoretical studies by Bryden and Stommel (1984) and Armi and Farmer (1984).

Superimposed on the thermohaline circulation, there are tides, Coriolis force and atmospheric changes that modify the flow. The timescale of the circulation change depends on the influence of these forces. On the seasonal timescale the current fluctuations may be associated with the seasonal cycle of evaporation *minus* precipitation for the Mediterranean, or with seasonal changes in water stratification. The measurement in the Strait of Gibraltar by Lacombe (1961) and Lacombe et al. (1964) showed that the mean flow, tidal currents and sub-tidal currents, all have considerable variability, in the order of 0.5 to 1 m/s^{-1}.

However, fluctuations with periods of days to months are most likely to be associated with meteorological forcing, as the Atlantic and Mediterranean respond to large-scale patterns of atmospheric pressure and wind, and the 'inverted barometer' response was investigated by Lacombe et al. (1964), Crepon (1965) and Garrett (1983).

These variations should be detectable in the Alboran Sea because the ratio of the cross-sectional areas between the Strait of Gibraltar and the Alboran Sea indicates the barotropic current changes for the deep current to be of the order of a few cm/s. Measurements in 1982 (Pistek, 1985) did not show any strong cross-correlation

between current meter or float data and the atmospheric pressure integrated over the Alboran or the Western Mediterannean.

The circulation in the Western Alboran Basin involves both Atlantic and Mediterranean waters. The three types of water considered are those identified by Bryden and Stommel (1982): Atlantic Water, Levantine Water, and Western Mediterranean Deep Water. The Atlantic Water forms the inflow to the Alboran Sea, and the Levantine and Western Mediterranean Deep Waters comprise the outflow of Mediterranean water through the Alboran Sea to the Atlantic.

Atlantic water in a top layer about 150 m thick flows into the Alboran Sea from the Atlantic as a 20 km wide jet at a speed of several km/h. It has a characteristic average salinity of 36.5% and a temperature that depends on the season. This energetic layer often creates anticyclonic circulation in the south-western part of the Alboran Sea. Its extension and depth are quite variable. It is documented by Ovchinnikov et al. (1962), Lacombe (1971), Lanoix (1974), Cheney and Doblar (1978), Gallagher et al. (1981), Bucca and Kinder (1984), and by participants of the 'DONDEVA' experiment (Parilla, 1984). Laboratory and numerical modelling has been reported by Whitehead and Miller (1979) and Preller (1981), respectively. The anticyclonic circulation is clearly visible on the satellite infrared images of the sea-surface temperature, as shown by Wannamaker (1979), Philippe and Harang (1982) and La Violette (1983). In spite of this effort the dynamics are still not clearly understood.

Under the 150 m thick surface layer there is the deep water of Mediterranean origin. Uppermost in this layer is the intermediate Levantine water formed near Rhodes (Ozturgut, 1976) and characterized throughout the Mediterranean by a mid-depth maximum in both temperature and salinity (Wust, 1961). Under this is the Western Mediterranean Deep water formed south of France (Medoc Group, 1970), which is less saline but cooler, with a potential sigma of 29.10 kg/m^3 or greater and a potential temperature of less than 12.90 °C (Sankey, 1973; Stommel, 1972).

Stommel et al. (1973), Porter (1976), Bryden and Stommel (1982), Pistek (1984), Kinder (1984) and Pistek (1985) have addressed the deep flow. Bryden and Stommel (1982) found the enhanced flow near the southern boundary from geostrophic calculations; their current-meter data from one mooring showed a current directed along the Moroccan continental slope towards Gibraltar, with small annual variability. Kinder's (1984) current-meter data taken in the northern Alboran showed slow (<1 cm/s) south-westerly flow at 500 m and very sluggish easterly flow at greater depth. Current meter and free-floating vertical current-meter data obtained in 1980 (Pistek, 1984) also indicated the slow flow in the center of the Alboran Sea with a westerly direction for the intermediate water and a changeable direction for the deep water; there was also an enhanced and accelerated flow along the Moroccan continental slope towards Gibraltar. Pistek's (1985) float and current-meter measurements showed that under the variable surface anticyclonic circulation in the southwestern Alboran there existed a cyclonic motion of deep water with the

boundary current along the Moroccan continental slope. Levantine water was found concentrated in the central Alboran and moving partly south along 4°30'W and partly west along 36°10'. The upward bending of isolines across the Moroccan continental slope showed the variable intensity in time and in longitudinal extension.

The relative contributions of Levantine and Deep Western Mediterranean waters to the outflow of Mediterranean water through the Strait of Gibraltar are important for Mediterranean circulation. The proportions of the different water masses in this outflow are established in the Alboran Sea and the knowledge of the deep flow pattern, its time variability, and eventual coupling with the upper layer are important for understanding the mixing and its dynamics. Recently published (Lacombe and Riches, 1982) results of the past measurements from the Strait of Gibraltar and some theoretical studies of the data by Armi and Former (1984) and Bryden and Stommel (1984) indicate the importance of dynamics in the Strait of Gibraltar for the main features of deep water circulation in the Alboran Sea.

The main purpose of the present work was to investigate the flow pattern in the western-most part of the Alboran Sea and with the help of hydrography to map the distribution of the different water masses and their contribution to the outflow.

2. Equipment and experimental procedure

Acoustically tracked free floats (swallow type) and current meters were used to investigate the circulation

The original float design is described by Tillier (1980) and Bradly and Tillier (1980); the float modification and preparation for deployment are described in Pistek (1984) and Pistek, de Strobel and Montanari (1984). The acoustic tracking was done by four moored autonomous listening stations (ALS), with the array of hydrophones at 400 m depth (for optimal reception of the float signal) and by the shipborne station. The latter was used after the experiment was finished, to track and release the retrievable floats. The ALS tracking of the floats and their recovery are also described in the cited references.

Both types of float, recoverable and expendable, were fitted in this experiment with modified electronics permitting the repetitive transmission of the float depth. Every 80 h the standard depth-code (used in float deployment) was repeated (4 depth soundings separated by 2 h intervals), giving the opportunity to check the float depth during the experiment.

The water displacement of a glass float is pressure dependent. In addition to the elastic response to pressure it shows a non-elastic 'creeping' effect, as observed in the past (J.C. Gascard, personal communication). Figure 2 shows the time series of the float depth for all floats, starting 8 h after deployment. These are the averaged depth data obtained from all four listening stations. Every 80 h four listenings, separated by 2 h, have been plotted as short lines. Float 08 descended about 100 m in 27 days and then stabilised. The change in depth for float 07 was 450 m. Both of these floats were of the recoverable type. Floats 03, 05 and 06 were expendable, and had less cables and equipment outside the glass spheres. Float 06 only descended 50 m in 40 days (linearly). Floats 03 and 05 were audible for only a short time, but float 05 showed the same rate of descent as float 06. The presence of the additional equipment outside the recoverable-type of float could explain the differences in the depth of descent.

Results of the repeated depth measurements indicate that 'creeping' compression is common to all floats. It is connected with the non-elastic response of the glass sphere to the pressure. In addition to this effect the non-linear compression of the float's 'rubber' parts (cables, sealing material), which was assumed to be important only to shallow depth (150 m), probably contributes as well (indicated by the difference in compression between the two types of floats).

Floats at 60 m were deployed as drogues, with the parachute attached at 58 m on the line which connected the float to the small surface floater. When they transmitted they were tracked from listening stations in the same way as the deep floats.

It was difficult to acoustically position the surface floats (at 60 m) from the ship-borne receiving station because they moved rather fast (>2 n.mi/h). This experience supports the view that satellite tracking of surface floats (or floats deployed at shallow depth) is desirable. The positions of the floats' deployments are given in Fig. 1.

In total four moorings were deployed with two current meters and an ALS station on each of them. All moorings were of the subsurface type, with an EG&G transponder and releaser positioned near the bottom, and the shallowest part at 280 m; they were made up with Kevlar rope. Four propeller-type current meters (three VACM and one Weller-VMCM) in addition to two acoustic 2-axis N. Brown type and two acoustic 3-axis N. Brown type were used. The mooring positions are given in Fig. 1.

3. Measurements and data processing

3.1. PURPOSE

The main purpose of the cruises carried out in August, September and October 1983 was to investigate the circulation in the western-most part of the Alboran Sea. To this end an experiment with combined float deployments, measurements by current meters, and three periods of CTD measurements was performed. Four current meter moorings (marked 1 to 4) were deployed with two current meters on each of them at depths corresponding to the Levantine and Deep Western Mediterranean waters; there was an automatic listening station (ALS) at 400 m on each of them in the period from the beginning of August to the end of October 1983. The positions and periods of deployment of the floats, CTDs and current meters are given in Fig. 1, and more details are displayed in Tables 1 and 2.

TABLE 1
Description of hourly current-meter data (1983)

Mooring	Current meter[1]	Deployment depth (m)	Original sampling (min)	Average velocity amplitude (cm/s)	Notes
1	NB acoustic	328	4	9.54	working only
	NB acoustic	712	4	11.98	31 days
2	VACM	346	15	1.29	
	NB acoustic	731	4	1.56	
3	VACM	294	15	1.28	
	NB acoustic	678	4	1.98	
4	Weller	298	4	3.97	
	VACM	403	15	4.80	

[1] NB acoustic: N. Brown acoustic current meter.
VACM: EG&G vector averaging current meter.
Weller: propellor type current meter (VMCM) - two perpendicular propellors in the horisontal plane.

Positions of moorings were chosen on the basis of 1982 measurements (Pistek, 1985) to fill the lack of data from the western-most part of Alboran Sea. Sites were

TABLE 2
CTD (N. Brown MKIII) casts 1983

Cruise	Julian day	Casts no.
Alboran I	216	1–9
(1980)	217	10–15
	218	16–20
	220	21–22
	221	23–33
	222	34–37
	223	38–41
Magnaghi	257	1–18
(1982)	258	19–31
Alboran II	279	1–9
(1982)	280	10
	281	23
	282	24–30, 34–35
	283	36–39, 44–48
	284	50–58, 62
	285	63–80
	286	81–96
	287	97–105
	288	106–117
	289	118–126
	292	129
	293	132
	295	133–134

chosen in deeper water to achieve the efficient acoustic tracking of floats. Site 1 was chosen south of Gibraltar to investigate the outflow of deep water and to track the floats in the Strait of Gibraltar. The mooring located in the southern Alboran on the Moroccan continental slope was chosen to measure the stability of boundary current. The moorings located in the central part, in the northern part of Alboran measured the contribution of Levantine and Deep Western Mediterranean waters to the outflow of deep water from Alboran.

The positions and deployment depths of floats 06, 08, 03, 05 were chosen on the basis of the same objectives as the locations of current-meter moorings. Two floats were planned for deployment near site 06 but after the failure of its transducer one was retrieved. Two floats were deployed in the central Alboran to verify the steadiness of cyclonic circulation which was found in 1982. One float failed to transmit after 2 days and only float 07 was left.

Three floats were deployed at 60 m at chosen sites to investigate the anticyclonic gyre often present in the southwestern Alboran and to verify the correlation with satellite images. All these floats were destroyed by fishermen after a few days. There were three periods of CTD measurements as indicated in Fig. 1 and Table 2, with locations of the casts as in Fig. 3. Their purpose was to map the different water-masses.

3.2. DATA RECORDING AND PREPARATION

Data from the moored instruments were recorded on magnetic-tape cassettes, transcribed onto 8-track HP tapes, transferred to UNIVAC disc storage, and then prepared for analysis by the replacement of 'bad' data values and truncation.

Onboard acquisition of XBT and CTD was through the use of SACLANTCEN's IOS (integrated oceanographic system) on a Hewlett-Packard 21MX computer. Data were stored on HP 8-track tapes and later transferred to UNIVAC 1106 disc storage, where they were cleaned by the removal of spikes and bad profiles.

3.3. SATELLITE DATA

On-board acquisition of satellite data was performed on a special satellite acquisition system (Wannamaker, 1983) connected to a HP-21MX computer with data display on line printer or Lexidata image processor, and a monitor for colour imagery. The data were stored on HP800-bpi magnetic tape and later processed in SACLANTCEN facilities. Resolution of these Automatic Picture Transmission (APT) satellite images is 4 × 4 km. The series of satellite images displayed in this report was taken from the Atlas of satellite images collected by Nacini (1985). All images were transmitted from NOAA-7 satellite. High Resolution Picture Transmission (HRPT) images were obtained on magnetic tapes from Dundee, Scotland, and processed at SACLANTCEN.

3.4. FLOATS AND ALS

The positions of the floats were computed from the transmissions on a two-hourly basis. The precision of float positioning depends on the precise localisation of the four listening stations, the precision of synchronization, the drift of the clocks in the floats and stations, multipath propagation of the sound (possibly reflections), and the sharpness of cross-correlation. The positions of the listening stations were established by radar and satellite navigation with an error of less than 1 km, which established the error in absolute positioning of the float tracks. Before deployment, each instrument was synchronised aboard the ship in the Alboran Sea to within 1 ms (by 5 MHz radio signals from the Instituto Elettrotecnico Nazionale Galileo Ferraris,

Torino, Italy). The drift of the oscillators was much smaller than specified by the company ($< 5 \times 10^{-7}$ Hz/Hz/yr) and was taken into account in the computation of the distance. The random variation of the oscillator was less than 2 ms/h. The frequency bandwidth allowed the arrival time to be established to an accuracy of 0.1 s.

Influences of multipath propagation and reflection were visible as a broadening of the cross-correlation. They are hard to evaluate because the bottom topography in the Alboran Basin is very variable. The average propagation path was less than 60 km long, but the positioning of floats was less precise than in the 1982 experiment (Pistek, 1985), probably because of the more complicated topography.

Acoustic tracking of the shallow depth floats (at 60 m) was quite difficult, their path being partly in shallow water (100 m) where acoustic propagation is complicated. The final precision in the position was less than 500 m.

The ALS installed on mooring 4 stopped functioning on day 278 because of the battery's low voltage.

The float-position data (one point every 2 h) were recomputed into average two-hourly velocities and linearly interpolated to hourly values. A Groves (1955) filter was used to remove tidal effects selectively and as a low-pass filter; only the variations of periodicity greater than $1\frac{1}{2}$ days were preserved after filtration. Data for the fast moving, shallow depth, floats are plotted in the original 2 h-sampling interval. Examples of the floats' paths plotted from the raw data and from the data after filtration are given in Figs. 15 and 13 respectively.

3.5. CURRENT METERS

A summary of all eight current meter measurements is given in Table 1. The original sampling interval for VACM current meters was 15 min and for the N. Brown acoustic and Weller (VMCM) current meters was 4 min.

After removal of spikes, original data were filtered by a low-pass filter and decimated to hourly values; they are presented in this form in Figs. 4 to 12.

Rather strong currents (40 cm/s) were measured at mooring 1 by two N. Brown 3-axis acoustic current meters. The deep (at 687 m) current meter (Fig. 6) failed totally after 31 days, and its vertical component had failed soon after deployment. On the basis of past measurements it had not been expected that the deep current in this site would be so strong, with the consequence that the subsurface mooring did not have enough buoyancy to counter it. As a result the measurement of the vertical velocity component in Fig. 5 is distributed (due to mooring motion).

To remove tides and to low-pass the data, a Groves (1955) filter was used as in the treatment of the float data. Examples of hourly values and filtered current meter data and the filter's spectral effect are presented in the report on Alboran I (Pistek, 1984).

3.6. HYDROGRAPHY

Three hydrographic surveys were made with a CTD N. Brown MKIII system. The August and September data sets are small because of limited time for the measurements and the casts were limited to the western Alboran area. In addition to a shift, corresponding to 0.01 in salinity, many of the casts from the August set have missing data for as much as 100 m, starting at a depth of about 200 m. The problem was related to computer software and was identified only after data acquisition. The October CTD set covers most of the western and central Alboran Sea.

The data from each cast were ordered progressively by depth (no return loops were permitted) and the different variables computed. Data relating to salinity and potential temperature variations were averaged to 10 m values. The importance of the high stability and resolution of the CTD system for the identification of the water masses and the geostrophic calculations in the Mediterranean are discussed in Pistek (1984).

4. Results

4.1. DEEP FLOATS

Figure 13 presents the tracks of floats deployed in deep water. These tracks have been created from low-pass filtered data. Float 07, originally deployed to 670 m, descended in 24 days to 1090 m and remained at that depth. It moved clockwise around the mountain-like feature in the central Alboran basin. Only a few positionings were made on the southern side of the mountain (day 245 to 265). Later, this float moved in the northwestern direction, in a motion resembling that of floats deployed in this area in 1982 (Pistek, 1985), and was finally retrieved. Float 06 was deployed near the Spanish continental slope at a depth of 525 m; it moved back and forth along the continental slope and later was trapped in a valley and upwelled almost 200 m (see Table 3 for details).

TABLE 3
Parameters for float upwelling

Float no.	Depth		Amount of upwelling	*Volume* of float at F	Buoyancy needed to keep the float	Vertical[1] speed
	F (after upwelling) (m)	O (before upwelling) (m)	(m)	(cm^3)	(g)	(cm/s)
06	350	550	200	43900.2	15.1	1.96
05	300[2]	435	135	43887.9	11.0	1.68
03	300[2]	330	30	43905.9	2.5	0.8

[1] Vertical speed is computed from the drag force determined by a buoyancy force, the density of the water, a drag coefficient (0.6), and the float's cross-sectional area.
[2] Sill.

Float 08 was deployed in the western central Alboran at a depth of 465 m and descended in 23 days to 560 m. It moved slowly and indecisively in the vicinity of the deployment site for about 35 days, until after a more southerly movement it was trapped in the Moroccan continental slope current. It marked the outer northern boundary of this current and moved with average speeds of 2.5 cm/s and 4.2 cm/s during days 260–270 and 270–280 respectively. It was retrieved near Gibraltar.

Floats 03 and 05 were deployed near the Morrocan continental slope to investigate the Moroccan continental slope current. Float 03 was deployed to 330 m, float 05 to 435 m; both of them moved along the continental slope, then travelled considerably north before moving through the Strait of Gibraltar to the Atlantic in 11 and 16 days from the deployment time respectively. Their speed was accelerated, starting at 2.5 cm/s near the deployment site and reaching 13 cm/s and 30 cm/s, without the tidal component, near 5°W and near the sill respectively.

Figure 14 shows the detail of the floats' tracks passing to the Strait of Gibraltar. These tracks have been plotted from data taken every 2 h. They clearly show the strong semi-diurnal tidal influence, with especially float 05 experiencing strong tidal variation in the area south of Tarifa. Float 08 was caught in a local eddy near Gibraltar and was retrieved. The floats moved in the northern part of the Strait of Gibraltar. They moved to the sill and even though their deployment depths were 435 m and 330 m, for floats 05 and 03 respectively, they were upwelled and passed over the sill (300 m) to the Atlantic with speeds greater than 120 cm/s and 70 cm/s respectively. Taking into account the glass-sphere compressibility, the buoyancy needed to upwell the floats is summarised in Table 3. Because there was an interval of 80 h between the transmissions of the depth information, the last depth information was received on days 236 and 231 (see Fig. 2) for floats 05 and 03 respectively, still too far from the sill to show upwelling.

The sill crossing for floats 05 and 03 can be established from Fig. 14 at 10 h on day 238 and at 22 h on day 232 respectively. Tidal prediction for Gibraltar taken from the tide tables (produced by the Italian Hydrographic Institute) shows that floats 05 and 03 respectively crossed the sill 5 h and 3 h before the high water in Gibraltar (all in GMT time). The high speed, reached by the floats during the sill crossing, and its timing are in good agreement with earlier current-meter measurements on the sill described by Lacombe and Richez (1982). Those measurements showed the presence of a strong westward current at 200 m between 1 h to 6 h, with the maximum at 4 h before the high water in Gibraltar.

Figure 15 shows the tracks of floats from original data (taken every 2 h). Tidal variations and inertial oscillations are visible. Vector velocity time series of all floats are displayed in Fig. 16. The time series of the floats' east-west and north-south velocity components are shown in Figs. 17 and 18 respectively. There are created from data filtered by Groves filter and decimated to 12 values. To display the velocity data for floats which passed through the Strait of Gibraltar in more detail, hourly values and Groves-filtered hourly values of the vector velocity time series of floats 03, 05 and 08 are displayed in Figs. 19 to 22. They show considerable tidal velocities, with the highest speed near the sill.

4.2. CURRENT METERS

Figure 23 shows the time series of the current velocity vectors from the current meters at mooring 1. Figure 24 shows the same for the rest of the current meters. These are the synchronized and decimated versions of the Groves-filtered data with a sampling interval of 12 h. They are marked according to mooring (2, 3 and 4), with the upper time series of each mooring corresponding to the shallow current meter while the lower time series corresponds to the deep current meter; the high correlation between the two series is clearly visible. The same information about currents in the form of velocity components is given in Figs. 25 to 27. The current meter deployed at the depth of 712 m on mooring 1 malfunctioned after about 31 days. The vertical velocity component of the current measured by the upper current meter on the same mooring shows very large vertical currents, probably due to the mooring's motion. Non-tidal currents measured at mooring 1 were rather large and match the speed of the floats which passed by. They show predominantly the south-westward or even south-eastward direction of current. This surprising result indicates the possibility of return current to the Alboran Sea, or perhaps the existence of a deep eddy to the south of this site.

Current speeds at mooring 2 were the lowest, with variable directions; there was no indication of persistent deep westward flow of Levantine or Deep Western Mediterranean water at this site.

Current meters on mooring 3 show predominantly north-western currents with variable amplitudes. In agreement with float 08 they probably indicate the northern boundary of the Moroccan continental slope current. Currents at mooring 4 were stronger and oriented predominantly in the north-western direction, and had considerable speed and directional variability.

The plots of progressive vector diagrams for all current meters are shown in Figs. 28 and 29. They emphasize the directional variability of the currents. Figure 28 was created from hourly data, and Fig. 29 from Groves-filtered data decimated to 12 h. Inertial oscillations and tidal variation are visible in Fig. 28 but they have been filtered out in Fig. 29.

4.3. CURRENT-METER FLOATS

To illustrate the time and space variability of the flow, current meter and float data are presented in Fig. 30 for each second day as a current vector field. The data were created from the filtered and decimated data displayed in Figs. 16, 23 and 24. There is evidence of surprisingly large variations in current speed and direction, in space and time.

4.4. CTD CROSS-SECTIONS

Several cross-sections of salinity and potential temperature were created from CTD data taken on three cruises (Alboran I, *Magnaghi* and Alboran II). The positions of the individual casts are shown in Fig. 3 and the times of taking the casts are presented in Table 2.

Figures 31a–f present the cross-sections of potential temperature and salinity from the Alboran I cruise (days 216 to 223). The casts from this cruise are not complete, as mentioned in the hydrography section, but they are good enough for contouring the salinity and potential temperature isolines. CTD casts were concentrated only in the western Alboran Sea. Isolines across the Moroccan continental slope bent strongly upwards. Levantine water was present in the western Alboran, with the main concentration north of 36°N. Contours of the potential temperature and the salinity for depths of 100 m, 150 m, 350 m, 500 m and 700 m are presented in Figs. 32 and 33. The contours at 100 m and 150 m show the anticyclonic gyre as being present in the southern Alboran but shifted somewhat to the east. The contours for salinity and potential temperature already at 350 m show the characteristic bending-up of isolines across the Moroccan continental slope. Figures 34a and b display the contours of the maximum salinity and its depth respectively. It is evident that the main mass of Levantine water is north of 36°N, with a tendency to spread south along the 4°50′W longitudinal; and the maximum salinity is reached in the shallower water in the north (north of 36°N) rather than in the south.

Figures 35a–c present the cross-sections of the potential temperature and salinity obtained from the *Magnaghi* cruise (days 257–258). All casts were concentrated in the western Alboran. There is a bending-up of isolines across the Moroccan continental slope, just as in the Alboran I cruise. A considerable difference exists in the upper structure of the western Alboran layer, with no deepening of isolines observable, indicating the non-existence of anticyclonic circulation in the south. The contours of potential temperature and salinity in Figs. 36 and 37 indicate the same result. The contours at 100 m and 150 m show a structure similar to those for greater depths. The mass of Levantine water is again present near and north of latitude 36°N, with its salinity maximum located in the same area—as indicated in Figs. 38a and b. The difference from the Alboran I cruise is the shallower depth for the salinity maximum and the southward extension of Levantine water along the 4°20′W longitude (as against the 4°50′W longitude).

Cross-sections of the potential temperature and salinity from the Alboran II cruise (days 270 to 296) are presented in Fig. 39a–l. The cross-sections across the Moroccan continental slope from the west (Fig. 39b) to the east (Fig. 39j) again show the bending-up of isolines with the strongest effect in the western Alboran (Fig. 39e), and weaker bending-up east of 4°W (Figs. 39h–j). Figures 39a,b,k and l show the mass of Levantine water extending deep along the western Spanish continental slope. Even in the deep channel near Alboran Island (Fig. 39i) there is a bending-

up of isolines towards the southern slope of the channel, with the Levantine water present in its northern part. Again, as for the *Magnaghi* cruise, there is no indication of the existence of the upper layer anticyclonic gyre in the southwestern Alboran. Contours of salinity and potential temperature for depths of 30 m, 60 m, 70 m, 100 m, 150 m, 350 m, 500 m and 700 m are given in Figs 40 and 41. In these contours too there is no indication of anticyclonic circulation. In the contours for the greater depth, especially that for 500 m, the bending-up of isolines is visible along the whole Moroccan continental slope. The contours of dynamic height anomaly for the same data are given in Fig. 42. They show the strong current to the east in the southwestern part of the Alboran; the cyclonic circulation in the centre for the upper layer; and the westward flow along the Moroccan continental slope with the eastward return near the Spanish continental slope at 350 m, although the contours for 500 m and 700 m indicate a generally eastward flow (which is only partly in agreement with the current-meter data in Fig. 30—days 279 to 289).

The contours of the maximum salinity and its depth (in Fig. 43a,b) show a tongue of Levantine water along the Spanish continental slope. This maximum is located very deep (>500 m). Another tongue of Levantine water extends south along the longitude 3°40'W until reaches the Moroccan continental slope, where it appears at a much shallower depth (<400 m). To further illustrate the bending-up of isolines, contours of the depth for water with a potential temperature of 12.9 °C are displayed in Fig. 44a, and two three-dimensional views of the same variable from different angles are given in Fig. 44b. The water-type which corresponds to this potential temperature is the Deep Western Mediterranean Water. It is more evident that this is present at the shallower depth in the western Alboran than in the eastern part, indicating an upwelling in its path from the east to the west.

A comparison of CTD cross-sections reveals that the bending-up of isohalines in August (Fig. 31b) closely follows the Moroccan continental slope, while September and October cross-sections from the same area (Fig. 35a, Fig. 39d) show a northward shift of about 8 km for this feature. In addition to CTD casts, yo-yo measurements were performed. Their purpose was to investigate the non-linear internal waves, but the measurement performed in the Strait of Gibraltar, near the sill, also gave important information about the composition of the water outflowing to the Atlantic. CTD casts in this experiment were repeated every 5 min during a period lasting 3 h. Measurement started at the time of 'dead' water (2 h before high water in Gibraltar, in GMT), when the ship had no drift, and initially was close to and east of the sill. The strong tidal dependence of the currents is known from past current-meter measurements (Lacombe and Richez, 1982) on the sill. The yo-yo measurement started during a period of enhanced outflow. Results in terms of the time variation of potential temperature and salinity are presented in Fig. 45. The salinity plot, especially in the first phase shows the presence of Mediterranean water from almost 70 m. The Deep Western Mediterranean water is clearly visible, with its outflow across the sill to the Atlantic indicated. One hour after the yo-yo measurement, CTD cast 62 was taken about 8 km to the east of

the sill; this revealed the presence of Deep Water Mediterranean water at depth of less than 300 m. Figure 46 shows the potential temperature/salinity diagram with potential sigma curves for cast 62 and casts 74 and 30 for comparison. Cast 74 was taken in the Alboran Sea at a position where the strong Moroccan continental slope current was detected by floats. Cast 30 was also taken in the Alboran Sea, but in a position outwith the outflow current. It is evident that the water between 300 to 500 m at station 62 had the same characteristics as the water between 450 to 500 m at station 74 and between 700 to 750 m at station 30. This is in agreement with the now-well-documented idea that the upwelled Deep Western Mediterranean water, mixed with Levantine water in the area of the Moroccan continental slope, is transported by the Moroccan continental slope current through the Strait of Gibraltar to the Atlantic.

It is important to establish the water mass in which floats 03, 05 and 08 were positioned. From the deployment depths of 330, 435 and 565 m for floats 03, 05 and 08 respectively–and from the CTD cross-sections, it appears that the floats were positioned in the lower boundary of Levantine water or the upper boundary of the Deep Western Mediterranean water.

4.5. GEOSTROPHIC CURRENTS

Many of the casts from the Alboran I cruise (days 216 to 223) were not complete (see Sect. 2.5) and were therefore not suitable, except for one cross-section, for geostrophic calculation. Schematic results of the geostrophic current calculations from the *Magnaghi* cruise (days 257–258) are summarised in Fig. 47 and detail cross-sections are given in Figs. 48a–c. These cross-sections correspond to the salinity and potential temperature cross-section of Figs. 35a–c. They show that the main jet of Atlantic water in the upper layer turned south, and the anticyclonic gyre did not exist in the western Alboran, which is in agreement with Figs. 36 and 37. Results for the deep-water current show the existence of the Moroccan continental slope current towards Gibraltar at a depth of 400 m. This current is clearly visible in Figs. 48a and b, and possibly exists to the south of CTD station 20 in Fig. 48c. Comparison of this result with the current-meter measurements at mooring 2 and with the motion of float 08 reveals that the computed slope current is restricted too much in the south. This is because too deep a level of no-motion was chosen (250 m).

Schematic results of the geostrophic current calculation for the Alboran II cruise (days 279 to 289) are summarised in Fig. 49. The detail cross-sections of the geostrophic current are given in Figs. 50a–j and correspond to the cross-sections of salinity and potential temperature in Fig. 39. The results for the upper layer resemble the results from the *Magnaghi cruise*, i.e. the absence of the significant anticyclonic gyre in the southwestern Alboran; the cyclonic circulation in the central Alboran; and the small cyclonic vortex northeast of Gibraltar. An important result

for the deep layer was the existence of a westward-directed Moroccan continental slope current along the slope from 3°15'W to Gibraltar, at a depth of 400–450 m and stronger in the western Alboran than in the south-central Alboran. Slightly north, and deeper than this continental slope current, there is a current directed to the east. Cross-section X taken across the deep Alboran Sea channel shows the deep water in the central and northern part of the channel as moving westward into the Alboran Sea. The existence of an anticyclonic circulation around the mountain-like bottom feature in the central Alboran (as indicated by the track of float 07) is implied in the geostrophic calculation; likewise the existence of a cyclonic vortex in the south-central Alboran, as was indicated by 1982 float measurements (Pistek, 1985), is evident.

Depending on the chosen level of no-motion, there is a considerable difference between the results of the computed geostrophic current near the Moroccan continental slope. Results for the two different levels of no-motion, one at 250 m and the other at 150 m, are shown in Fig. 50 for almost all cross-sections, as the left and right side display respectively. The shallower level (150 m) fits the spatial extension and amplitude of the observed current better. It is possible that an even shallower level of no-motion, as indicated by the salinity and potential temperature cross-sections in Fig. 39, could be chosen. Figure 51 shows the cross-sections of geostrophic current computed from the CTD cross-section displayed in Fig. 39b for different levels of no-motion. This CTD cross-section is located close to Gibraltar. Floats 03 and 05 passed across it 50 days earlier, near the location of cast 75, on days $229\frac{1}{2}$ and $233\frac{1}{2}$, with speeds of 14 and 12.5 cm/s respectively. If it is assumed that the amplitude and location of the Moroccan continental slope current did not change appreciably in 50 days, the best choice for the level of no-motion would be about 75 m, to match the speed and location of the floats' passage. Figure 52 shows the overlay of the corresponding geostrophic current cross-section with its salinity and potential temperature structure. This figure indicates the water composition of Alboran outflow and the ratio of the volumes of Levantine and Deep Western Mediterranean waters participating in it.

4.6. SATELLITE DATA AND FLOATS AT 60 m

There were no current meters deployed in the upper layer, and therefore only satellite infrared images, CTD data, geostrophic calculations, and the tracks of the near-surface (60 m) floats for a short period were used to interpret its motion.

Satellite infrared images are displayed in Fig. 53. They cover the period of measurement unevenly. There are two types of images: APT and HRPT, as described in Sect. 2. Some of them are not mercator projected, but they are good enough to give a qualitative indication of circulation.

Three images taken in August (days 220, 228 and 238) show the well-developed

anticyclonic gyre slightly shifted to the east. The infrared image from day 238 (not mercator projected) shows the more confined gyre. An example of agreement between the satellite infrared image (day 220) and geostrophic current as computed from the CTD cross-section is given in Fig. 54. The edge of the gyre is clearly visible. The cross-section of the geostrophic current also indicates the existence of a smaller anticyclonic vortex on the western side of the gyre, which is likewise visible in the infrared image.

The surface structure changed considerably in September (days 250, 255 and 260). Images for days 250 and 255 are APT data; day 260 is HRPT data. A considerable shift in the anticyclonic gyre to the east is visible in the image from day 250 (September 7). It is even more pronounced later on, at day 255. HRPT data from day 260 show the gyre 'anomalously' positioned east of 3°50'W, and the western and the central Alboran filled with the water about 3 °C colder than the water which was present in the eastern Alboran. The jet of Atlantic water leaving the Strait of Gibraltar bent southward and was following the Moroccan continental slope to the east. This result is in agreement with the CTD measurements taken during the *Magnaghi* cruise (days 257–258)—as mentioned in the sections which describe the CTD contours and geostrophic current.

The October satellite infrared images relate to days 275, 283, 291, 292 and 293. The satellite image from day 275 is not very clear. It resembles the previous images: low temperature in the western and central Alboran, with unclear structure. The next image—from day 283—shows, as before, the jet of Atlantic water bending southward and than meandering eastward. These results are in agreement with the CTD contours and geostrophic calculations created from the CTD data which were taken during the Alboran II cruise (days 279–289).

The remaining satellite images, days 291, 292 and 293, show the growth and consolidation of a new anticyclonic gyre. One image from day 292 shows the jet which moved from the Strait of Gibraltar strait eastward, in contrast to the southward bending which was visible in the earlier images.

Three subsurface floats were released at a depth of 60 m, and acoustically tracked between the days 279 to 285 from the ALS positions, in the same way as for deep floats. The locations of the deployment sites and the tracks of the floats are given in Fig. 55. Velocity vector time series for all floats are presented in Fig. 56. The results show that all floats, even one deployed north-east of Gibraltar, moved south—and in agreement with the satellite image (day 283) they indicate that the anticyclonic gyre did not exist. The floats moved close to the Moroccan continental shelf and then meandered to the east. The average speed of the floats in the jet of Atlantic water was 41 cm/s and 50 cm/s for floats 07 and 06 respectively (all of them were finally destroyed by fishermen). Figure 57 (day 283) illustrates the agreement between the surface temperature distribution as registered by satellite and the tracks of the three subsurface (60 m) floats (days 279–285).

4.7. METEOROLOGICAL FORCING

In the Alboran II report (Pistek, 1985) there is a discussion of meteorological forcing and of the cross-correlations between the pressure integrated over the Western Mediterranean (or over the Alboran Sea) and current meter or float measurements computed in 1982. The results did not support meaningful cross-correlation between the deep currents and the atmospheric pressure. Current-meter measurements in this experiment were taken in the westernmost part of the Alboran Sea and near the Strait of Gibraltar, and therefore the cross-correlations had been expected to be more pronounced.

The average pressure over the western Mediterranean was evaluated daily from the weather maps of the European Meteorological Bulletin (D6050), for the period of 115 days (Julian days 196 to 311), overlapping the period of measurement. Integration over the area between each two isobars was done by planimeter, and the resulting surface was multiplied by the average pressure for each strip. Summation of all contributions and its division by the total surface produced the average pressure. Figure 58 shows the time series of the average western Mediterranean pressure (called WESTMED).

On average, the atmospheric pressure was lower in August than in September and October—but in September three very low pressure perturbations passed over the western Mediterranean. The time series was too short to establish the low frequency spectra with confidence; the autospectrum is presented in Fig. 59 with probable periodicities (15, 10, 7, 5, 3 to 2.7 days). The autocorrelation, in Fig. 60, shows the periodicity of about 10 days.

Wind data are displayed in Fig. 61. They represent the daily midday observations from the three land stations situated near the Alboran Sea. These were the data published in the weather maps of the European Meteorological Bulletin (D6050).

4.7.1. Correlation with deep currents. To illustrate the correlation between the average atmospheric pressure and current-meter data, coherence between each current-meter component and pressure was computed, and results are presented in Fig. 62. A linear-predictive spectral analysis method (as described by Nuttall, 1983), which 'efficiently' depicts the frequencies with higher coherences was utilized. Although this non-linear analysis could have been used for the short-time series it had a drawback in that it does not specify the confidence limits. The results show only a weak coherence in general, with higher values for deep current meters. It had been expected that currents near the Strait of Gibraltar would have been more correlatable (mooring 1) with the atmospheric pressure variation, in accordance with the literature.

Figure 63 shows the results relating to coherence between the float velocity and the average atmospheric pressure. The coherence is in general higher than that between the current-meter readings and pressure, but the time series for floats 03 and 05 are short—which diminishes the confidence limits of the resulting coherence. The coherence between the velocity of this float and atmospheric pressure was computed for the short time series (20 days) when float 08 was caught in the Moroccan continental slope current, and did not increase. The coherence between the current speed measured by the upper meter at mooring 1 and the corresponding atmospheric pressure was computed for the short-time series (16 days) when floats 03 and 05 were caught in the Moroccan continental slope current, and showed high correlation. As before. this time series was too short to yield results with adequate confidence.

4.7.2. Correlation between atmospheric conditions and position and extension of anticyclonic gyre. The set of satellite images which are displayed in Fig. 53 and the corresponding CTD measurements indicate the development of a rather 'unusual' upper layer circulation in the western Alboran during the course of the experiments. After a period of a well-developed anticyclonic gyre in the August of 1983, the gyre was shifted eastward on 7th September (day 250)—and the jet of Atlantic water, after leaving the Strait of Gibraltar, bent southward. This situation persisted until 18th October (day 291), at which time a new gyre started to grow.

It is not clearly understood how the changes of position, extension or disapearance of an anticyclonic gyre are forced. Numerical studies by Preller and Hulbert (1982) and Preller (1984) indicate the important effect of the vorticity attributable to the Alboran inflow, and that of the amplitude of the inflow velocity on the extension and location of the gyre. An earlier hypothesis that the gyre and its changes are forced by the wind field anomalies is not plausible (Whitehead and Miller, 1979), since Cheney and Doblar (1978) observed that the low pressure over the western Mediterranean with westerly wind causes the migration of the gyre to the east, while the opposite conditions favor the development of a large gyre in the western Alboran Sea.

Observations of pressure and wind in conjunction with satellite images for the 1982 Alboran experiment are described in Pistek (1985). While supporting the Cheney and Doblar (1978) assertion, they also showed that additional variables are involved in order to explain the creation and growth of a new vortex and the partition of a large gyre during the stable conditions.

Observations for the Alboran III period of measurement are summarised below. The times of CTD measurements, float deployments, satellite infrared images and pressure variation, were registered, are displayed in Fig. 58; wind conditions are presented in Fig. 61 and satellite images in Fig. 53.

(a) The average August WESTMED pressure was 1014 mb; prevailing winds were from the west with a maximum speed of 15 n.mi/h; satellite images for days 220, 228 and 238 showed the well-developed gyre shifted slightly estward (probably because of wind). CTD results (days 216 to 223) are in agreement with the satellite images. This situation is in agreement with the explanation by Cheney and Doblar (1978).

(b) September atmospheric pressure showed several deep lows; prevailing winds were from the east with a maximum amplitude of 15 n.mi; satellite images for days 250, 255, 260 coincided with the low pressure period and show (a) the complete shift of the anticyclonic gyre eastward, (b) the presence of cold water in the western Alboran, and (c) bending of the jet of Atlantic water southward, after passing the Strait of Gibraltar. CTD data (days 257–258) agree with the satellite images. These results indicate the importance of atmospheric pressure in shifting the gyre.

(c) The average atmospheric pressure in October was high (1020 mb). The lows were less pronounced than in September. Winds were weak and variable in direction during the first half of October, but they were stronger and from the east during the second half.

Following the smaller low pressure variation and variable wind that existed, the satellite images for days 275 and 283 show the absence of the anticyclonic gyre. CTD data (days 279–289) and floats deployed at a depth of 60 m (days 279–285) agree with the satellite images. Satellite images for days 291, 292 and 293 (which were after the smaller low pressure variation but during the period of stronger winds from the east) show the growth of a new gyre in the south-western Alboran. These results cannot be explained solely as an outcome of the wind and pressure interplay c.f. Cheney and Doblar (1978).

4.8. SPECTRA OF THE CURRENT AND FLOAT VELOCITIES

Autospectra for each current velocity component and rotational spectra for all eight current meters are presented in Fig. 64; the 90% confidence limits are indicated. The high-frequency spectra were produced from the original data. The lower-frequency spectra were obtained from the hourly data and the low-frequency spectra were obtained from the Groves-filtered data. The *rms* fit, to remove the trend in spectral computation, helped at least partly to also remove the aliasing of high-frequency spectra by low-frequency components.

The high-frequency spectra show internal waves and solitons. For many of the current meters there was a 6 h peak. Tidal variation, mainly the semidiurnal tide, and inertial oscillation are clearly identifiable at frequencies in the middle of the high-frequency range.

Individual plots of low frequency current-meter spectra do not have enough degrees of freedom. They indicate peaks that are evident also in the atmospheric data. Figures 65a and b present the spectra of current velocity data obtained by averaging the individual spectra of the upper and lower current meters at moorings 2, 3 and 2, 3 and 4 respectively. Figure 65c shows the spectra of float velocity data obtained by averaging the individual spectra of floats 06, 07 and 08. The numbers beside the peaks are the wave periods in days.

4.9. OTHER COHERENCES

Coherence between the current-meter data and between the current-meter and float data were computed in order to improve the interpretation of the circulation.

4.9.1. Current meter-to-current meter coherence. It is evident from the data sets that currents measured by current meters on individual moorings (upper and lower) are correlated (see Fig. 66). The highest correlation is that between the current velocity components on mooring 4. Vertical separation between the two current meters on this mooring was only 100 m; on the others the separation was 400 m.

Figure 67 displays several instances of coherence between the upper current meters on different moorings. The coherence between the currents at moorings 1 and 2 is low, indicating that there is a small contribution of the Levantine water located in the northern Alboran to the outflow of Mediterranean water into the Atlantic; on the other hand, the higher coherence between the current components at mooring 1 and the west current components at mooring 3 or mooring 4 indicates the important contribution of the water mass located in these areas to the outflow.

The higher correlation between the east-west current component at mooring 2 and the north-south component at mooring 3 indicates the existence of the cyclonic return current in the north-western Alboran.

4.9.2. Current meter-to-float and float-to-float coherence. Coherences between the float and current-meter data and between the float and float data are displayed in Fig. 68a–e.

Float 05 is highly correlated with the current-meter data at moorings 1, 3, and 4, and to a lesser extent with the current-meter data at mooring 2, indicating that the main contribution to the outflow comes from the Moroccan continental slope current. The same observation is valid for float 03.

Float 08 data shows high coherence only with the upper current-meter data at mooring 3 because of the spatial proximity to this mooring.

Float 06 data is highly correlated with the upper current-meter data at mooring 2, again because of spatial proximity to the mooring. For the whole period of measurement, coherence of float data with mooring-1 current-meter data is small, indicating that the contribution of this water mass to the Mediterranean outflow is not at all significant. Partial coherence for the period before float 06 was trapped in the valley of the Spanish continental slope (marked SHORT) is higher, but is not comparable to that between float 05, or float 03, data and mooring-1 current-meter data.

Float 06 and float 07 data show a peak coherence after 2.2 days for the east-west component of velocity, and after 3.4 days for the north-south component of velocity. Float 05 and float 03 data show sharp coherence in the east-west components of velocity after 2.8 days. All coherences involving float 07 are solely for the period of 25 days when tracking of float 07 was good. Several of the coherences pertaining to the north-south current velocity components peak after 3.3 days.

5. Conclusions

The upper-layer circulation during the experiment was observed through the agency of satellite infrared images, CTD casts and, in the last part of the experiment, by acoustic tracking of floats deployed at a depth of 60 m. Considerable variability in this circulation was revealed. Although the anticyclonic gyre was present in the southwestern Alboran in the first month of the experiment the gyre subsequently shifted eastward—leaving the western Alboran with an 'unusual pattern' of flow. The jet of Atlantic water bent southward after leaving the Strait of Gibraltar, and moved with an average speed of 40–50 cm/s, in general meandering eastward. Cyclonic circulation existed in the central Alboran and a small cyclonic eddy was present north-east of Gibraltar. This situation persisted for several weeks and finally, at the end of the experiment, a new anticyclonic eddy grew near Ceuta. Qualitative correlation between the gyre's extension (or its longitudinal position) and the wind speed and direction (or the average atmospheric pressure) over the western Mediterranean often agreed with the observations and hypothesis of Cheney and Doblar (1978). Likewise our observations in 1982 (Pistek, 1985) were also often in agreement with it. The disappearance of the anticyclonic gyre in this experiment and the creation and the growth of new vortexes near Ceuta, as shown in Pistek (1985), reveal that the dependence between the variables is more complex.

Computer modelling of the upper layer dynamics by Preller and Hulbert (1982) and by Preller (1984), shows the importance of inflow parameters (velocity, angle of inflow) on the longitudinal position and the strength of the gyre, but the southward bending of the jet, as observed in this experiment, could not be achieved without putting clockwise vorticity into the jet in the Strait of Gibraltar (Preller, personal communication).

All of the current meters (8) and the floats (4) were deployed deeper than 250 m in the western Alboran Sea, and one float was deployed in the central Alboran. The main intention was to investigate the deep circulation in the westernmost part of the Alboran as a continuation of measurements made in 1982 (Pistek, 1985) and to study the stability of the circulation pattern in the central Alboran. Floats 05 and 03, which were deployed near the western Moroccan continental slope, showed the existence of the Moroccan continental slope current—guided by bottom topography, reaching the level of Gibraltar in latitude, and bending into the Strait of Gibraltar. This was in agreement with previous measurements (Bryden and Stommel, 1982); (Pistek, 1985). Also float 08 (which was deployed in the central part of the western Alboran Sea) drifted southward after stagnating for about 30 days and was caught in this slope current; the trajectory probably traces the current's northward extent. The floats had an accelerated motion reaching, after the removal of tidal motions, a speed of 13 cm/s near longitude 5° W and 30 cm/s in the Strait

of Gibraltar. They moved in the northern side of the Strait of Gibraltar, and their tracks exhibit the large semi-diurnal tidal motion. In particular float 05 experienced strong tidal variation south of Tarifa. Both floats (05 and 03) moved to the sill, and even when their deployment depths were greater than the depth of the sill (300 m) they moved over it into the Atlantic with speeds greater than 120 cm/s and 70 cm/s (respectively). Taking float compressibility into account, the vertical velocities needed to upwell the floats over the sill were 1.7 cm/s and 0.8 cm/s for floats 05 and 03 respectively. The times of float passage over the sill relative to the time of tidal high water, were −5 h HW (i.e. 5 h before high water at Gibraltar) for float 05 and −3 h HW for float 03. This is in the time-window when the outflow over the sill is strongest (the maximum being −4 h HW), as shown by Lacombe and Riches (1982), and renders the upwelling and horizontal velocities acceptable. Two floats were deployed in the northern Alboran and after one failed the remaining one, 06, was left at a depth of 525 m. It moved indecisively westward and back eastward, and was finally caught in the valley on the Spanish continental slope, where it was upwelled about 200 m. It was ascending during the 3-week period and the vertical velocity needed to keep it at the final depth of 350 m was 1.98 cm/s, too large to be permanent. One explanation is that the float was only periodically pushed up by the current near the bottom and was in fact lying on the bottom during the intervening periods. There are, however, several mechanisms which can cause intermittent upwelling (e.g. strong surface currents, wind, breaking solitons).

Float 07 was deployed in the central Alboran at a depth of 670 m and descended during 30 days to a depth of 1090 m (the cause is not known). It moved clockwise around the mountain-like bottom topographic feature in the central Alboran, which was a circulation also observed in the 1982 experiment for floats 03 and 01 (Pistek, 1985); later float 07 was moving with a cyclonic tendency in a north-western direction, finally stagnating in the central Alboran around 4°30'W. This behaviour again resembled that of floats in the previous deployment. Wherever the tracking in its path was good (northern part of track), the large north-south velocity variation was detected with a periodicity of 3.4 days.

Two current meters were deployed on every mooring (one at about 300 m and the other at 700 m) except at mooring 4, where the lower current meter was deployed to 400 m. Currents at the upper and lower level on each mooring were strongly correlated and in addition the computed coherence was high. Currents were very strong at mooring 1, south of Gibraltar, with average upper and lower current-meter amplitudes of 9.5 cm/s and 12 cm/s; and at mooring 4 they were 4 cm/s and 4.8 cm/s—these values were not biased by the tide, tidal variations at mooring 1 were several times higher. Currents in the northern and central Alboran, moorings 2 and 3, were small—of the order of 1 to 2 cm/s. Current at mooring 1 had a very large tidal component and the filtered speed without tides was suprisingly southward-oriented, indicating a strong meander or return current at that location. The north-south current component of the velocity at mooring 1 was coherent with the east-west current velocity component at moorings 3 and 4, indicating that

the main contribution to the outflow comes from the slope current; on the other hand the very low coherence between the currents at moorings 1 and 2 indicates that the contribution to the outflow from the north side was small. The same observation holds for the coherences between the float and current-meter velocities. Float velocities for floats 03 and 05 were coherent with the current velocities at the moorings 1, 3 and 4 but not 2; the float velocity for float 06 was coherent only with the current velocity of the upper current meter at mooring 2, even when the coherence was computed for the shorter period before the float 06 was trapped in the underwater valley.

Slightly higher coherence between the east-west current velocity component at mooring 2 and the north-south current velocity component at mooring 3 may signify the return cyclonic flow from the northwestern Alboran.

Geostrophic velocities calculated from the October 1983 CTD cross-sections clearly show the existence of Moroccan continental slope current extending almost from Alboran Island to Gibraltar, and reveal it as being weaker in the central section.

Bending-up of isolines towards the Moroccan continental slope was clearly visible in every period of CTD measurement (August, September, October 1983). The bending-up of isolines in the western part of the Alboran (4°40'W) was shifted northward in September and October, while in August it followed the sloping bathymetry more closely. October CTD cross-sections were extended eastward, close to Alboran Island, and the 'bending-up' was observable in these cross sections too. Floats 03 and 05 were deployed in the lower strata of Levantine water and the upper strata of Deep Western Mediterranean water. Their upwelling and passage over the sill indicates that this water mass flows to the Atlantic. CTD and yo-yo measurements taken near the sill, on its eastern side, during 'dead' water, showed the presence of Deep Western Mediterranean water at a depth that was less than the sill depth. This result and the times of float passage over the sill, −3 and −5 h (HW at Gibraltar)—which is when the well-known large upward movement of deep water isolines occurs—show that the Deep Western Mediterranean water gets over the sill into the Atlantic.

Computed coherence between the average atmospheric pressure over the western Mediterranean and current-meter data at 300 and 700 m shows a significant dependence of current on atmospheric pressure change. This holds true even for the current measured by the current meters deployed near Gibraltar. Only floats which were deployed in the Moroccan continental slope current show higher coherence with the atmospheric pressure, indicating that the Alboran outflow is influenced by atmospheric pressure. This influence could be generated in the Strait of Gibraltar. The time series involved in this computation of coherence were too short to yield good confidence limits.

Rotary and auto spectra obtained from current meter and float velocity data, indicate the presence of nonlinear waves in the high frequencies. Spectral peaks at 6 h and higher harmonics are often present. The semidiurnal tide is very prominent and inertial oscillation and diurnal tides are clearly visible. Float 07 displayed very pronounced variation, at 3.4 days periodicity, in the north-south velocity component. Many low-frequency spectral peaks coincide with those of atmospheric pressure in spite of the low coherence between their time series.

The floats used in this experiment transmitted information about depth every 80 h, in four 2 h intervals. Analysis of this information revealed the existence of 'creeping' float compression. Benthos expendable floats descended linearly to about 50 m in 45 days, while more complicated recoverable floats, which were built in SACLANTCEN's Ocean Engineering Department Laboratory, reached equilibrium depth sooner: in 23 and 30 days, descending 100 and 420 m, for floats 08 and 07 respectively. Floats 03 and 05 which were deployed deeper than the depth of Gibraltar sill, leaked over the sill into the Atlantic, but the final depth information, from east of Tarifa, did not indicate any upwelling.

A brief comparison of the results from all three sets of Alboran Sea experiments (years 1980, 1982 and 1983) showed that the results from the three sets are consistent in their description of the western and the central Alboran Sea circulation: clockwise vortex around the topographic feature in the central Alboran, cyclonic circulation southwest of it and bounded by Moroccan continental slope current in the south, and of variable extension to the north and west. In addition to the Moroccan continental slope current, which flows westward there is an eastward current which is deeper and to the north, and some of the floats deployed in 1982 were trapped in it. The hydrography, and also the motion of the floats, combine to demonstrate that the flow along the Spanish continental slope is to the west and that Levantine water is concentrated there. This motion is slow in general, with periods of enhanced westward currents—but it is not clear how much it contributes to the Mediterranean outflow, because most of the flow turns south (as indicated by the floats) along the longitude 4°40'W. In addition the augmentation of the westward current near the Spanish continental slope was coincident with the augmentation of the eastward current (as measured by current meters which were positioned in the southern locations), indicating an intensification and a larger extension of cyclonic circulation but not a greater contribution to the outflow. The Moroccan continental slope current towards Gibraltar (which was calculated from geostrophic data from 1983 CTD data) extended from Alboran Island to Gibraltar, and was weaker in the central section. Floats 03 and 05, deployed in summer 1983, moved almost in identical tracks and with identical speeds to those of the free-floating vertical current meters deployed in summer 1980, in the locations where these deployments overlapped. The locations of the current-meter moorings in the southern Alboran were identical for 1983 and 1980, but the variability in current speed and direction was much greater in 1983 than in 1980. Currents measured near the Spanish continental slope were stronger in the winter of 1982 than in the

summer of 1983 (identical location for moorings E-1982 and 2-1983). Currents measured by current meters on the mooring in the central part of the western Alboran (mooring 3) showed a prevailing westward direction, while the measurements from 1982 in the same location (mooring F) and in the location close to it (mooring A) showed currents which were stronger, with eastward components prevailing for long periods. This result was connected with the stronger cyclonic circulation observed in the winter period of 1982, as described above. The Moroccan continental slope current was also in existence in the winter of 1982 but it was weaker in its central section than it was in the summer of 1983. Bending-up of isolines towards the Moroccan continental slope was always detected in cross-sections, but it was only in 1983 that cross-sections were carried out further to the east, almost to Alboran Island. Location of the bending-up in the western Alboran was close the to sloping bottom topography of the Moroccan continental slope in 1980 and in 1982, and in the August of 1983—but was shifted about 8 km northward in the September and October of 1983.

Cross-correlations or coherences between the average atmospheric pressure over the western Mediterranean or Alboran Sea and deep currents were not significant in the 1982 and the 1983 measurements, while the upper layer responded often to the atmospheric and wind changes in agreement with the qualitative rule of Cheney and Doblar. Creation and growth of new anticyclonic vortexes near Ceuta, even during the time when the necessary stable conditions for the existence of anticyclonic gyre were satisfied, as was the case in 1982 and 1983 when the gyre was not present, cannot be satisfactorily explained by the above rule. These cases need a large vorticity input and another parameter in order to explain the mechanism for the insertion of vorticity into the inflowing jet of Atlantic water in the Strait of Gibraltar.

The apparently independent behaviour of the upper and deep layers partially justifies the assumption of two independent layers in the description of the Alboran Sea dynamics. It was found in the 1982 measurements that the large anticyclonic gyre does not extend very deep. But observations in 1982 also showed that the very energetic vortex near Ceuta (a surface geostrophic velocity of 80 cm/s) caused considerable mixing of Levantine and Deep Western Mediterranean waters, possibly influencing the composition of the outflow from the Alboran. Likewise, the shift of location in the western Alboran, where the isolines bent up in September and October 1983, was connected with different circulation pattern in the upper layer. The southward flow of Levantine water along longitude 4°40'W from the northern Alboran and the weakening of the Moroccan continental slope current in the central Alboran are probably influenced by the upper layer circulation.

There is no clear understanding of the forcing for the bending-up of isolines towards the Moroccan continental slope.

The 1980, 1982 and 1983 current meter and float data were spectrally analysed.

In the high frequency region of the current-meter data there is definite evidence of internal waves (also solitons) in all Alboran Sea locations; the semidiurnal tide is dominant and its higher harmonics point to its nonlinearity. A signal with a 6-hour periodicity is often clearly visible in the current velocity data, and its spectral peak cannot be explained as solely the result of tidal non-linearity. Inertial oscillations and diurnal tides are also clearly visible in the lower frequencies. In the low-frequency spectra many spectral peaks coincide with the spectral peaks of the atmospheric pressure spectra.

On two occasions during the Alboran Sea investigations (1982 and 1983) Swallow-type floats were tracked from autonomous listening stations moored in the area. Both experiments lasted about 90 days and were fully successful. They showed that it is feasible to use autonomous listening stations and track floats even in a very variable bathymetric environment. The floats used in these experiments were of the glass-sphere type. Their modification to recoverable-type was very useful in improving the economy of deployments, but the problem related to 'creeping' compression will need attention.

References

ALLAIN, C. L'hydrologie et les courants du détroit de Gibraltar pendant l'été de 1959. *Revue des Travaux, Institut de Pêches Maritimes*, **28**, 1964: 1–99.

ARMI, L. and FARMER, D. The internal hydraulics of the Strait of Gibraltar and associated sills and narrows. *Oceanologica Acta*, 1984 (in press).

BETHOUX, J.P. Mean water fluxes across sections in the Mediterranean sea, evaluated on the basis of water and salt budgets and of observed salinities, *Oceanologica Acta*, **3**, 1980: 79–88.

BETHOUX, J.P. Budgets of the Mediterranean sea. Their dependence on the local climate and on the characteristics of the Atlantic waters. *Oceanologica Acta*, **2**, 1979: 157–163.

BRADLY, A., TILLIER, P. Mesoscale Lagrangian measurement system. ICES Hydrographic Committee, Proceedings CM-1980/C7. Copenhagen, Comité International pour l'Exploration de la Mer, 1980.

BRYDEN, H.L. and STOMMEL, H.M. Limiting processes that determine basic features of the circulation in the Mediterranean Sea. *Oceanologica Acta*, **7**, 1984: 289–296.

BRYDEN, H.L. and STOMMEL, H.M. Origin of the Mediterranean outflow. *Journal of Marine Research*, **40** (supplement), 1982: 55–71.

BRYDEN, H.L., MILLARD, R.C., PORTER, D.L. Technical Report: CTD observations in the western Mediterranean sea during cruise 118, LEG2 of R/V CHAIN, February, 1975. WHOI-78-26, Woods Hole, Massachusetts, Woods Hole Oceanographic Institution. 1978.

BUCCA, P.J. and KINDER, T.H. An example of Meteorological effects on the Alboran Sea gyre. *Journal of Geophysical Research*, **89**, 1984: 751–757.

CHENEY, R.E. and DOBLAR, R.A. Structure and variability of the Alboran Sea frontal system. *Journal of Geophysical Research*, **83**, 1978: 4593–4597.

CREPON, M. Influence de la pression atmosphérique sur le niveau moyen de la Méditerranée occidentale et sur le flux à travers le détroit de Gibraltar. *Cahiers Océanographiques*, **17**, 1965: 15–32.

DEACON, M. Scientists and the Sea, 1650–1900: A Study of Marine Science. New York, NY, Academic Press, 1971: p. 445.

DEFANT, A. Physical Oceanography, Volume 1, New York, NY, Pergamon Press, 1961: p. 729.

FRASSETTO, R. Short-period vertical displacements of the upper layers in the Strait of Gibraltar, SACLANTCEN TR-30, Parts 1 and 2. La Spezia, Italy, SACLANT ASW Research Centre, 1964. [AD 808 764/AD 808 765]

GALLAGHER, J.J., FECHER, M. and GORMAN, J. Project HUELVA, Oceanographic/acoustic investigation of the western Alboran Sea, NUSC 6023. New London CT, Naval Underwater Systems Center, 1981.

GARRETT, C. Variable sea level and strait flows in the Mediterranean: A theoretical study of the response to meteorological forcing. *Oceanologica Acta*, **6**, 1983: 79–87.

GROVES, G.W. Numerical filters for discriminating against tidal periodicities. *Transactions, American Geophysical Union*, **36**, 1955: 1073–1084.

KINDER, T.H. Current-meter measurements in the northwestern Alboran sea. *In*: PARILLA, G. *ed.* Preliminary Results of the 'Donde Va' Meeting in Fuengirola, Malaga (Spain) 18–21 October 1983. *Inf. Tec. Institut Esp. Oceanografia*, No. 24, 1984. Madrid, Spain. Instituto Español de Oceanografia. Alcala, **27**, 1984: 159–167.

LACOMBE, H. Contribution à l'étude du régime du détroit de Gibraltar. I. Etude dynamique. *Cahiers Océanographiques*, **13**, 1961: 73–107.

LACOMBE, H., RICHEZ, C. Contribution à l'étude du régime du détroit de Gibraltar. II. Etude hydrologique. *Cahiers Océanographiques*, **13**, 1961: 276–291.

LACOMBE, H., TECHRNIA, P., RICHEZ, C., GAMBERONI, L. Deuxième contribution à l'étude du régime du détroit de Gibraltar (Travaux de 1960). *Cahiers Océanographiques*, **16**, 1964: 283–314.

LACOMBE, H. Le Détroit de Gibraltar, Océanographique physique. *Notes et Mémoires du Service Géologiques du Maroc*, **22**, 1971: 111–146.

LACOMBE, H. and RICHEZ, C. The regime of the Strait of Gibraltar. *In*: NIHOUL, J.C.J., *ed.* Hydrodynamics of semi-enclosed seas. Amsterdam, Elsevier, 1982: pp. 13–73.

LANOIX, F. Projet Alboran: étude hydrologique et dynamique de la Mer d'Alboran d'après les travaux effectués dans le cadre du Projet Alboran (juillet et août 1962), Rapport Technique OTAN no. 66. Bruxelles, Belgique, Organisation du Traité de l'Atlantique Nord, Sous-comité océanographique, 1974.

LA VIOLETTE, E.P. The advection of submesoscale thermal features in the Alboran sea gyre. NORDA TN 240. NSTL Station, MS, Naval Ocean Research and Development Activity, 1983.

MEDOC Group. Observation of formation of deep water in the Mediterranean sea. *Nature*, **227**, 1970: 1037–1040.

NACINI, E. An atlas of HRPT and APT satellite data images of the Alboran sea, August–October 1983. SACLANTCEN SR–89. La Spezia, Italy, SACLANT ASW Research Centre, 1985. [AD A161 898]

NUTTALL, A.H. Two-channel Linear-predictive spectral analysis; Program for the HP9845 desk calculator. NUSC TR 6533, New London, CT, Naval Underwater Systems Center, 1983.

OVCHINNIKOV, I.M., KRIVOSHEYA, V.G. and MASKALENKO, L.V. Anomalous features of the water circulation of the Alboran sea during the summer of 1962. *Oceanology*, **15**, 1976: 31–35.

OZTURGUT, E. The sources and spreading of the Levantine intermediate water in the eastern Mediterranean, SACLANTCEN SM–92. La Spezia, Italy, SACLANT ASW Research Centre, 1976. [AD B 018 619]

PARILLA, G. *ed.* Preliminary results of the 'Donde Va' meeting in Fuengirola, Malaga (Spain) 18–21 October 1983. *Inf. Tec. Institut Esp. Oceanografia*, No. 24, 1984. Madrid, Spain. Instituto Español de Oceanografia. Alcala 27, 1984.

PHILIPPE, M. and HARANG, L. Surface temperature fronts in the Mediterranean sea from infrared satellite imagery. *In*: NIHOUL, J.C.J. *ed.* Hydrodynamics of Semi-Enclosed Seas. Amsterdam, Elsevier, 1982: pp. 91–128.

PISTEK, P. Deep circulation in the Alboran sea. SACLANTCEN CP-33. La Spezia, Italy, SACLANT ASW Research Centre, 1983: pp. 5–1 to 5–16. [AD C 952 418]

PISTEK, P. Deep water mass circulation in Alboran Basin: Measurements from January to April 1982, ALBORAN II experiment, SACLANTCEN SM-195. La Spezia, Italy, SACLANT ASW Research Centre, 1985.

PISTEK, P. Deep water mass circulation in the western Alboran basin: measurements in July and September 1980, SACLANTCEN SR-81. La Spezia, Italy, SACLANT ASW Research Centre, 1984. [AD A 148 566]

PISTEK, P., de STROBEL, F. and MONTANARI, C. Low-frequency recoverable acoustic swallow floats for measuring mid and deep water circulation. Atti del 6° Congresso dell' Associazione Italiana di Oceanologia e Limnologia. 1984. Livorno, Italy.

PISTEK, P., de STROBEL, F., MONTANARI, C. Deep Sea Circulation in the Alboran Sea. *Journal of Geophysical Research*, 90, 1984: 4969–4976.

PISTEK, P., de STROBEL, F., MONTANARI, C. The use of SACLANTCEN-engineered floats for oceanographic research, NATO UNCLASSIFIED. *In*: NATO SACLANT ASW Research Centre. Papers presented to the 37th Meeting of the SACLANTCEN Scientific Committee of National Representatives, 14–16 October 1980. SACLANTCEN CP-28. La Spezia, Italy, SACLANT ASW Research Centre, 1980: 8–1 to 8–5 [AD C 024 237]

PORTER, D.L. The anticyclonic gyre of the Alboran sea, independent research report from MIT-WHOI joint program. Woods Hole MA, Woods Hole Oceanographic Institution, 1976.

PRELLER, R. and HURLBURT, H. A reduced gravity numerical model of circulation in the Alboran Sea. it In: NIHOUL, J.C.J. *ed.* Hydrodynamics of Semi-Enclosed Seas. Amsterdam, Elsevier, 1982: pp. 75–90.

PRELLER, R.H. A Numerical Model Study of Circulation in the Alboran Sea. Doctoral Thesis, Florida State University, 1984.

SANKEY, T. The formation of deep water in the northwestern Mediterranean. *Progress in Oceanography*, 6, 1973: 159–179.

STOMMEL, H. Deep winter-time convection in the western Mediterranean Sea, *In*: GORDON, A.L., *ed.* Studies in Physical Oceanography, volume 2. New York, NY, Gordon and Breach, 1972: p. 232.

STOMMEL, H.M., 3RYDEN, H. and MALGELSDORF, P. Does the Mediterranean outflow come from great depth? *Pure and Applied Geophysics*, 105, 1973: 879–889.

TILLIER, P. Expendable mid-range SOFAR floats and shipborne receiver. *Polymode News*, 73, 1980: 7–8.

WANNAMAKER, B. A system for receiving and analysing meteorological satellite data at small meteorological/oceanographic centres or aboard a ship, SACLANTCEN SR–74. La Spezia, Italy, SACLANT ASW Research Centre, 1983.

WANNAMAKER, B. The Alboran sea gyre: ship, satellite, and historical data, SACLANTCEN SR–30. La Spezia, Italy, SACLANT ASW Research Centre, 1979. [AD A081 852]

WHITEHEAD, J.A. Jr. and MILLER, A.R. Laboratory simulation of the gyre in the Alboran Sea. *Journal of Geophysical Research*, **84**, 1979: 3733–3742.

WUST, G. On the vertical circulation of the Mediterranean sea. *Journal of Geophysical Research*, **66**, 1961: 3261–3271.

ZIEGENBEIN, J. Spatial observations of internal waves in the Strait of Gibraltar, SACLANTCEN TR–147. La Spezia, Italy, SACLANT ASW Research Centre, 1969. [AD 856 028]

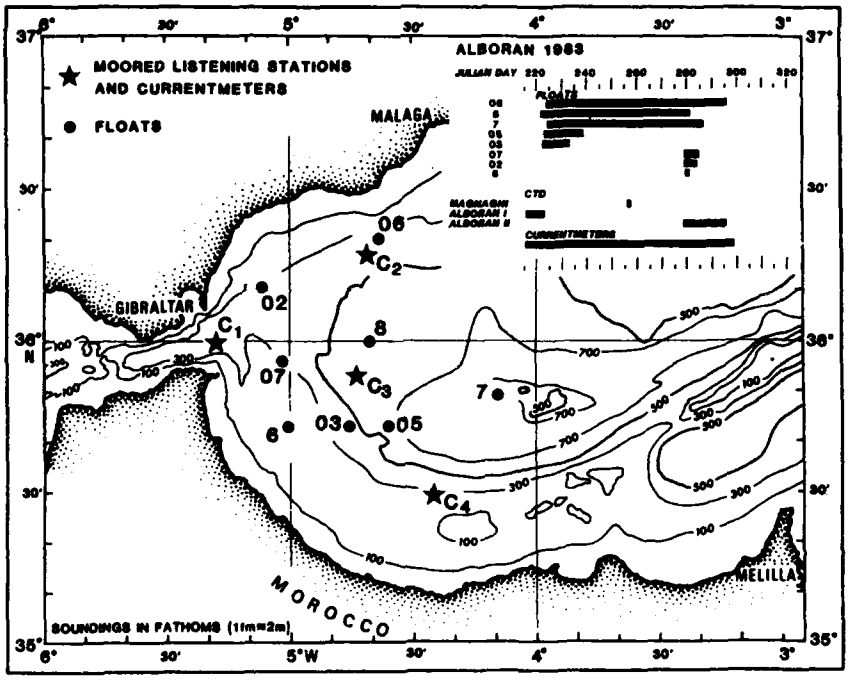

Fig. 1. Positions and deployment period for floats and current meters. 1, 2, 3, 4 mark the sites of moorings' deployment. Two current meters and one listening station were deployed on each mooring. Dots marked with numbers signify the deployment positions of individual floats. Schematic diagram of the deployment period for floats, CTDs and current meters in the righthand corner.

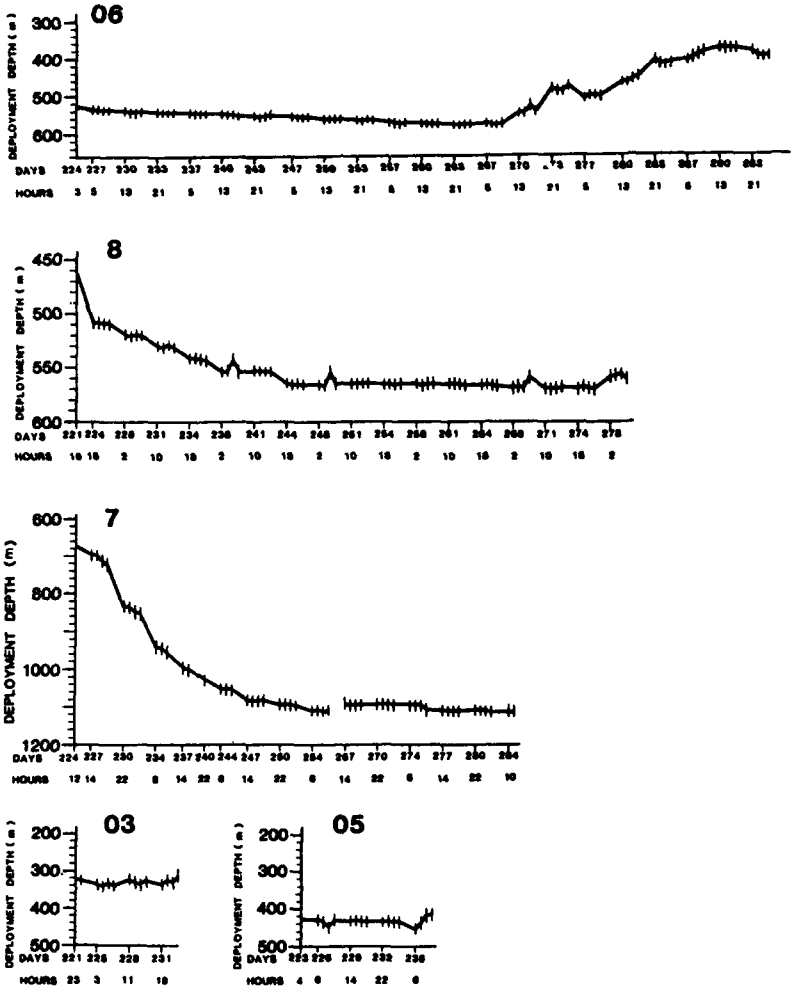

Fig. 2. Time series of float depths. Starting time is 8 h after deployment. These are the averaged data from all four listening stations. 4 short lines represent four listenings separated by 2 h each after every 80 h. Days are Julian days of deployment. Floats 06, 03, 05 are expendable type; floats 08, 07 are recoverable type.

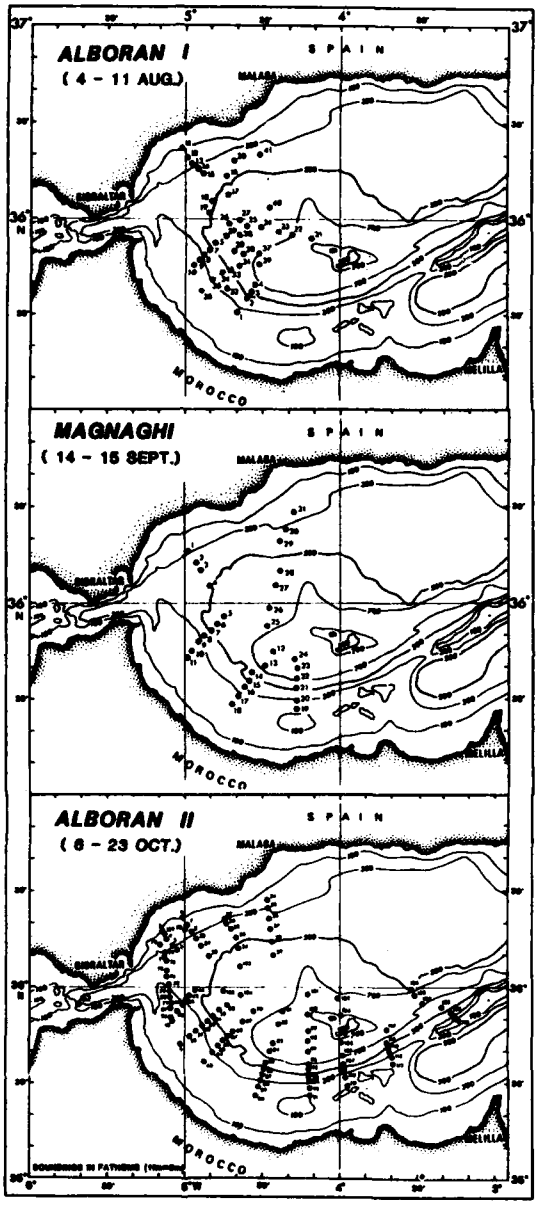

Fig. 3. Positions of CTD casts: Alboran I – CTD casts during August 1983 (days 216 to 223); Alboran II – CTD casts during September 1983 (days 257 to 258); Alboran III – CTD casts during October 1983 (days 279 to 295).

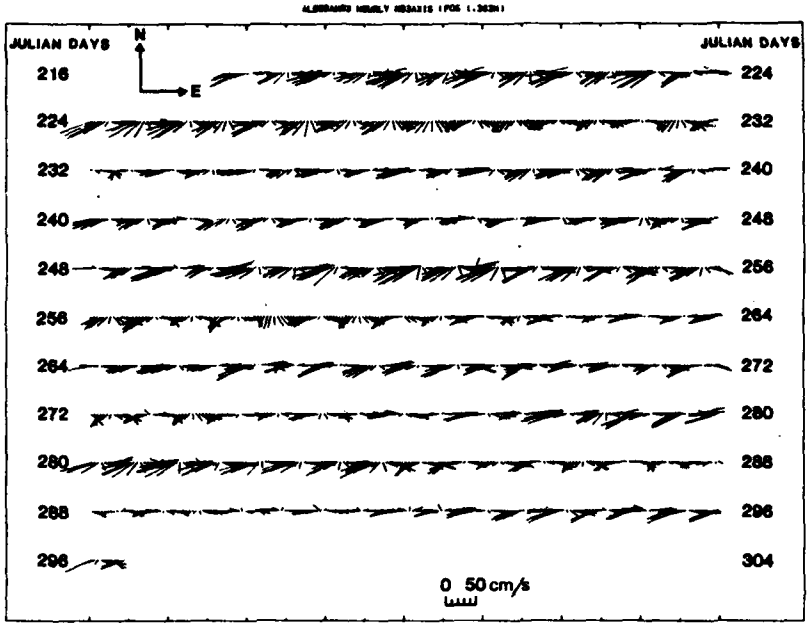

Fig. 4. Velocity vector time series of hourly N. Brown 3-axis acoustic current-meter data. Position 1, depth 328 m, August–October 1983.

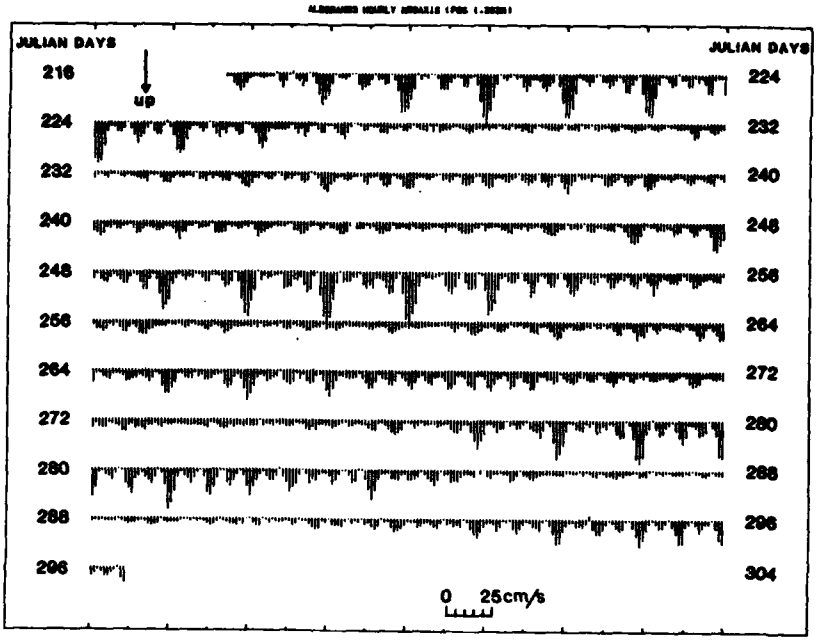

Fig. 5. Time series of vertical velocity component of hourly N. Brown 3-axis acoustic current-meter data. Position 1, depth 328 m, August–October 1983. Rather large velocity is probably the result of mooring motion.

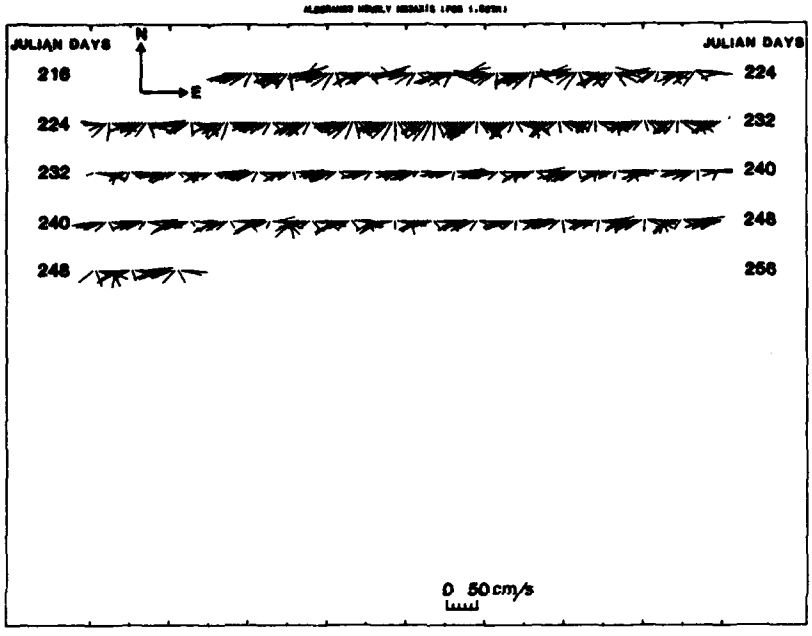

Fig. 6. Velocity vector time series of hourly N. Brown 3-axis acoustic current-meter data. Position 1, depth 712 m, August–October 1983. Current meter malfunctioned after 31 days (water penetrated into sensors), vertical component did not work.

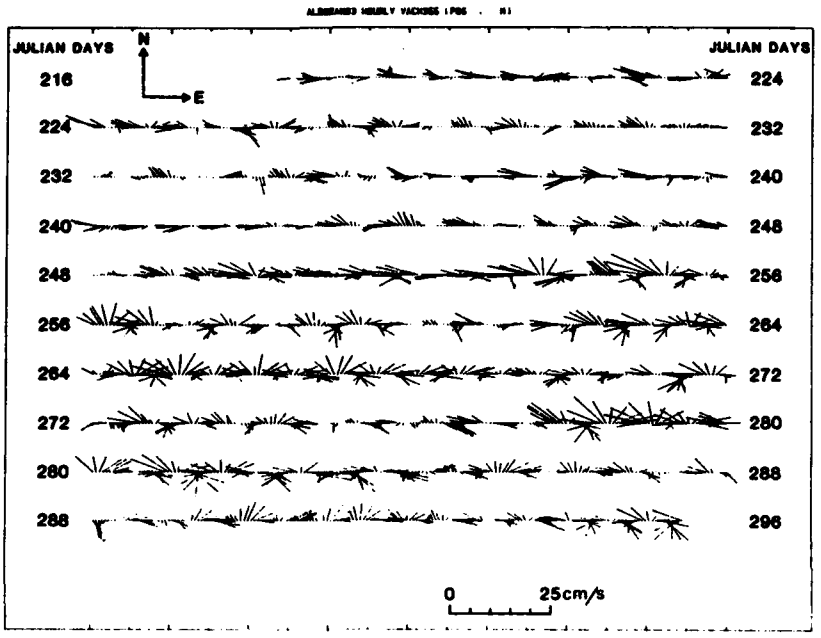

Fig. 7. **Velocity vector time series of hourly VACM current-meter data. Position 2, depth 346 m, August–October 1983.**

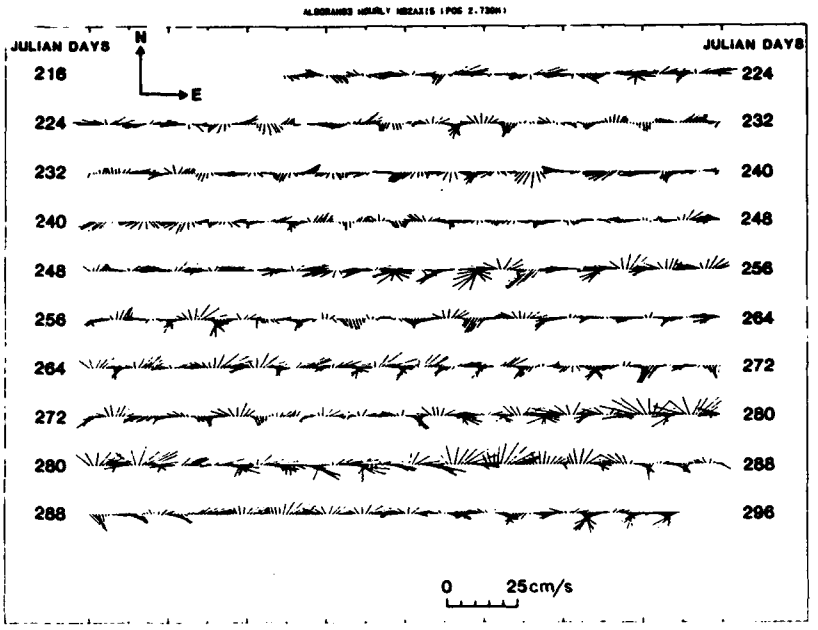

Fig. 8. **Velocity vector time series of hourly N. Brown 2-axis acoustic current-meter data. Position 2, depth 731 m, August–October 1983.**

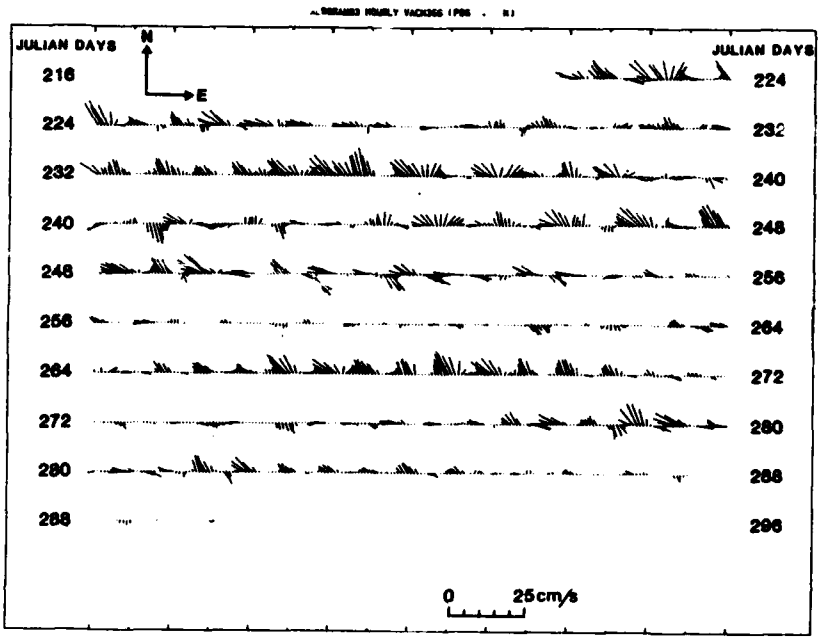

Fig. 9. Velocity vector time series of hourly VACM current-meter data. Position 3, depth 294 m, August–October 1983.

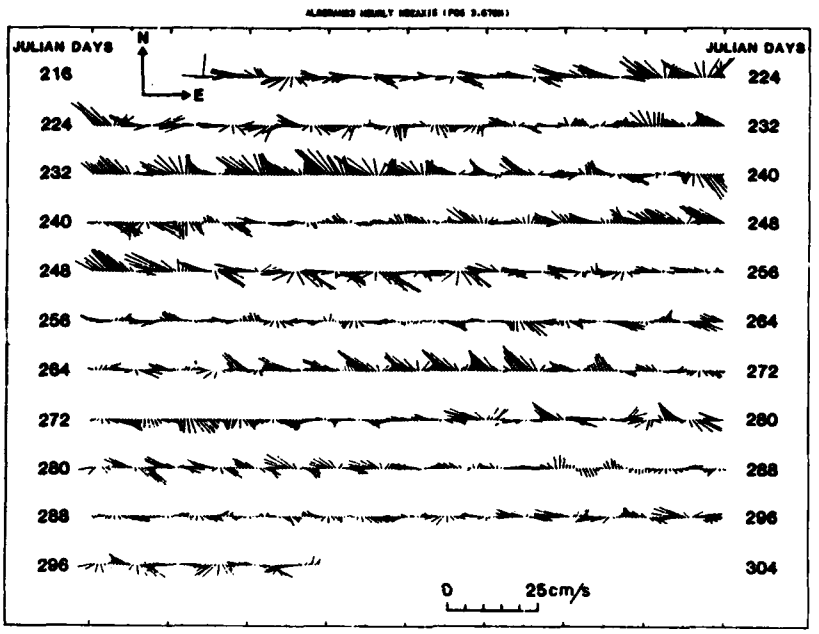

Fig. 10. **Velocity vector time series of hourly N. Brown 2-axis acoustic current-meter data. Position 3, depth 678 m, August–October 1983.**

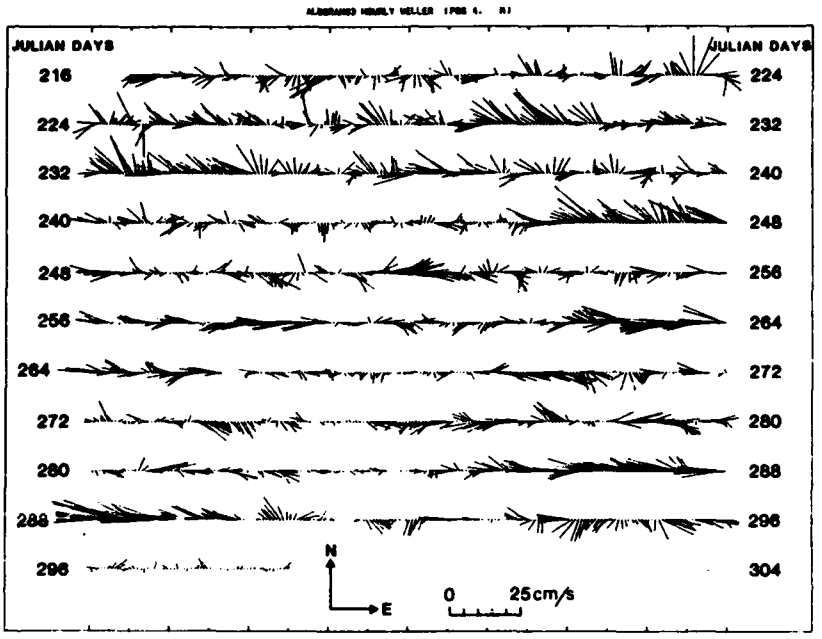

Fig. 11. **Velocity vector time series of hourly Weller (VMCM) current-meter data. Position 4, depth 298 m, August–October 1983.**

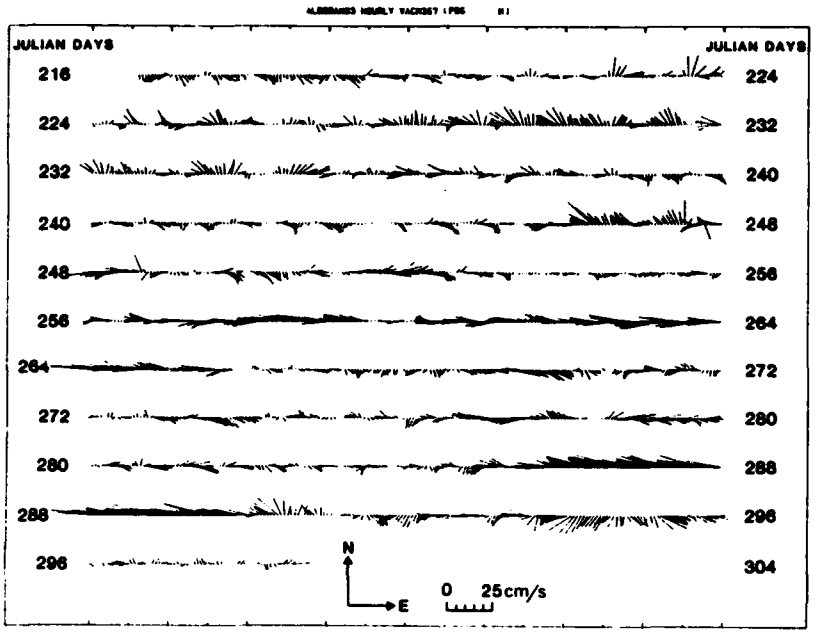

Fig. 12. **Velocity vector time series of hourly VACM current-meter data. Position 4, depth 403 m, August–October 1983.**

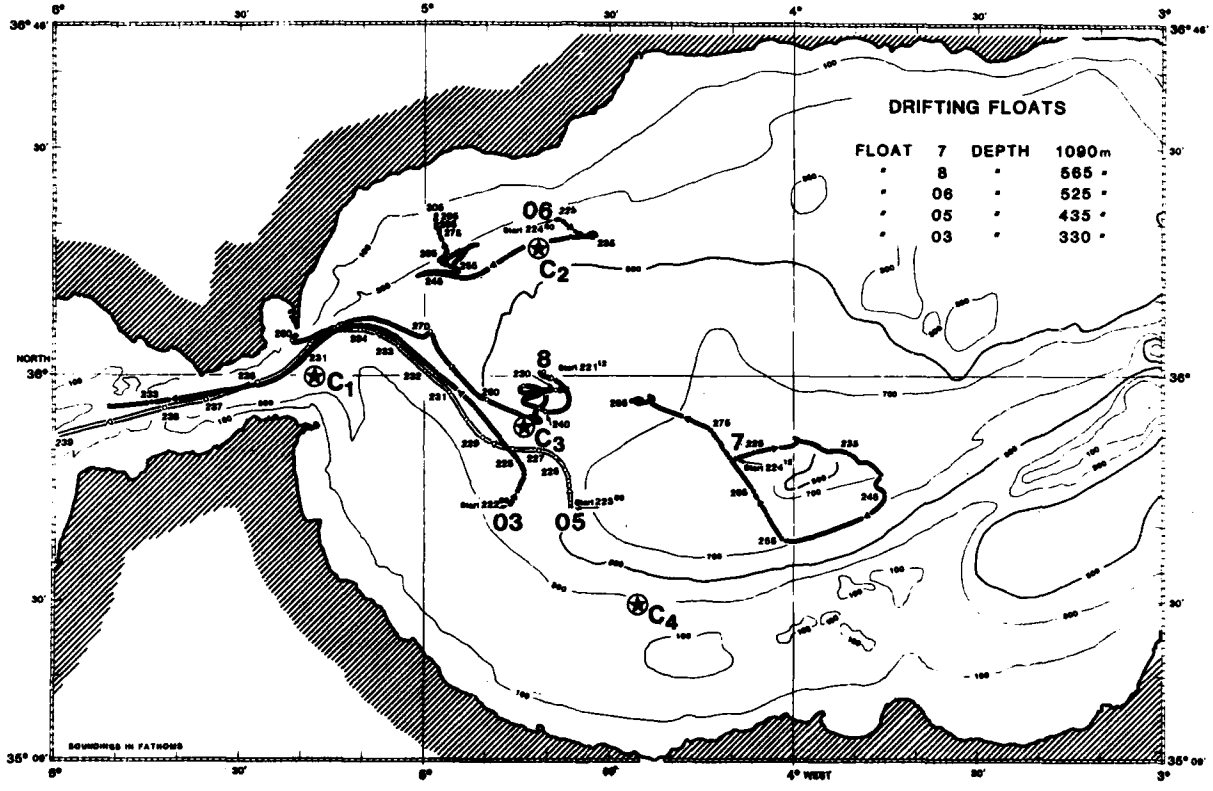

Fig. 13. Tracks of deep floats. 'Start' indicates the starting point and numbers near the tracks are Julian days. C1, C2, C3, C4 are the positions of autonomous listening stations. Floats 07 and 08 were retrieved after the experiment was finished. Tracks are created from data filtered by Grove's filter, without tides.

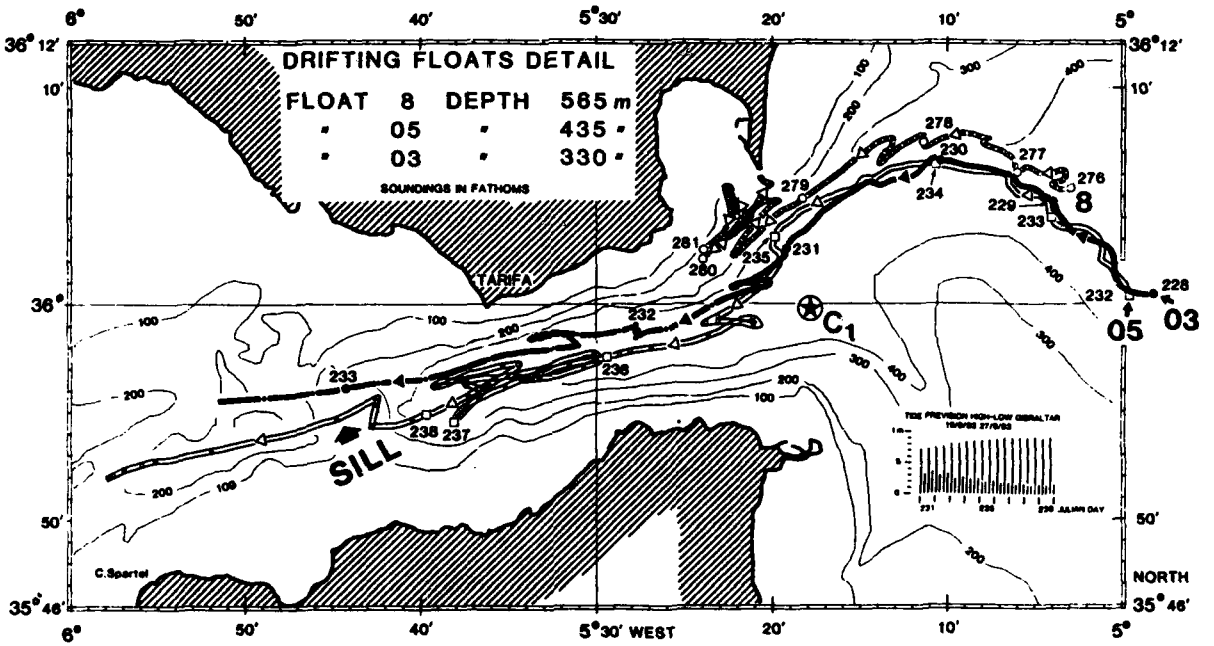

Fig. 14. Detail of the floats' tracks in the Strait of Gibraltar. Numbers near the tracks are Julian days and points in between indicate the location every 2 h. Tracks are created from 2-hour data. Tidal variation is very pronounced.

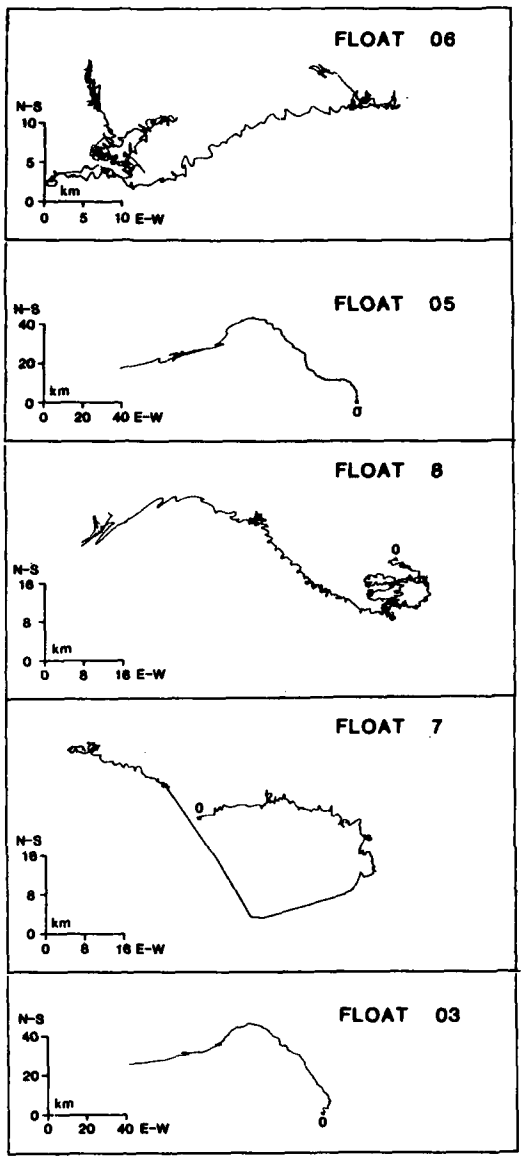

Fig. 15. Tracks of floats created from original 2-hour data. 0 indicates the starting point; E and N indicate the eastward and the northward direction.

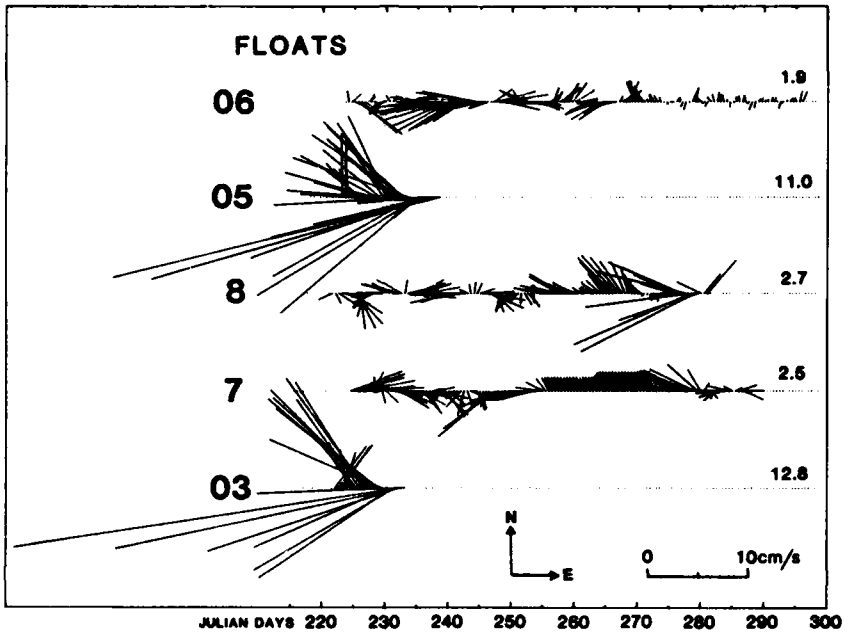

Fig. 16. Time series of the 12-hourly velocity vectors for all floats. Number signifies the float, number on the right signifies the average velocity amplitude in cm/s.

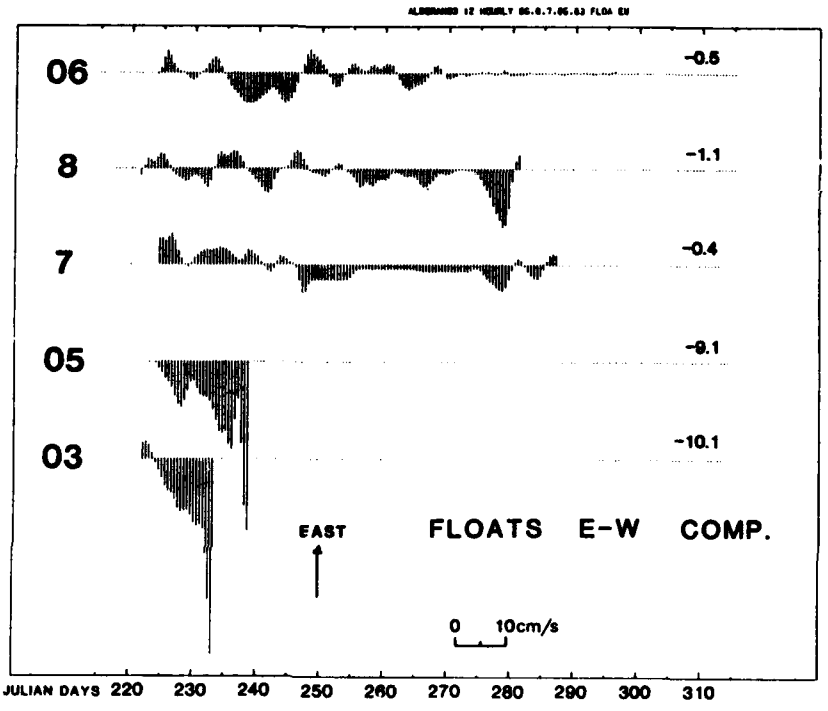

Fig. 17. Time series of the 12-hourly east-west velocity components for all floats. Number signifies the float, number on the right signifies the average value of the east-west velocity component in cm/s.

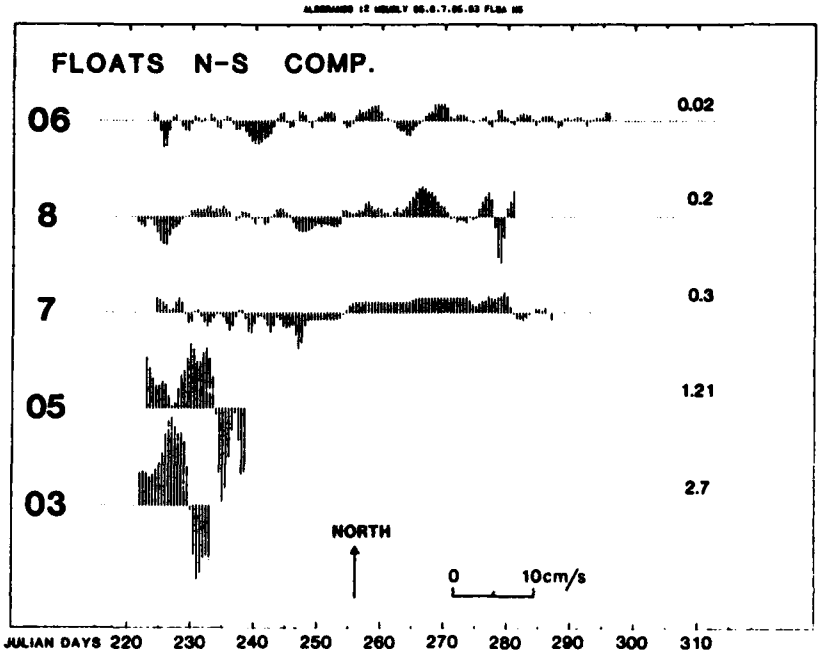

Fig. 18. Time series of the 12-hourly north-south velocity components for all floats. Number signifies the float, number on the right signifies the average value of the north-south velocity component in cm/s.

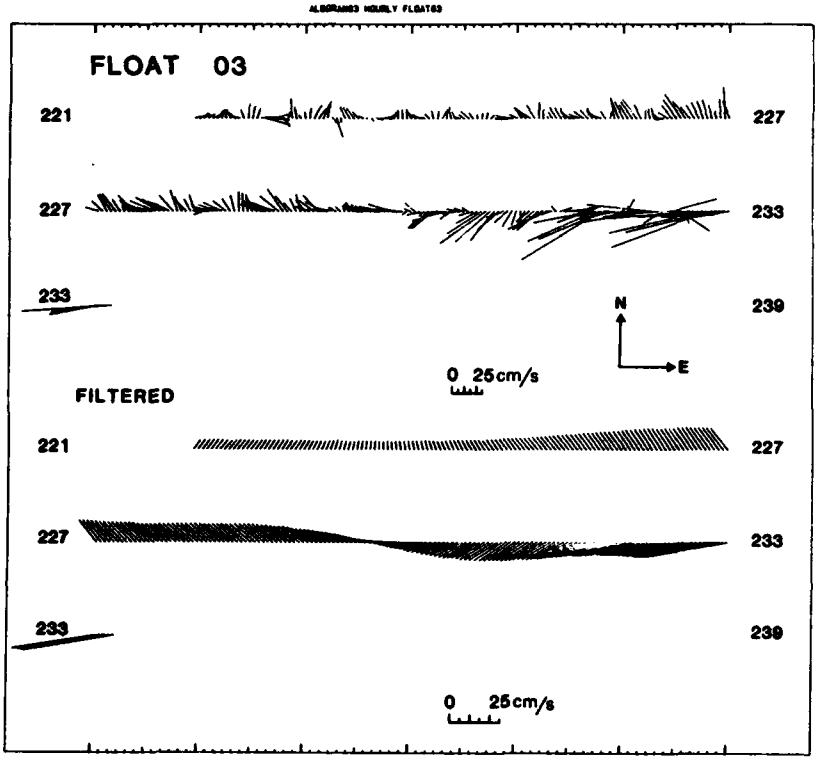

Fig. 19. **Time series of hourly velocity vectors of the original and Groves-filtered data for float 03. Numbers on the right and left signify the time of the beginning and the end of time series in Julian days. Original data show considerable tidal variation which is absent in the filtered time series.**

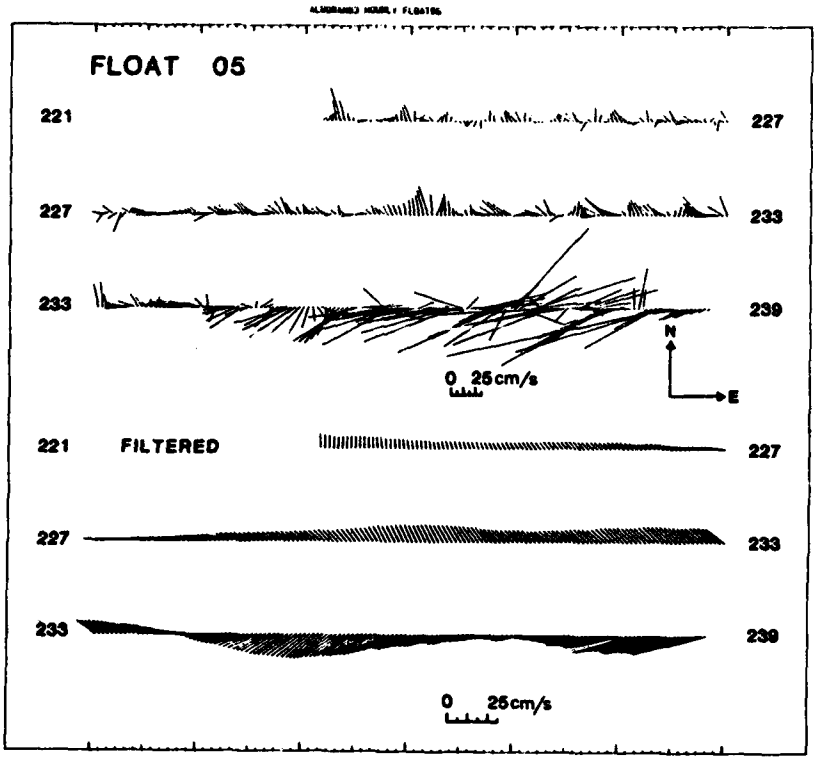

Fig. 20. **Time series of hourly velocity vectors of the original and Groves-filtered data for float 05. Numbers on the right and left signify the time of the beginning and the end of time series in Julian days. Original data show considerable tidal variation while it is removed in the filtered time series.**

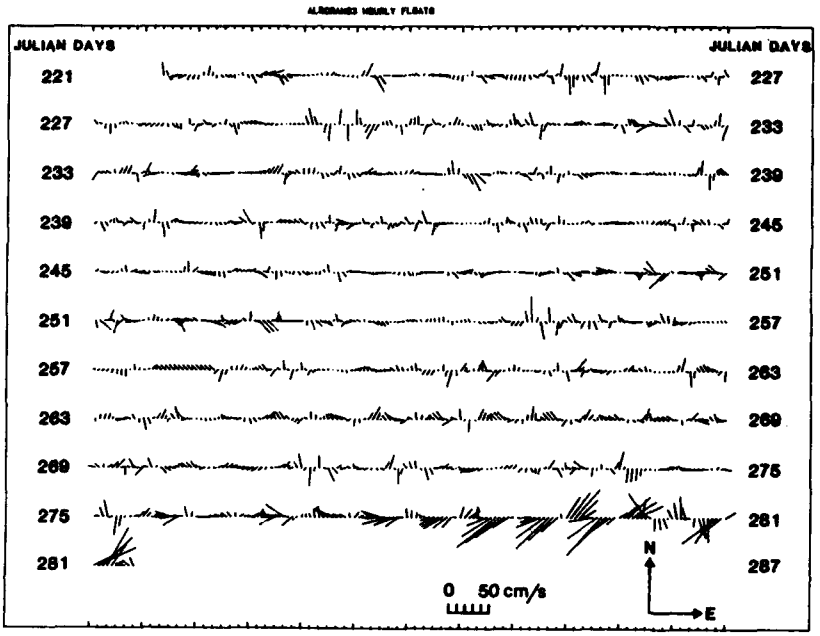

Fig. 21. **Time series of hourly velocity vectors of the original data for float 08. Numbers on the right and left signify the time of the beginning and the end of time series in Julian days.**

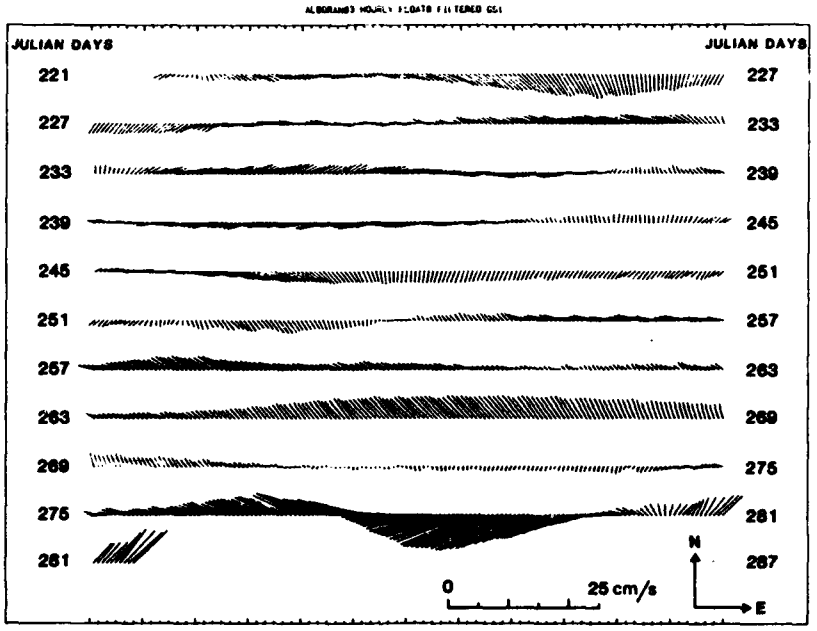

Fig. 22. **Time series of hourly velocity vectors of the Groves-filtered data for float 08. Numbers on the right and left signify the time of the beginning and the end of time series in Julian days.**

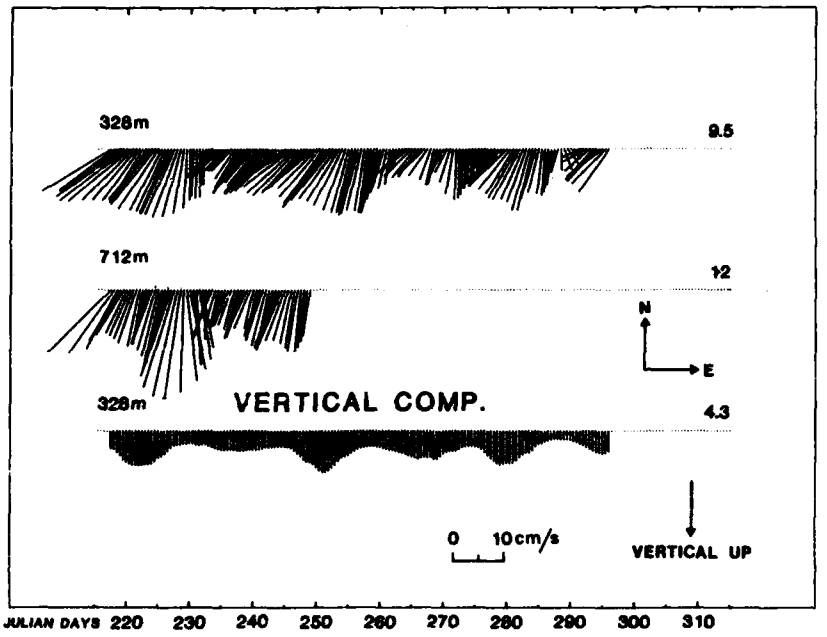

Fig. 23. **Time series of current velocity vectors at mooring 1. Numbers on the left signify the depth of the deployment of current meters; vertical velocity component was measured by the shallower current meter. Current meter at 712 m malfunctioned after 31 days. Numbers on the right signify the average velocity amplitude in cm/s. Data are Groves-filtered and decimated to 12 h.**

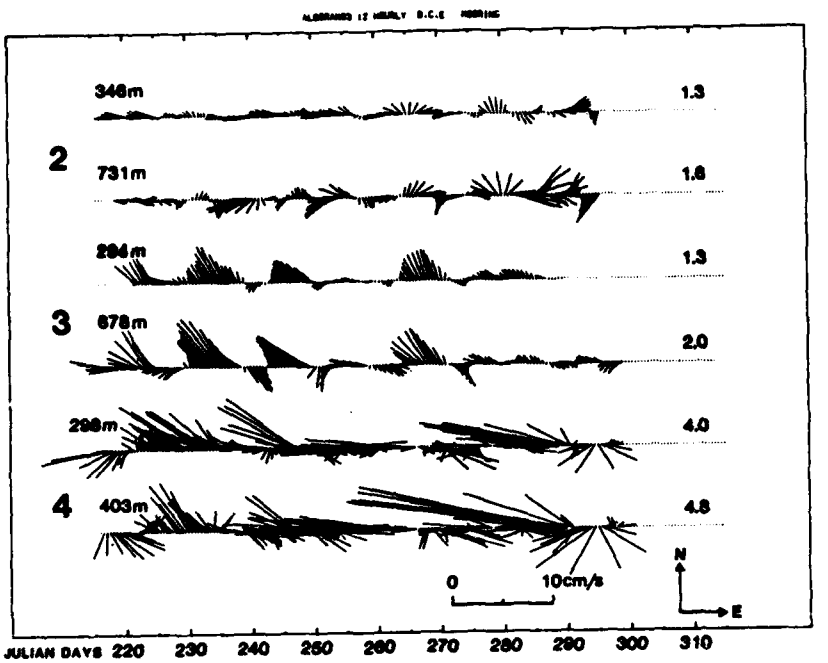

Fig. 24. Time series of current velocity vectors at moorings 2, 3 and 4. Two time series for each mooring display the data of the shallow and deep current meter. Deployment depth for each current meter is on the left of time series. Numbers on the right signify the average velocity amplitude in cm/s. Data are Groves-filtered and decimated to 12 h.

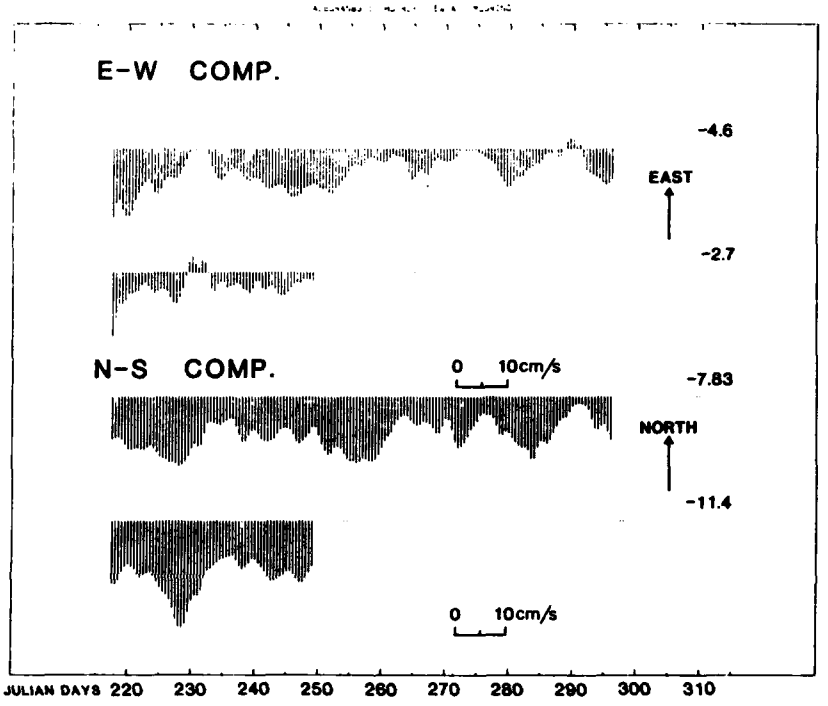

Fig. 25. Time series of current velocity components at mooring 1. Two time series for each component represent the data of the shallow and deep current meter respectively. Numbers on the right signify the average value of the velocity components in cm/s. Data are Groves-filtered and decimated to 12 h.

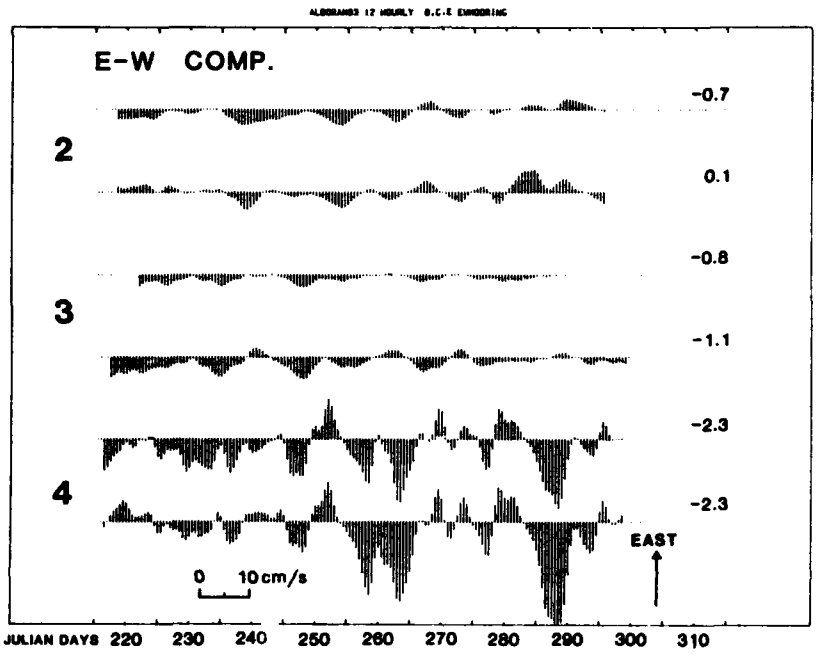

Fig. 26. **Time series of the east-west current velocity components at moorings 2, 3 and 4. Two time series for each mooring display the data for the shallow and the deep current meter respectively. Numbers on the right signify the average value of the velocity component. Data are Groves-filtered and decimated to 12 h.**

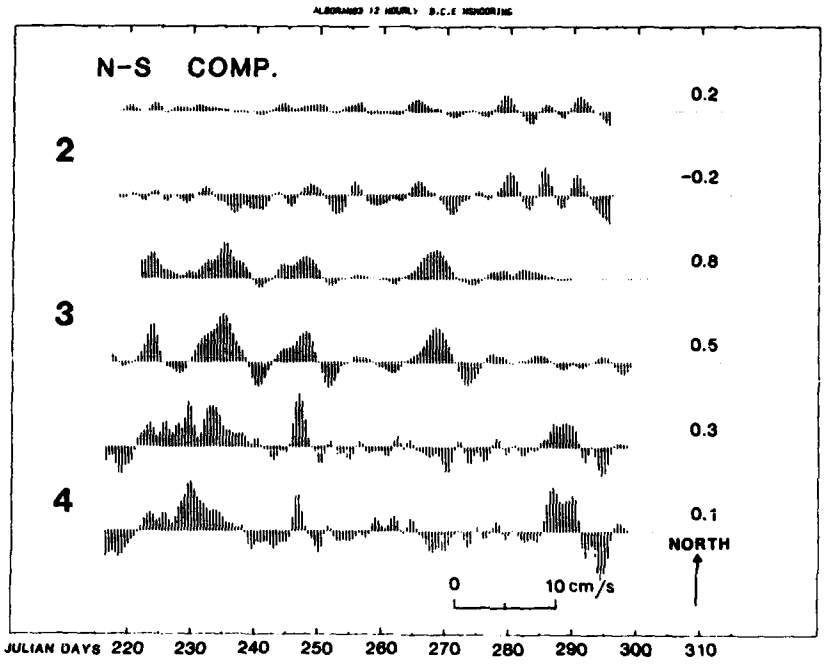

Fig. 27. Time series of the north-south current velocity components at moorings 2, 3 and 4. Two time series for each mooring display the data for the shallow and the deep current meter respectively. Numbers on the right signify the average value of the velocity component. Data are Groves-filtered and decimated to 12 h.

HOURLY VALUES

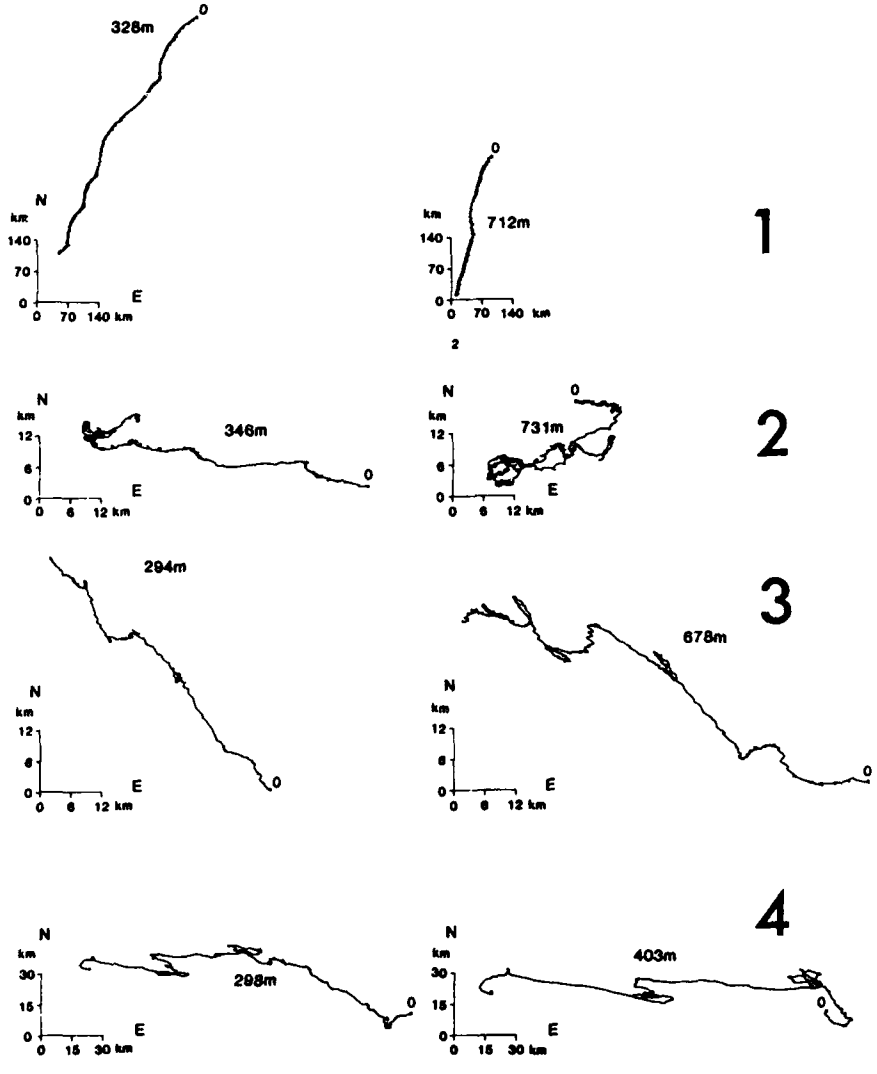

Fig. 28. Progressive vector diagrams for all current meters created from hourly value data. Moorings are marked by numbers 1 to 4. The depth identifies the current meter on each mooring. 0 identifies the starting point.

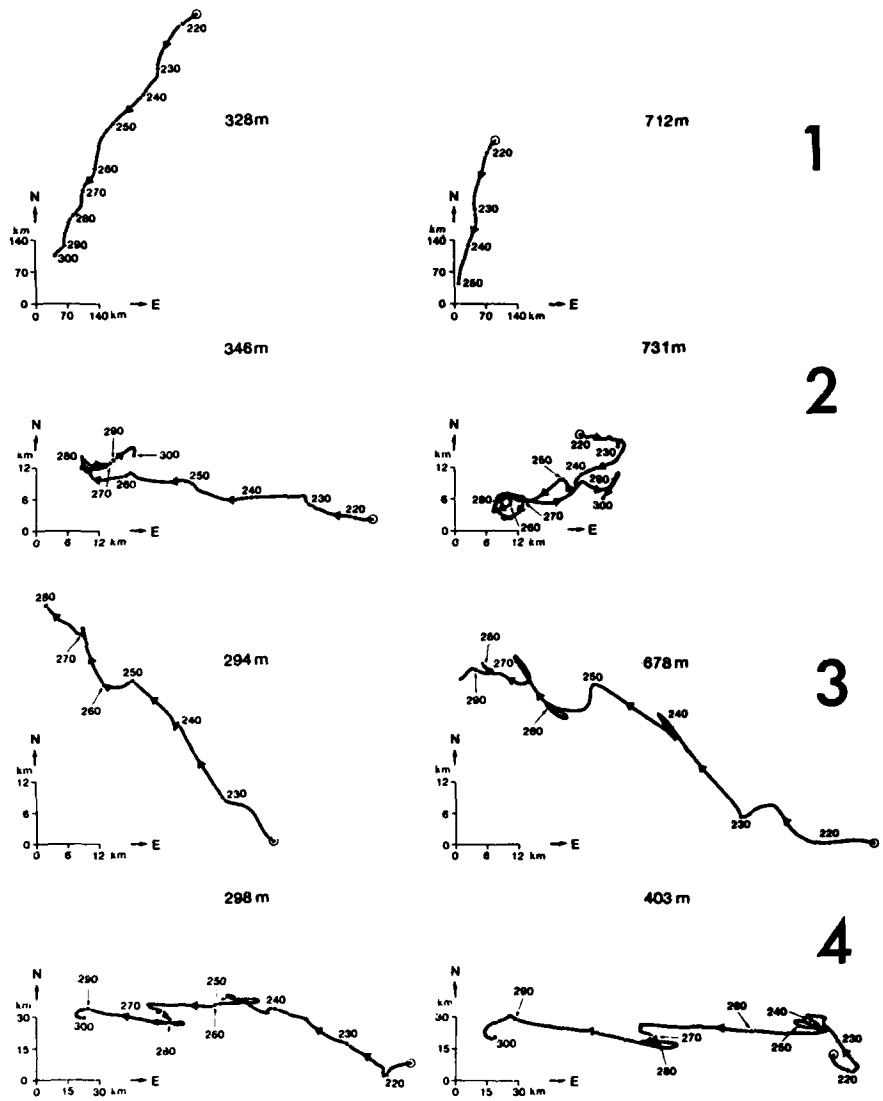

Fig. 29. Progressive vector diagrams for all current meters created from Groves-filtered data decimated to 12 h. Moorings are marked by numbers 1 to 4. The depth identifies the current meter on each mooring. Numbers near diagrams are Julian days.

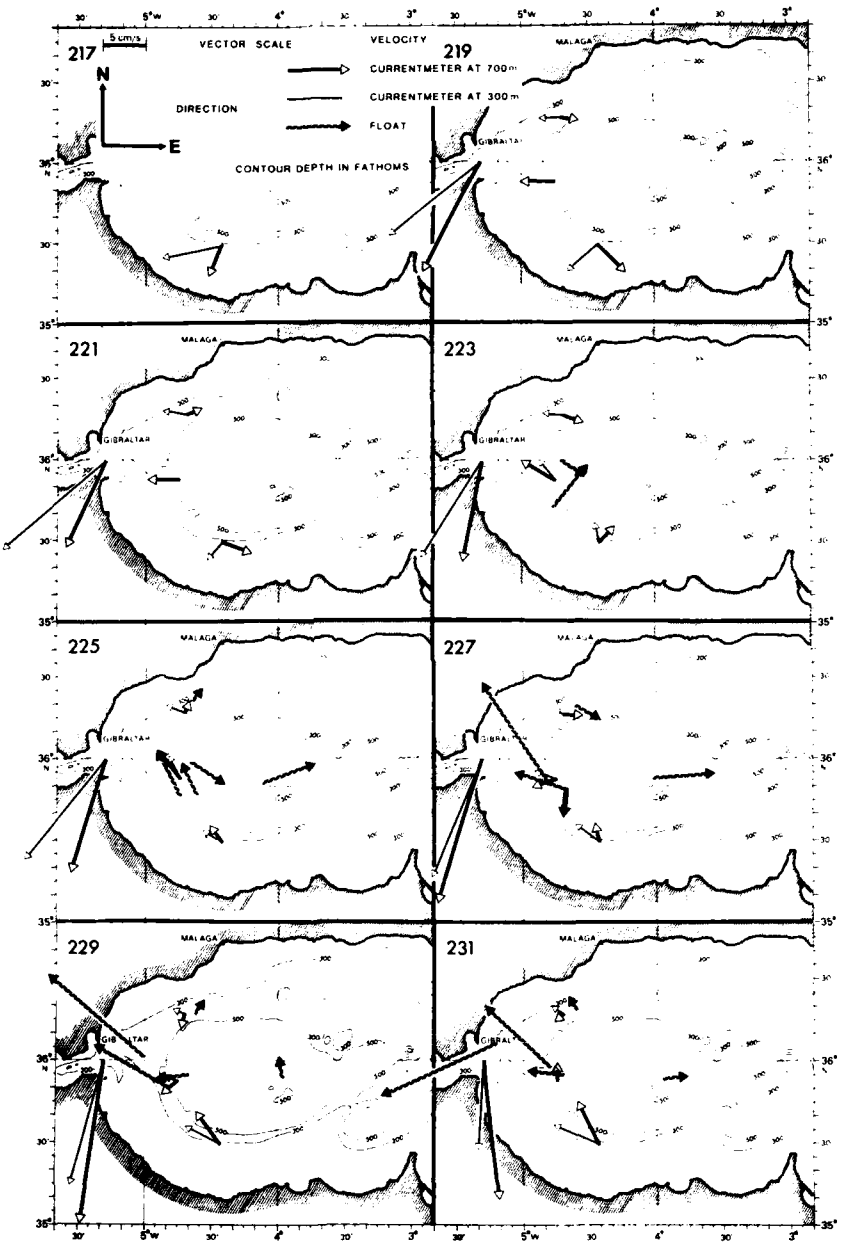

Fig. 30. **Two-day current vector field created from the float and current-meter data. Numbers signify Julian days.**

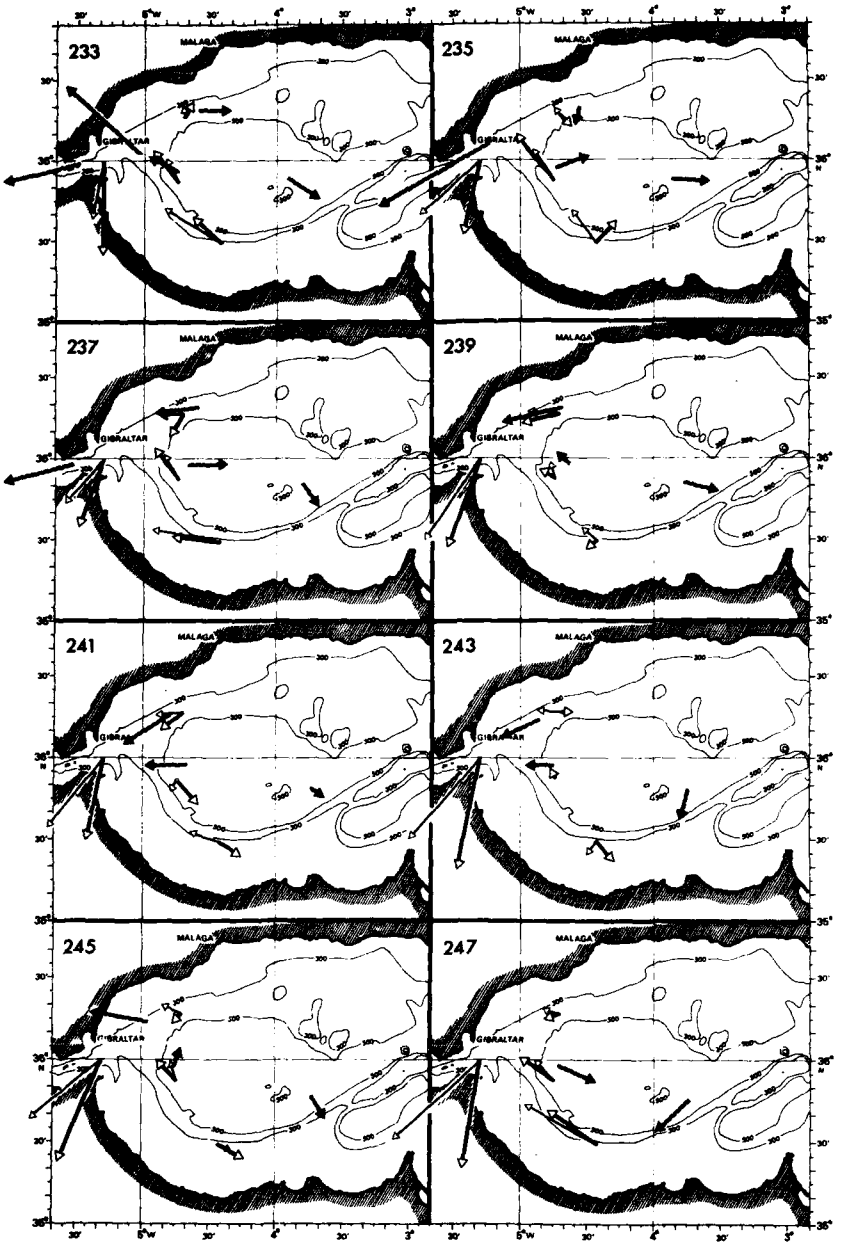

Fig. 30. (cont'd.)

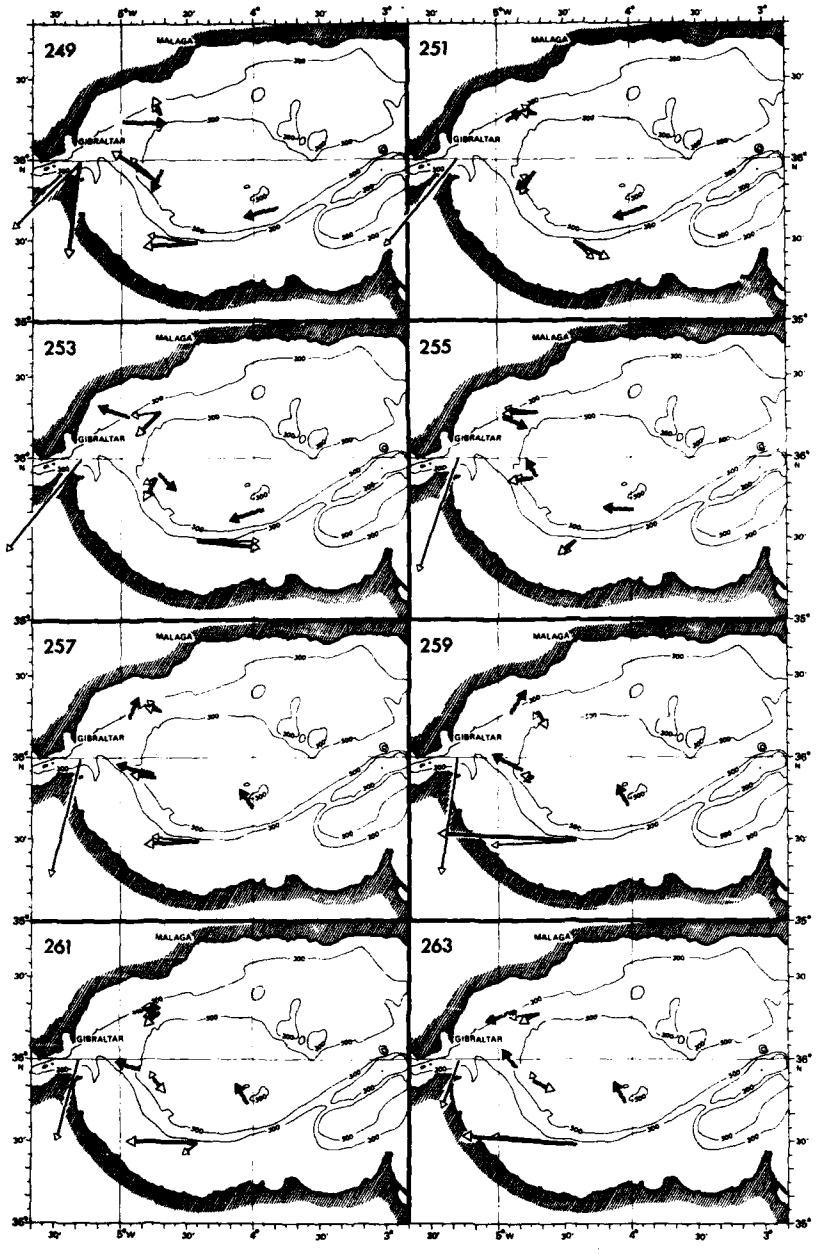

Fig. 30. (cont'd.)

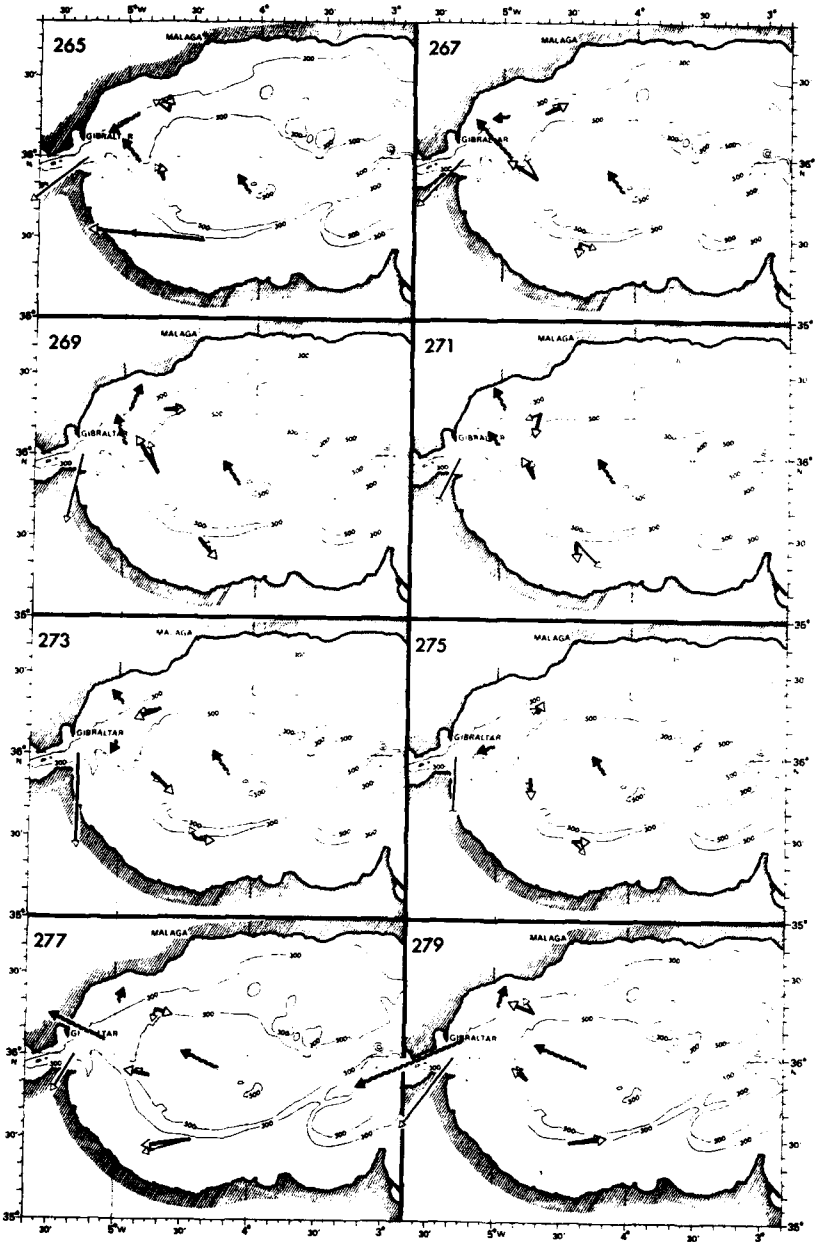

Fig. 30. (cont'd.)

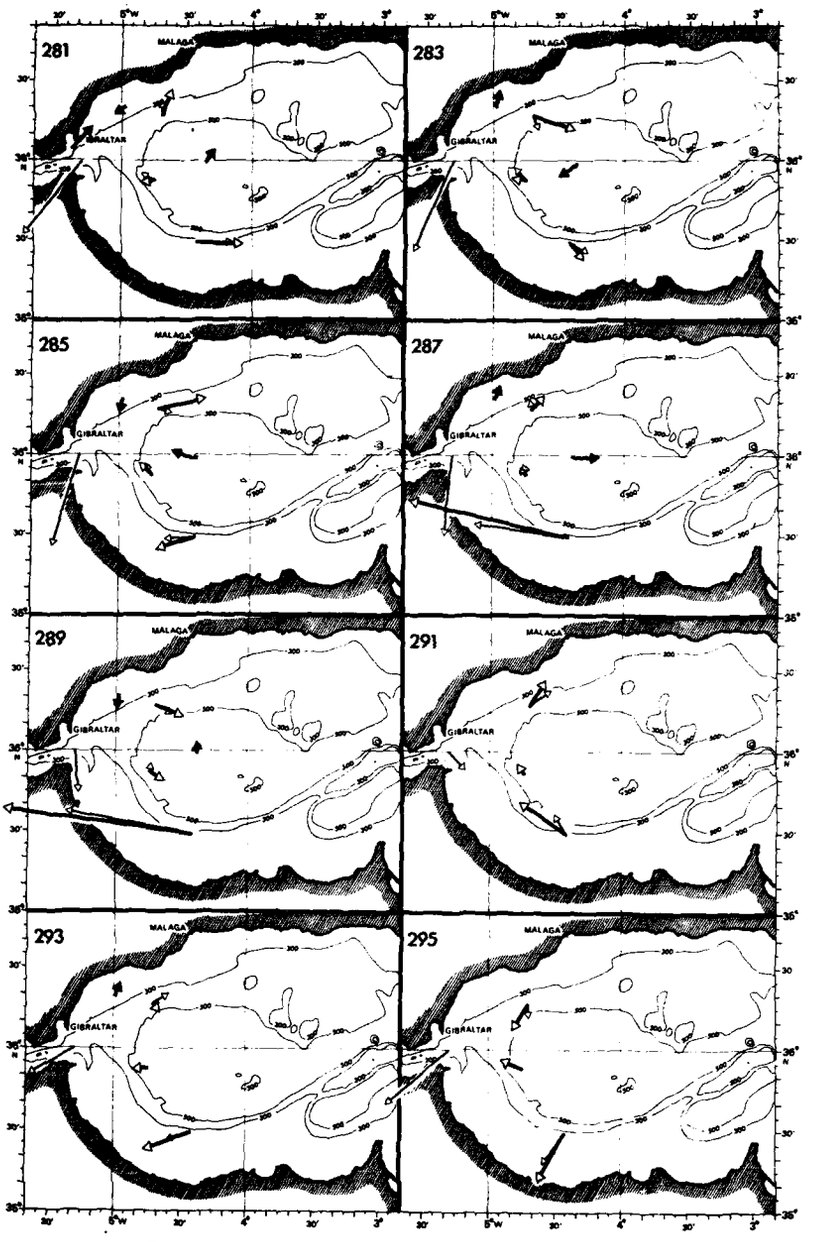

Fig. 30. (cont'd.)

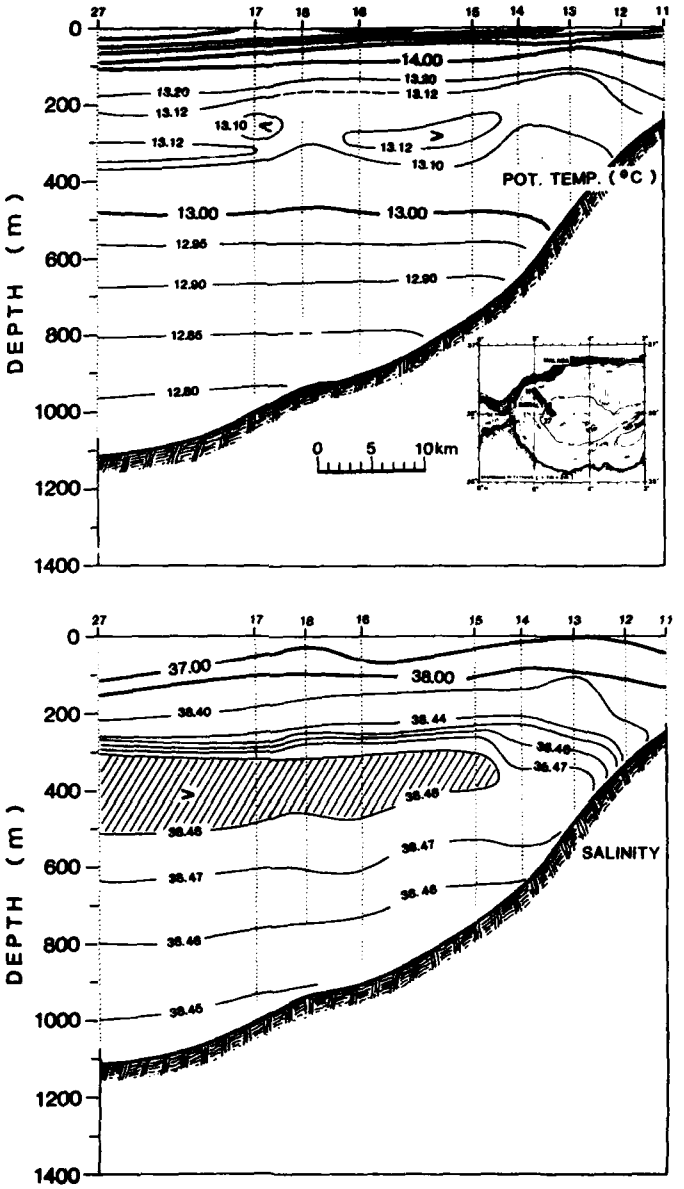

Fig. 31. Cross-sections of potential temperature and salinity. CTD, cruise: Alboran I, August 1983.

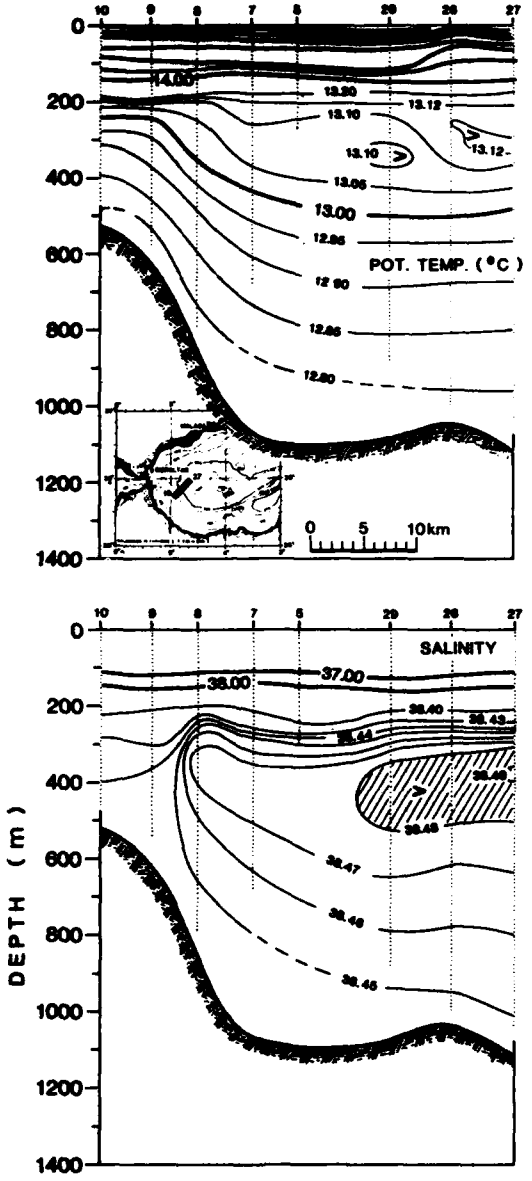

Fig. 31. (cont'd.)

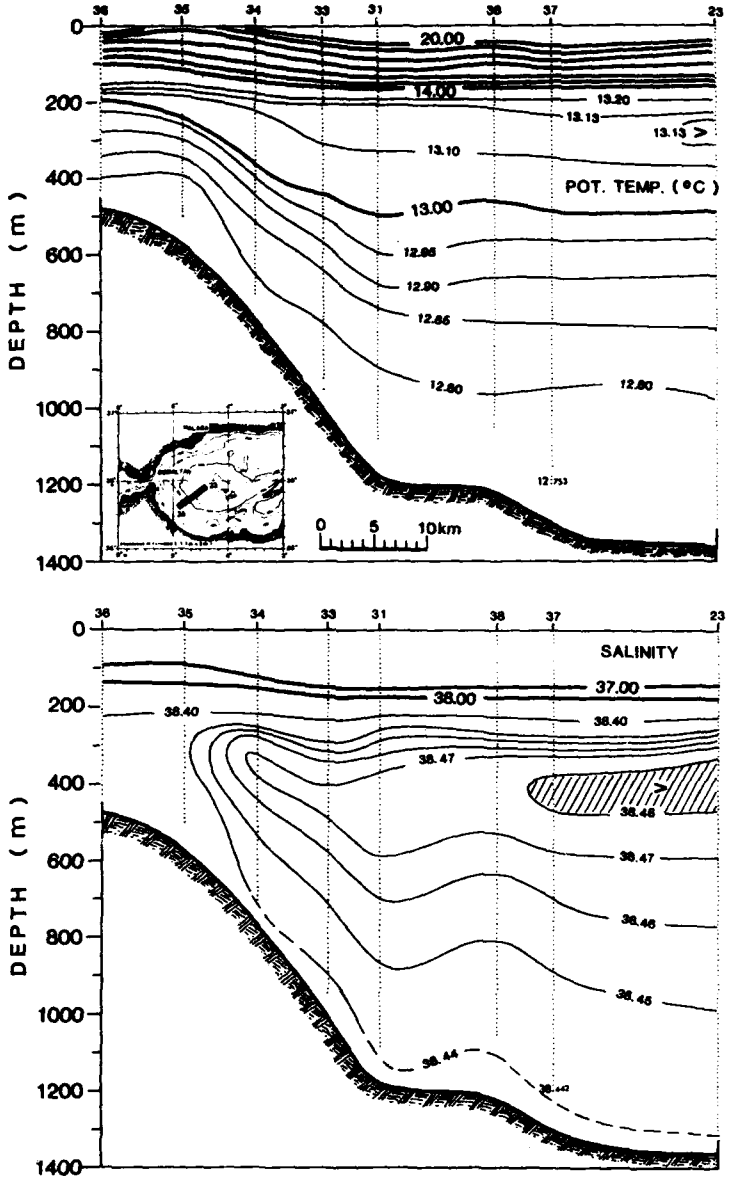
POT. TEMP. (°C)
20.00
14.00
13.20
13.13
13.10
13.00
12.95
12.90
12.85
12.80
DEPTH (m)
0
200
400
600
800
1000
1200
1400
0 5 10km
SALINITY
37.00
36.00
36.40
36.47
36.48
36.46
36.45
36.44

Fig. 31. (cont'd.)

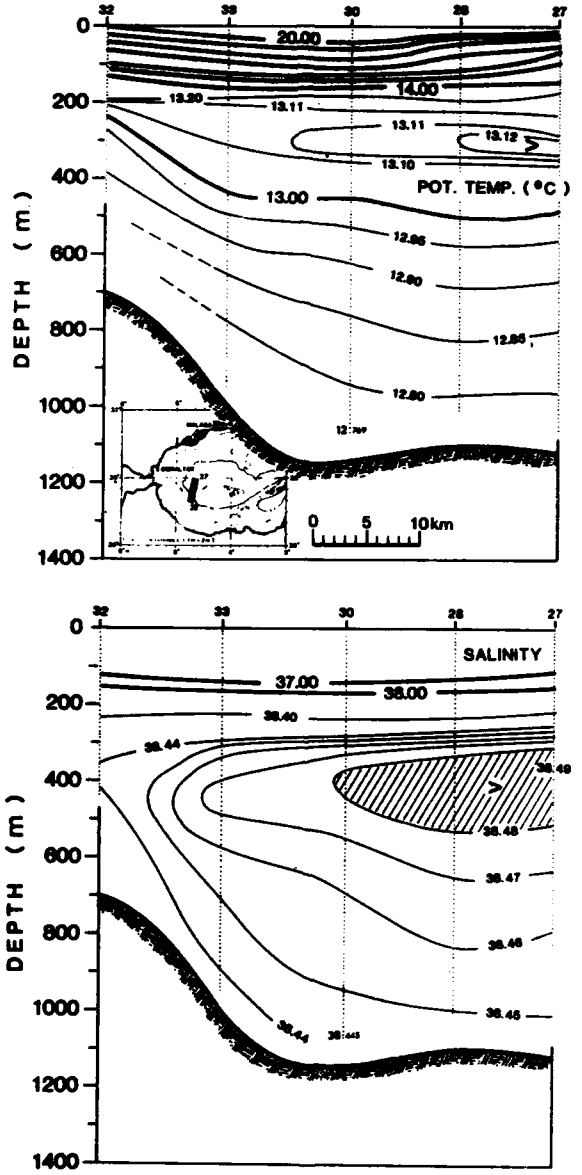
32
33
30
28
27
0
200
400
600
800
1000
1200
1400
DEPTH (m)
20.00
14.00
13.30
13.11
13.11
13.12
13.10
POT. TEMP. (°C)
13.00
12.95
12.90
12.85
12.80
0 5 10km
SALINITY
37.00
38.00
38.40
38.44
38.48
38.47
38.46
38.45

Fig. 31. (cont'd.)

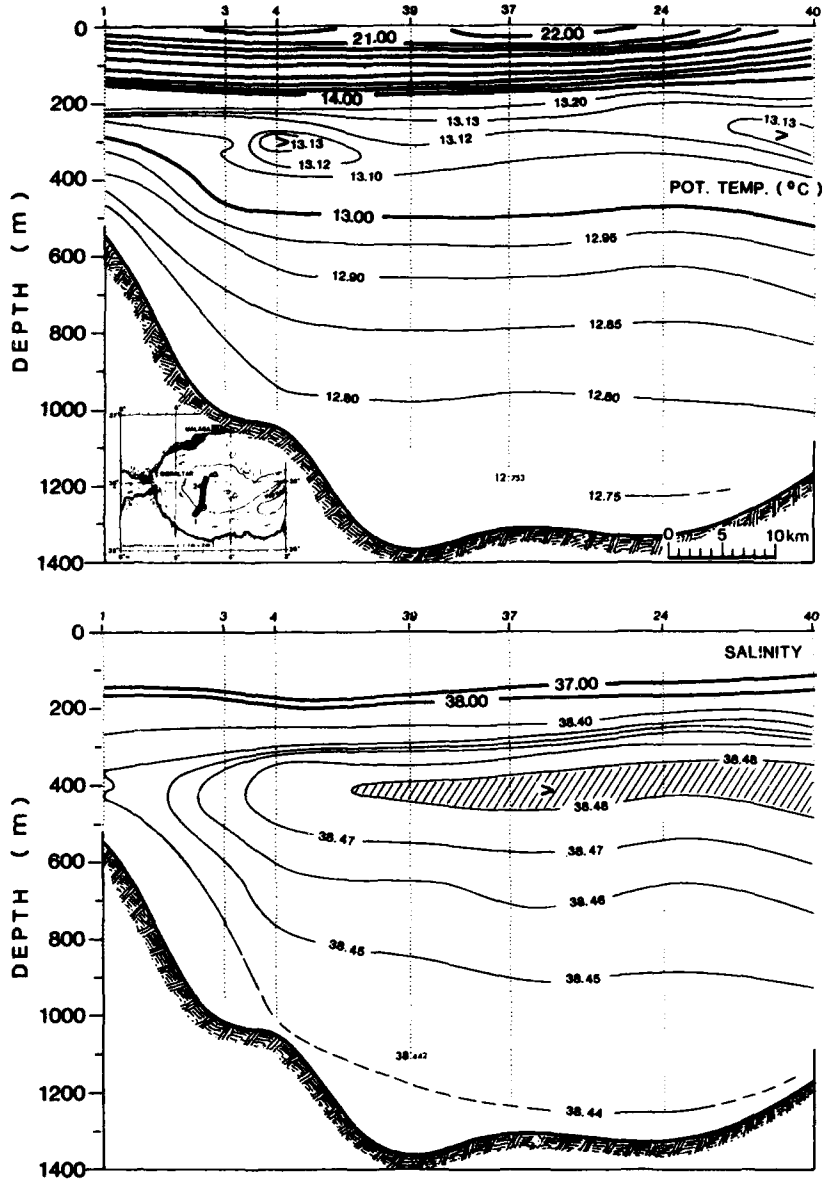
1
3
4
39
37
24
40
0
200
400
600
800
1000
1200
1400
DEPTH (m)
21.00
22.00
14.00
13.20
13.13
13.12
13.10
POT. TEMP. (°C)
13.00
12.95
12.90
12.85
12.80
12.75
0
5
10km
SALINITY
37.00
38.00
38.40
38.48
38.47
38.46
38.45
38.44

Fig. 31. (cont'd.)

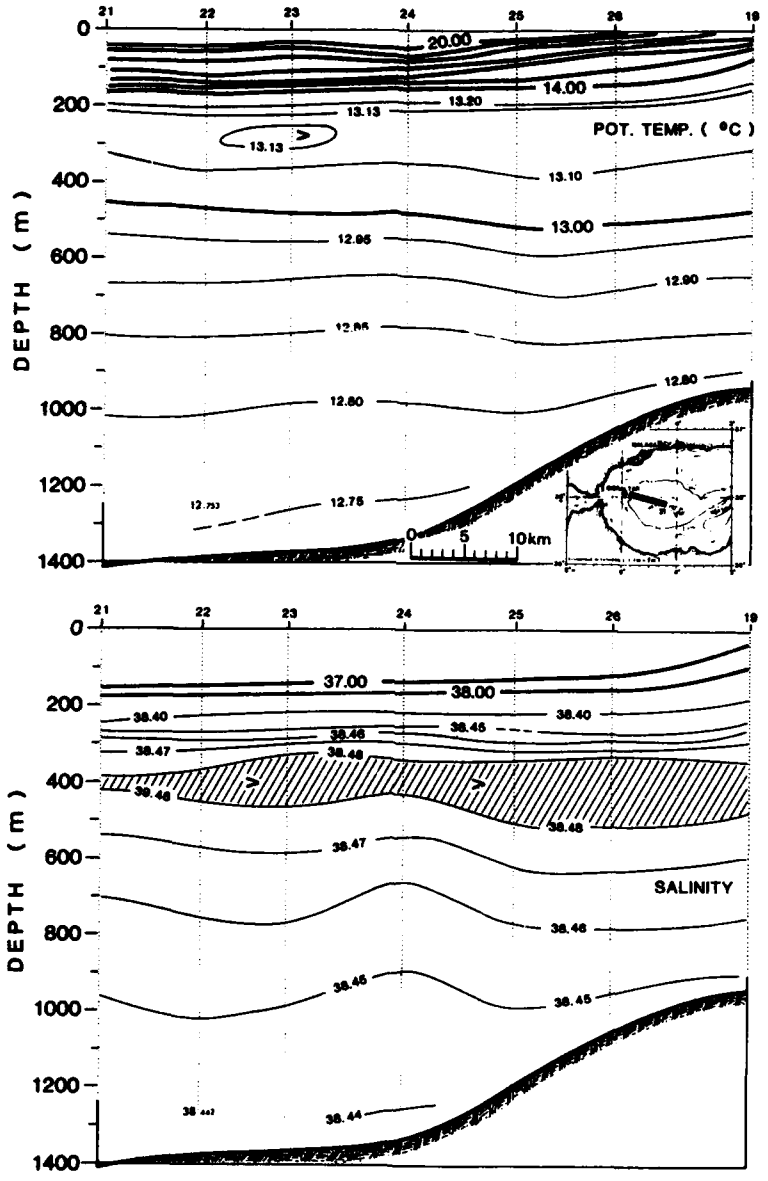
21
22
23
24
25
26
19
0
200
400
600
800
1000
1200
1400
DEPTH (m)
20.00
14.00
13.13
13.20
13.13
POT. TEMP. (°C)
13.10
13.00
12.95
12.90
12.85
12.80
12.80
12.753
12.75
0
5
10km
37.00
38.00
38.40
38.40
38.45
38.47
38.46
38.46
38.46
38.46
38.47
SALINITY
38.46
38.45
38.45
38.44

Fig. 31. (cont'd.)

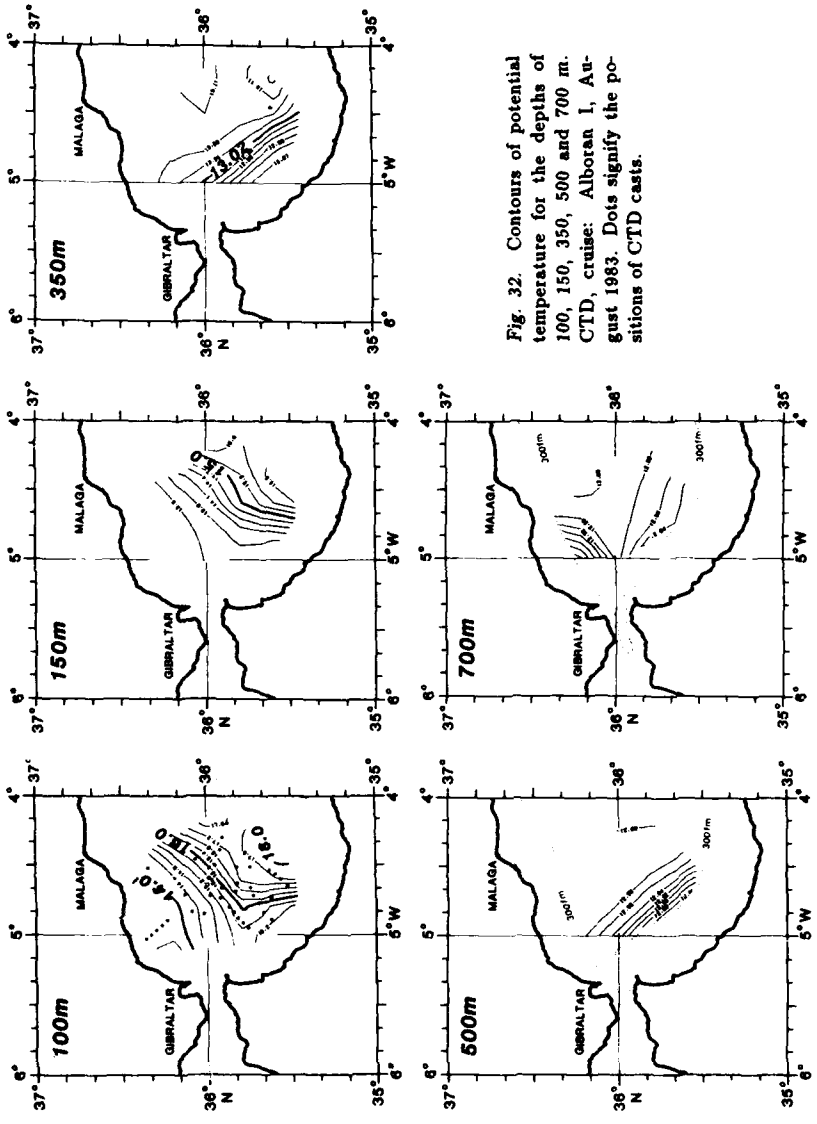

Fig. 32. Contours of potential temperature for the depths of 100, 150, 350, 500 and 700 m. CTD, cruise: Alboran 1, August 1983. Dots signify the positions of CTD casts.

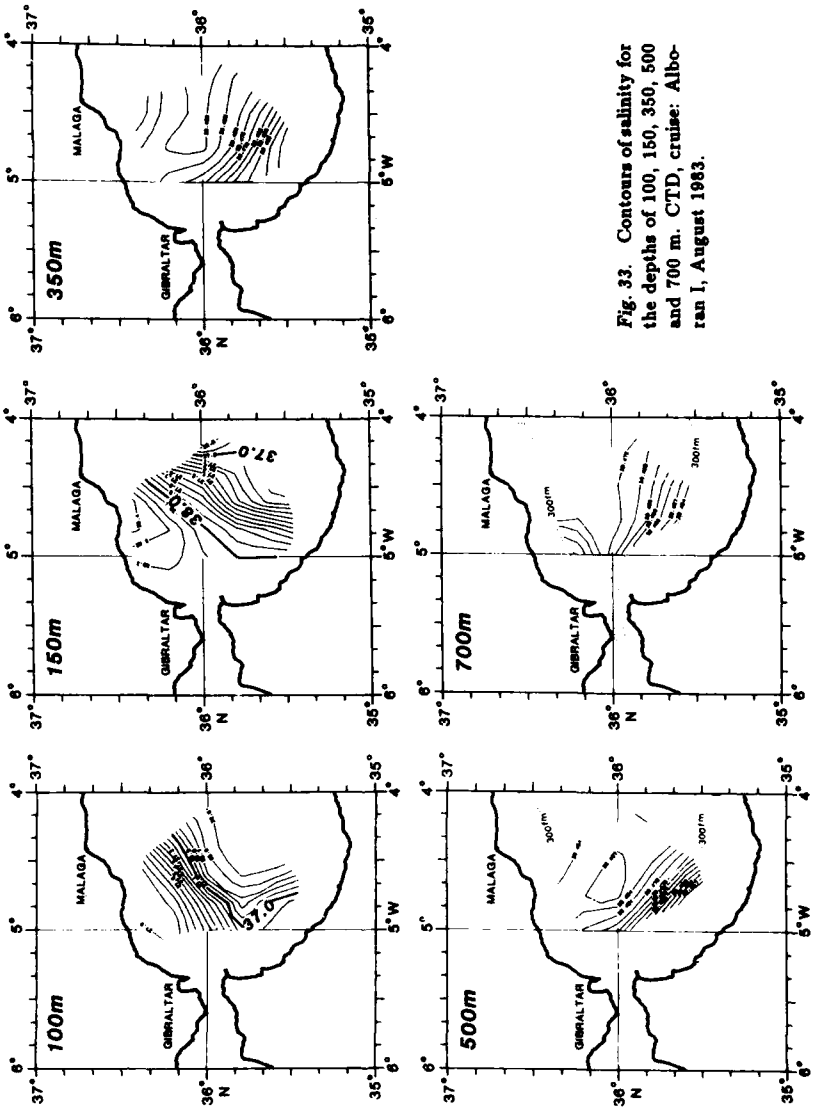

Fig. 33. Contours of salinity for the depths of 100, 150, 350, 500 and 700 m. CTD, cruise: Alboran I, August 1983.

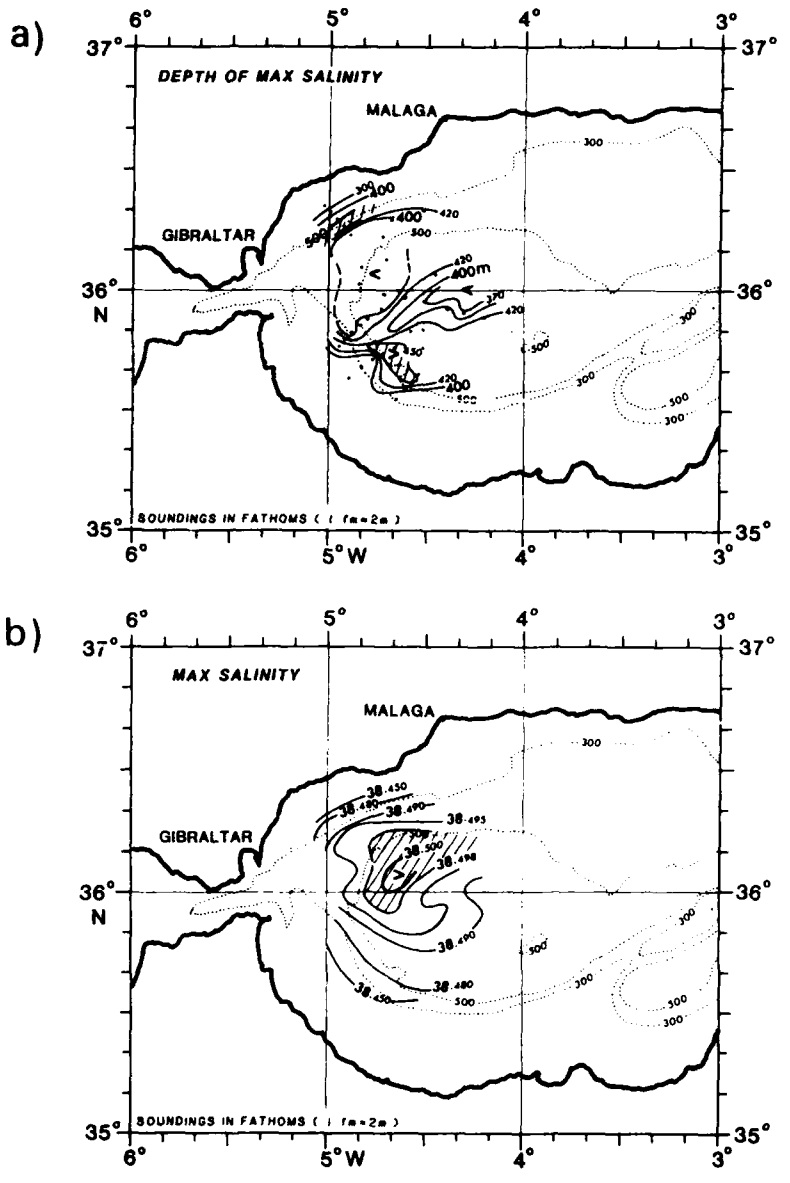

Fig. 34. (a) Contours of depth of maximum salinity; (b) contours of maximum salinity CTD, cruise: Alboran I, 1983. Dots signify the positions of CTD casts.

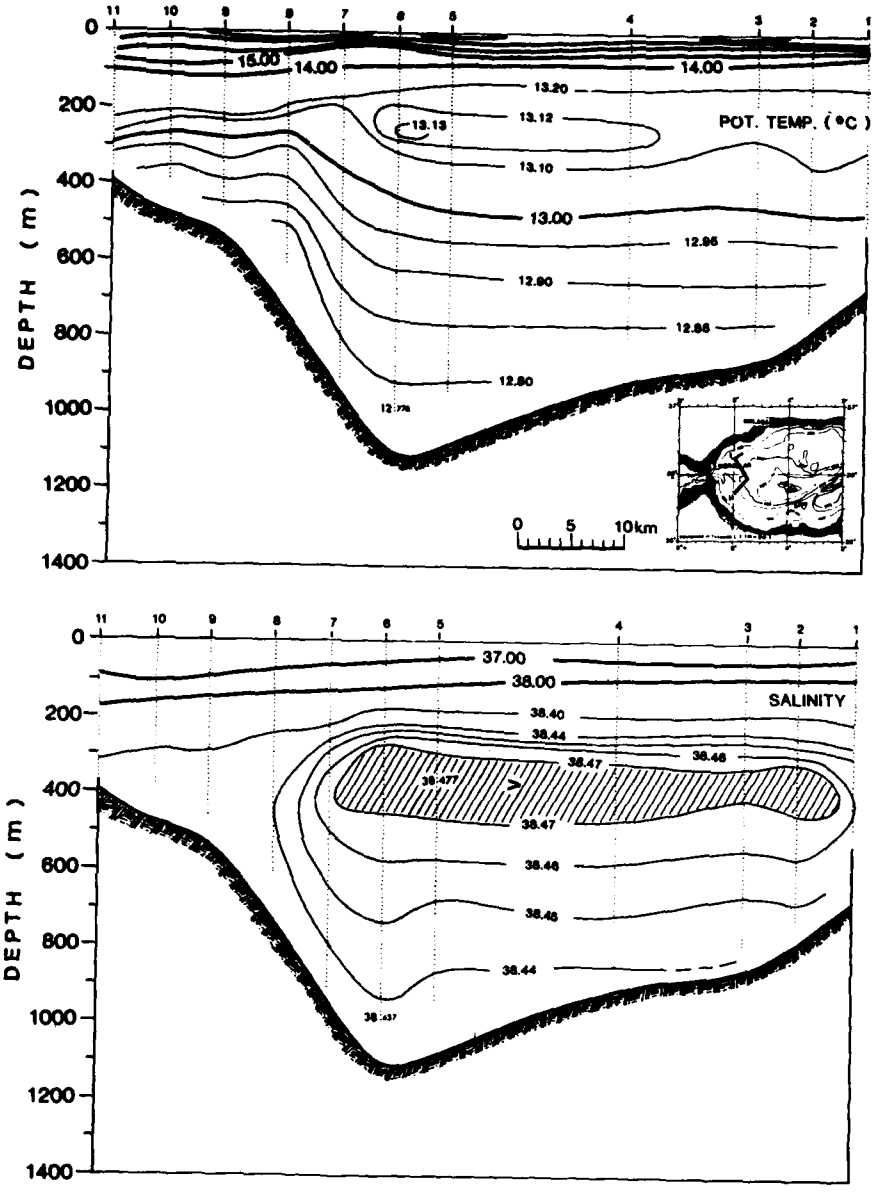

Fig. 35. Cross-sections of potential temperature and salinity. CTD, cruise: Magnaghi, September 1983.

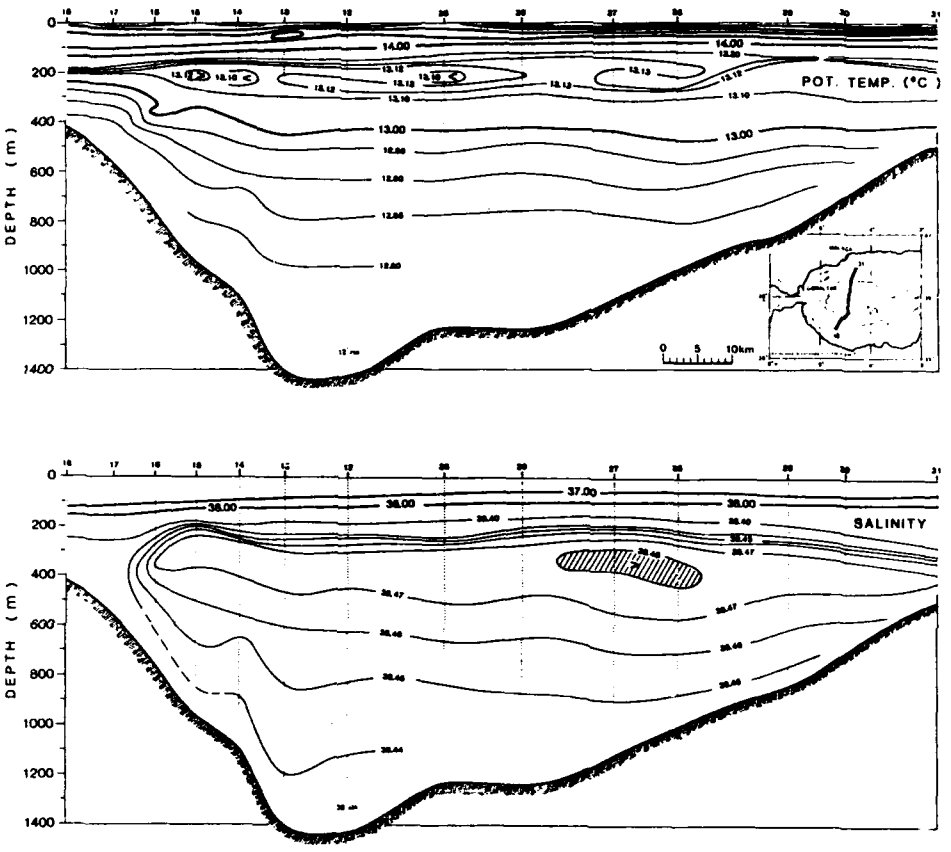
POT. TEMP. (°C)
DEPTH (m)
0
200
400
600
800
1000
1200
1400
14.00
13.00
0 5 10km
SALINITY
37.00
36.00

Fig. 35. (cont'd.)

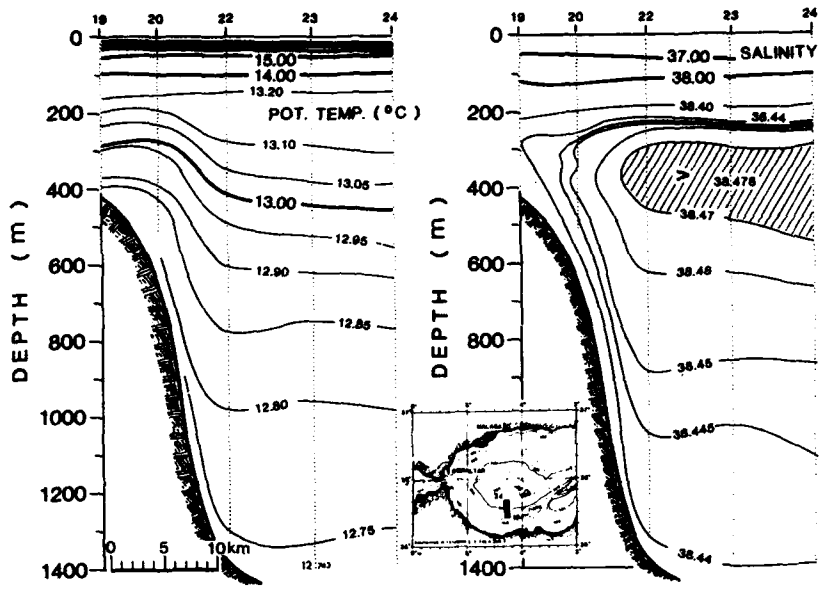
19
20
22
23
24
0
200
400
600
800
1000
1200
1400
DEPTH (m)
POT. TEMP. (°C)
15.00
14.00
13.20
13.10
13.05
13.00
12.95
12.90
12.85
12.80
12.75
0
5
10km
SALINITY
37.00
38.00
38.40
38.44
38.478
38.47
38.46
38.45
38.445
38.44

Fig. 35. (cont'd.)

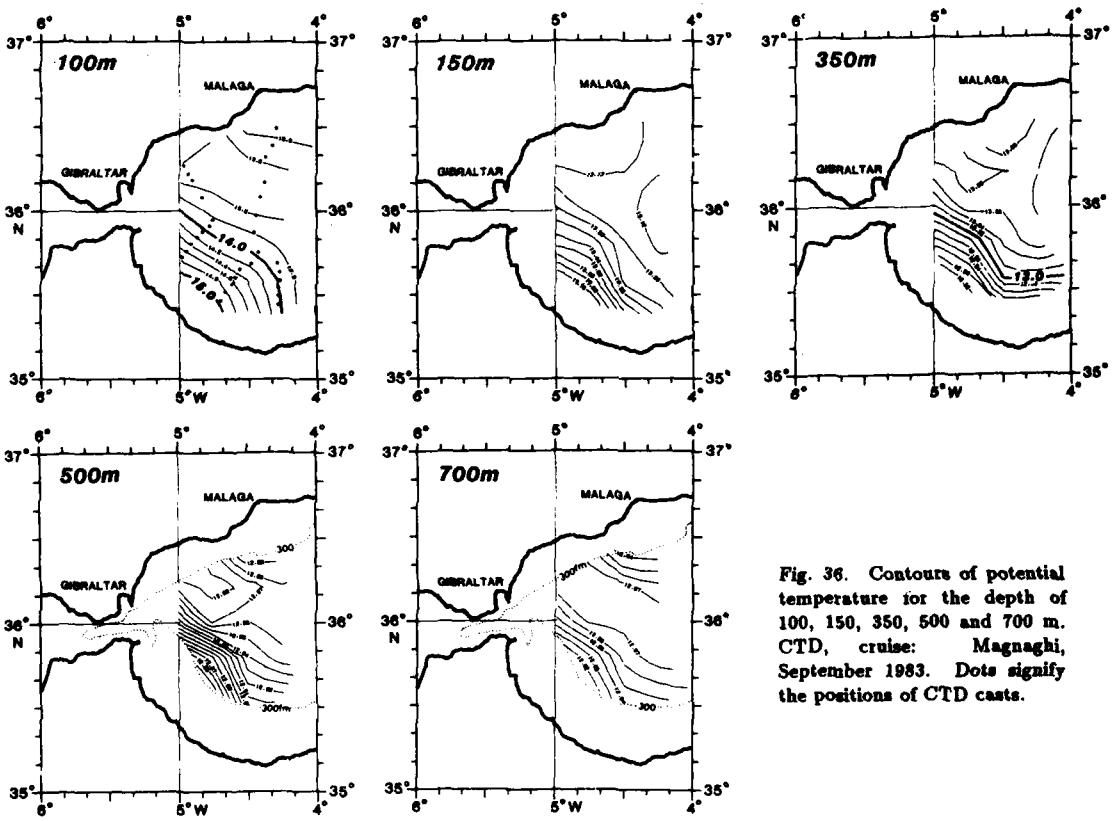

Fig. 36. Contours of potential temperature for the depth of 100, 150, 350, 500 and 700 m. CTD, cruise: Magnaghi, September 1983. Dots signify the positions of CTD casts.

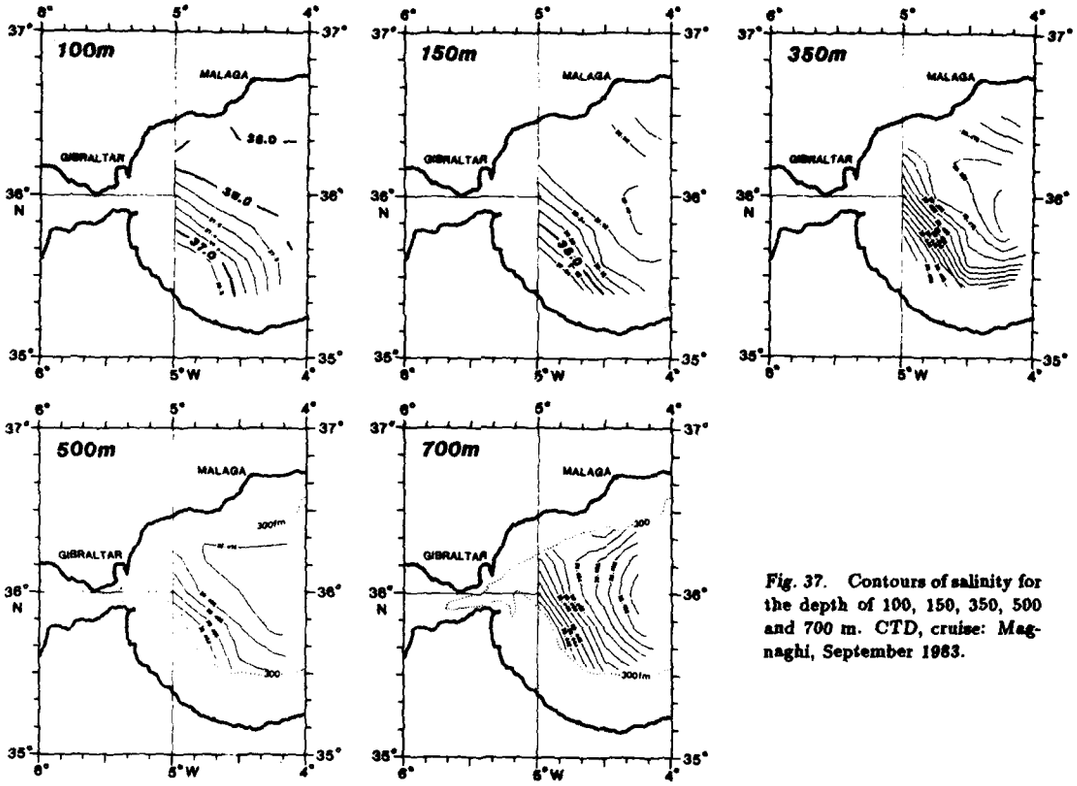

Fig. 37. Contours of salinity for the depth of 100, 150, 350, 500 and 700 m. CTD, cruise: Magnaghi, September 1983.

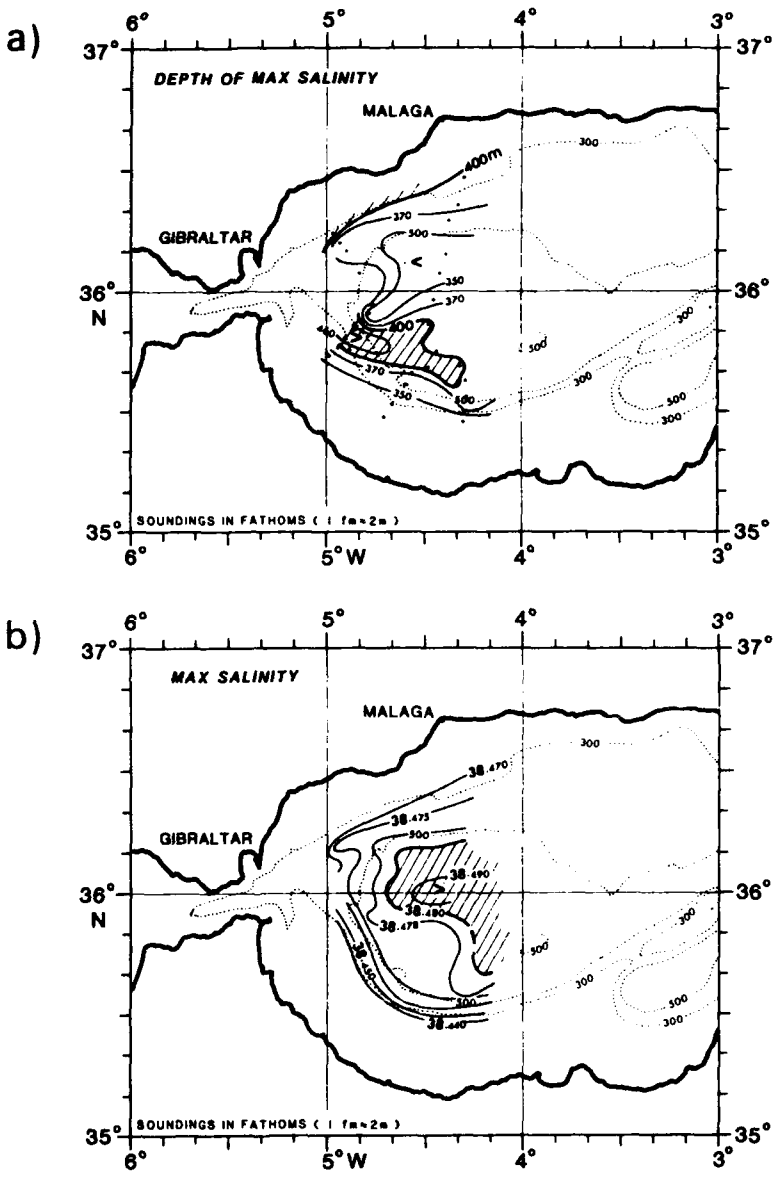

Fig. 38. (a) Contours of depth of maximum salinity; (b) contours of maximum salinity. CTD, cruise: Magnaghi, September 1983. Dots signify the positions of CTD casts.

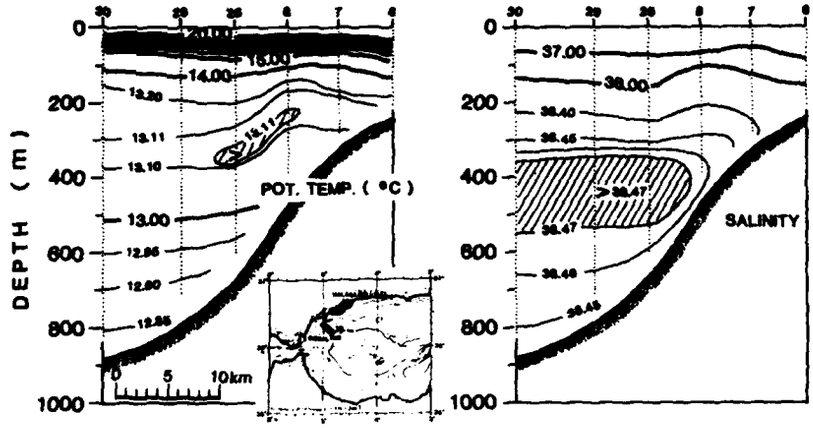

Fig. 39. Cross-sections of potential temperature and salinity. CTD, cruise: Alboran II, October 1983.

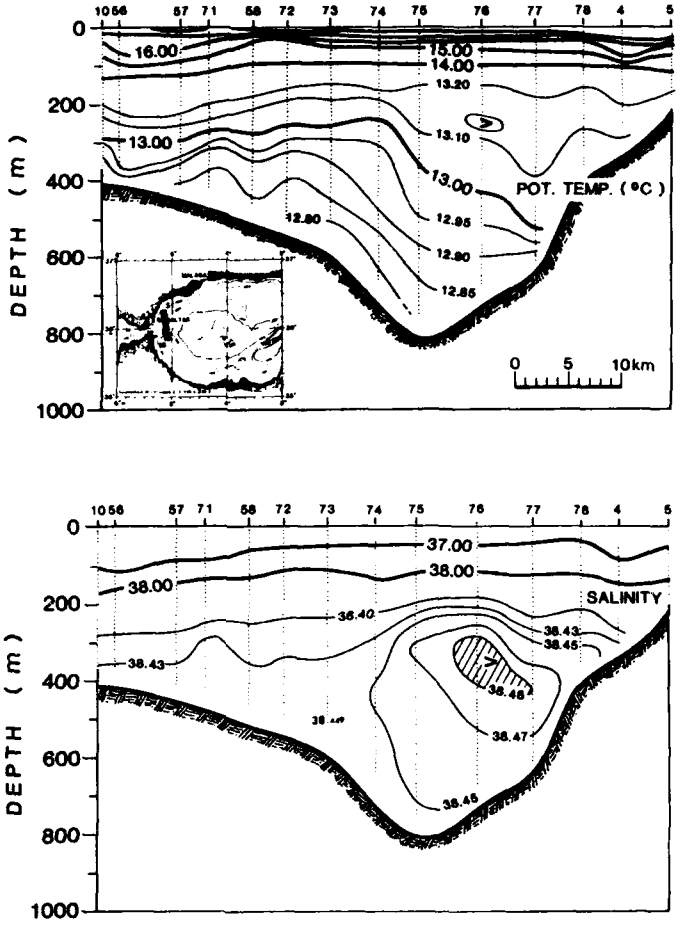
DEPTH (m)
POT. TEMP. (°C)
16.00
15.00
14.00
13.20
13.10
13.00
12.95
12.90
12.85
12.80
0 5 10km
SALINITY
37.00
38.00
36.40
38.43
38.45
38.47
38.48

Fig. 39. (cont'd.)

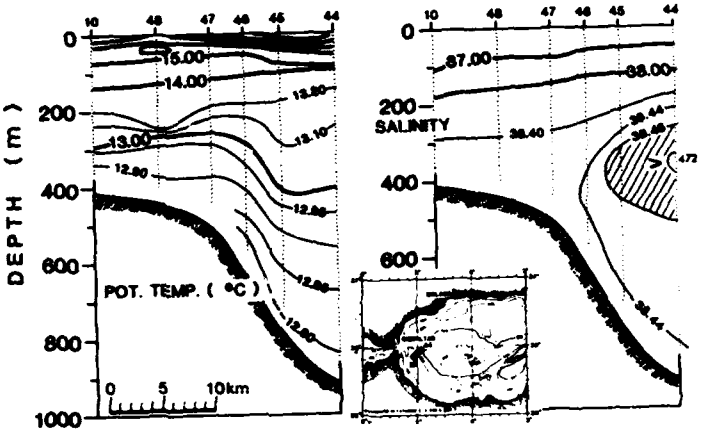

Fig. 39. (cont'd.)

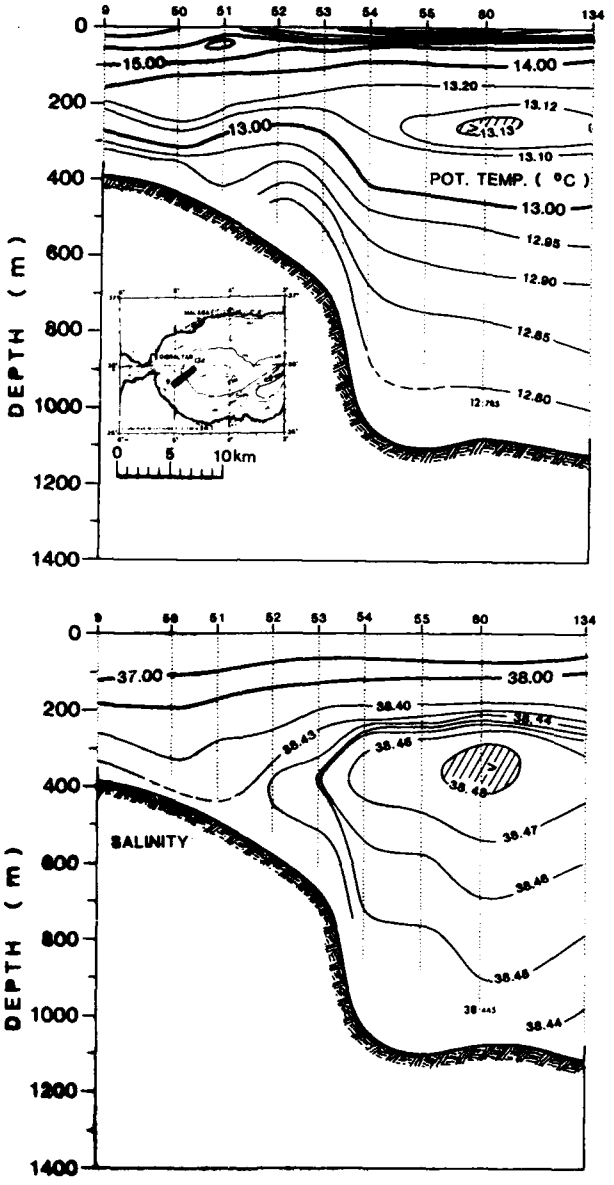
DEPTH (m)
POT. TEMP. (°C)
15.00
14.00
13.20
13.12
13.13
13.00
13.10
13.00
12.95
12.90
12.85
12.80
0 5 10km
SALINITY
37.00
38.00
38.40
38.44
38.43
38.46
38.47
38.48
38.49
38.44

Fig. 39. (cont'd.)

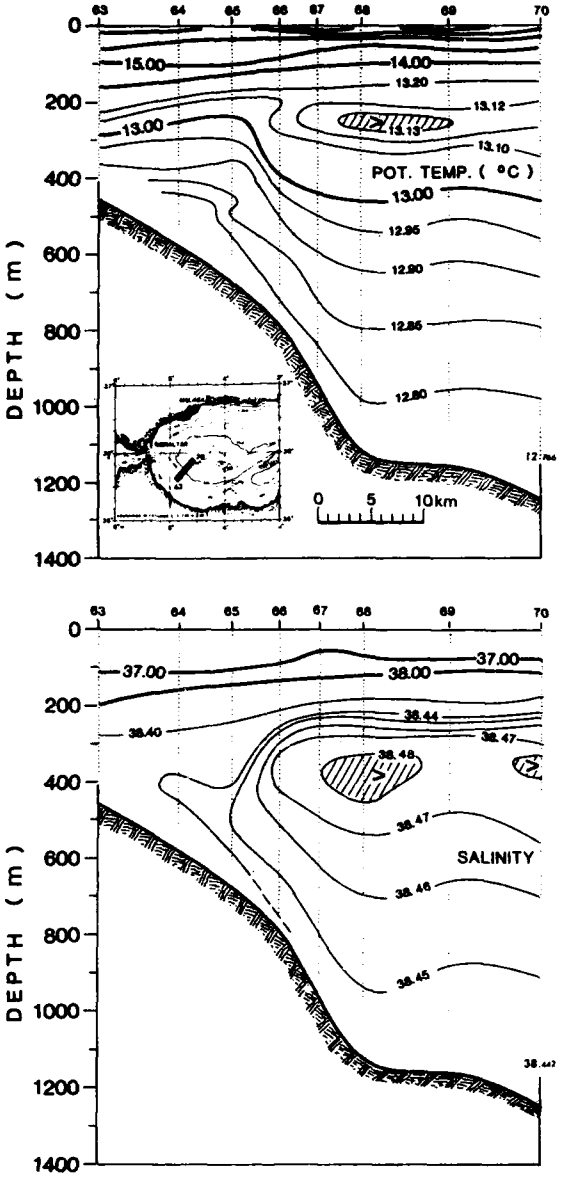
63
64
65
66
67
68
69
70
0
200
400
600
800
1000
1200
1400
DEPTH (m)
15.00
14.00
13.20
13.12
13.00
13.13
13.10
POT. TEMP. (°C)
13.00
12.95
12.90
12.85
12.80
0 5 10km
37.00
38.00
37.00
38.40
38.44
38.47
38.48
38.47
SALINITY
38.46
38.45

Fig. 39. (cont'd.)

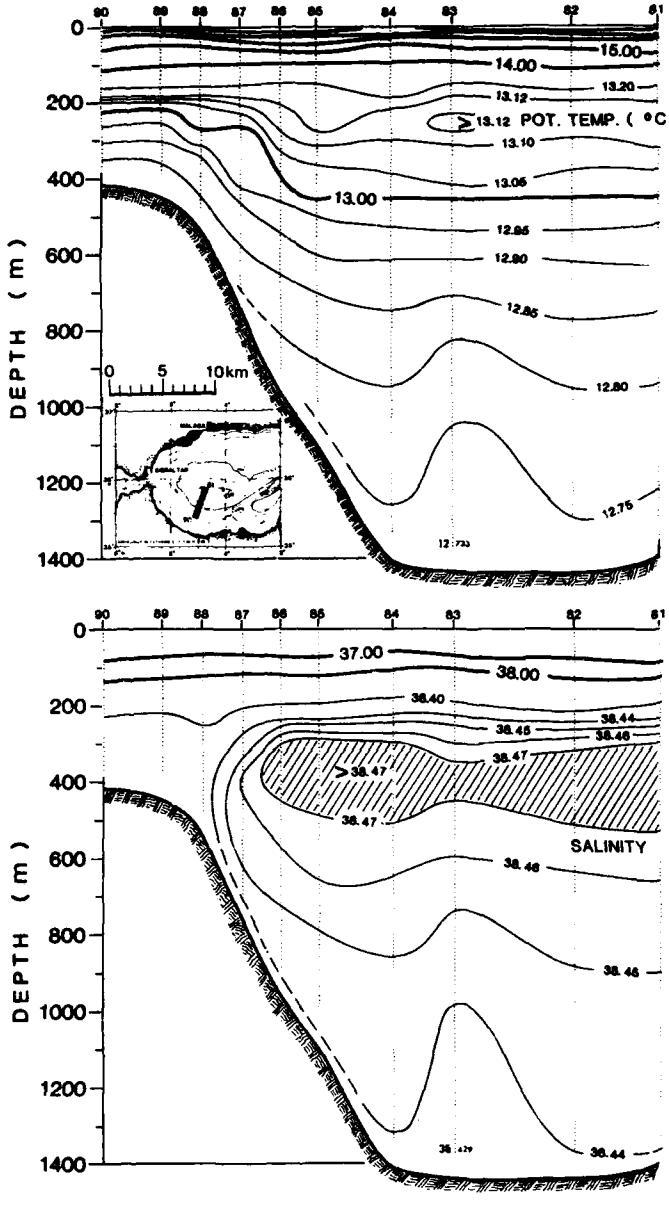
DEPTH (m)
POT. TEMP. (°C)
15.00
14.00
13.20
13.12
13.10
13.05
13.00
12.95
12.90
12.85
12.80
12.75
0 5 10km
SALINITY
37.00
38.00
38.40
38.44
38.45
38.46
38.47
38.46
38.44

Fig. 39. (cont'd.)

AD-A195 473 DEEP WATER MASS CIRCULATION IN THE ALBORAN BASIN: MEASUREMENTS - AUGUST 1... (U) SACLANT ASW RESEARCH CENTRE LA SPEZIA (ITALY) P PISTEK FEB 88 2/2

UNCLASSIFIED SACLANTCEN-SR-196 F/G 8/3 NL

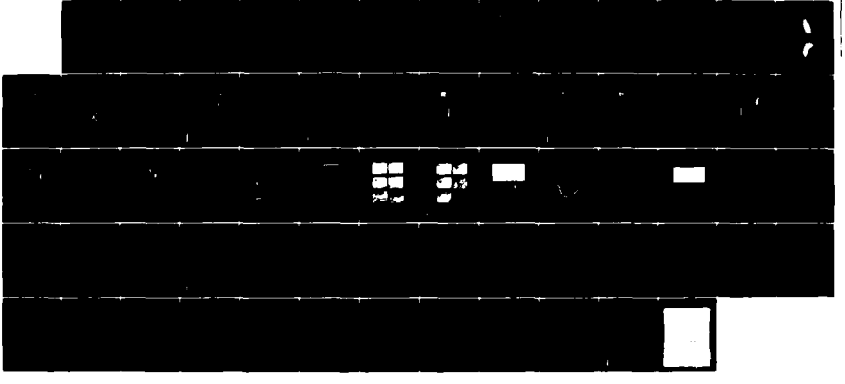

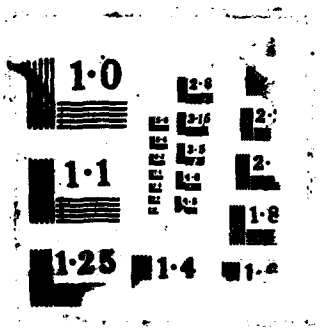
1·0
1·1
1·25
1·4
2·8
2·5
2·
1·8

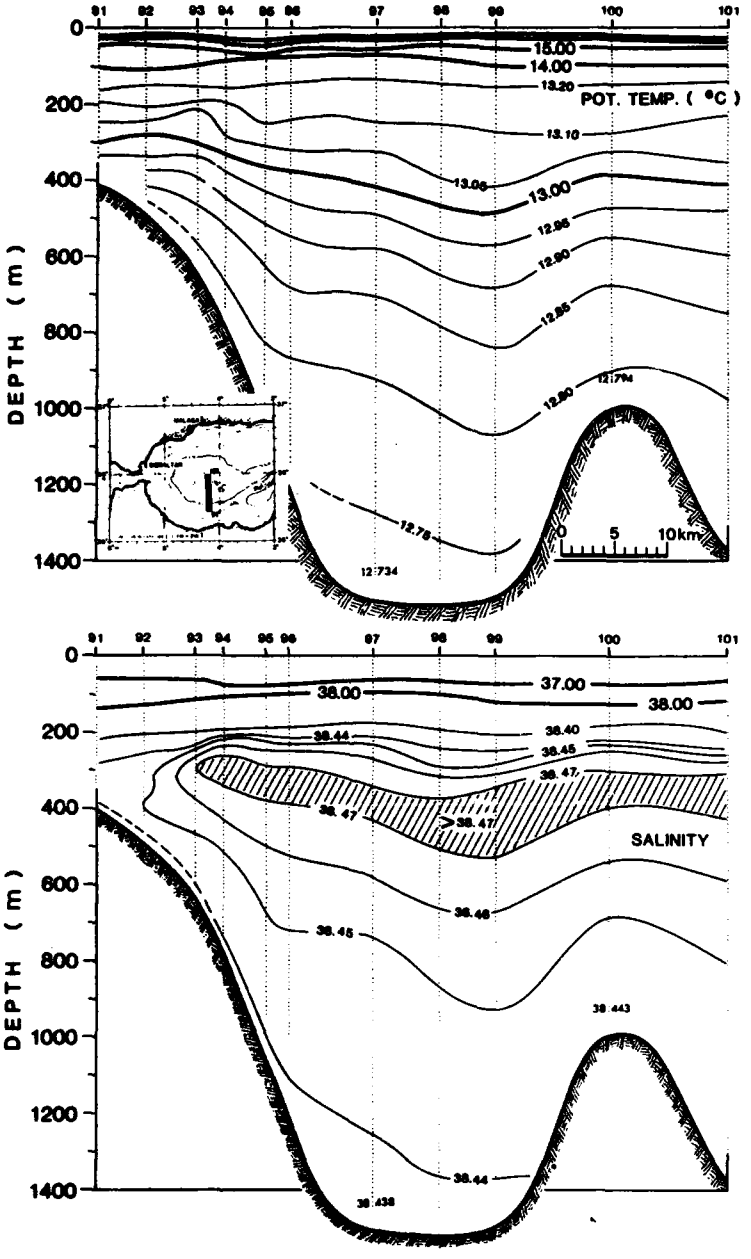
91 92 93 94 95 96 97 98 99 100 101
0
200
400
600
800
1000
1200
1400
DEPTH (m)
15.00
14.00
13.20
POT. TEMP. (°C)
13.10
13.05
13.00
12.95
12.90
12.85
12.80
12.794
12.78
12.734
0 5 10km
37.00
38.00
38.00
38.40
38.44
38.45
38.47
38.47
>38.47
SALINITY
38.46
38.45
38.443
38.44
38.438

Fig. 39. (cont'd.)

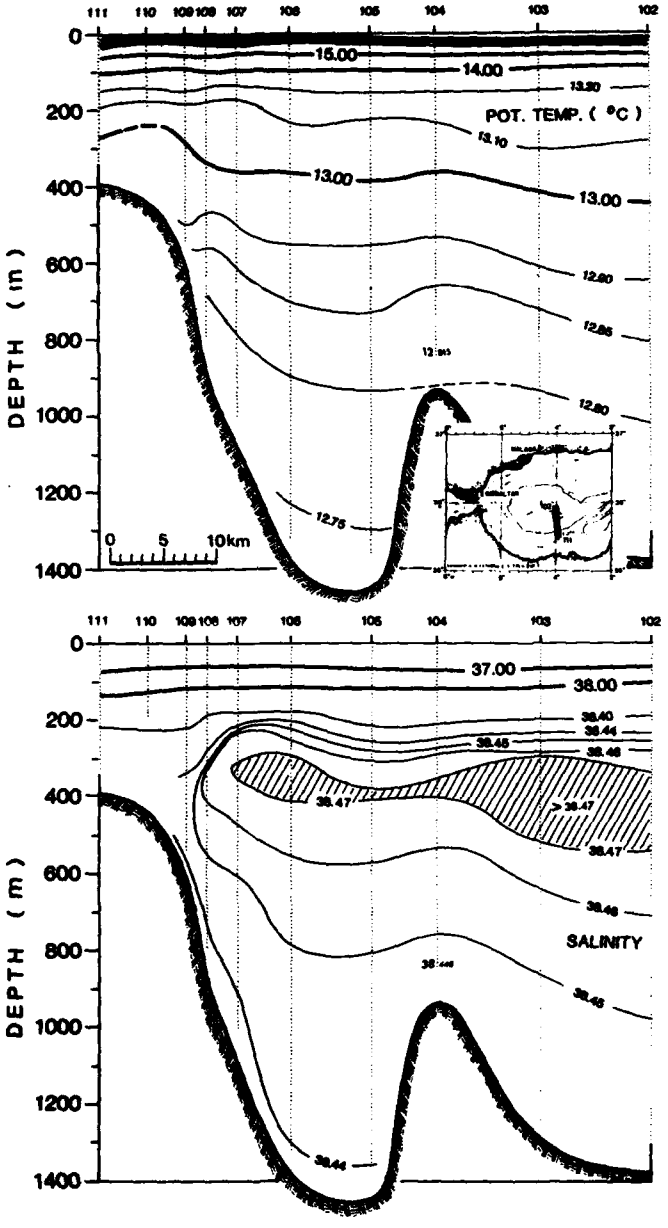
111 110 109 108 107 106 105 104 103 102
0
200
400
600
800
1000
1200
1400
DEPTH (m)
15.00
14.00
13.50
POT. TEMP. (°C)
13.10
13.00
13.00
12.90
12.85
12.80
12.75
0 5 10km
37.00
38.00
38.40
38.44
38.45
38.46
38.47
> 38.47
38.47
38.46
SALINITY
38.44

Fig. 39. (cont'd.)

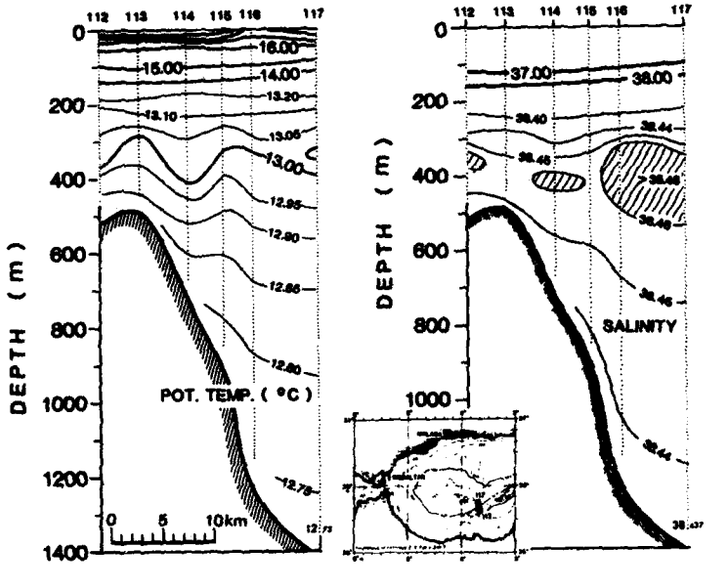
112 113 114 115 116 117
0
200
400
600
800
1000
1200
1400
DEPTH (m)
16.00
15.00
14.00
13.30
13.10
13.05
13.00
12.95
12.90
12.85
12.80
12.78
POT. TEMP. (°C)
0 5 10km
37.00
36.00
36.40
36.44
36.46
SALINITY

Fig. 39. (cont'd.)

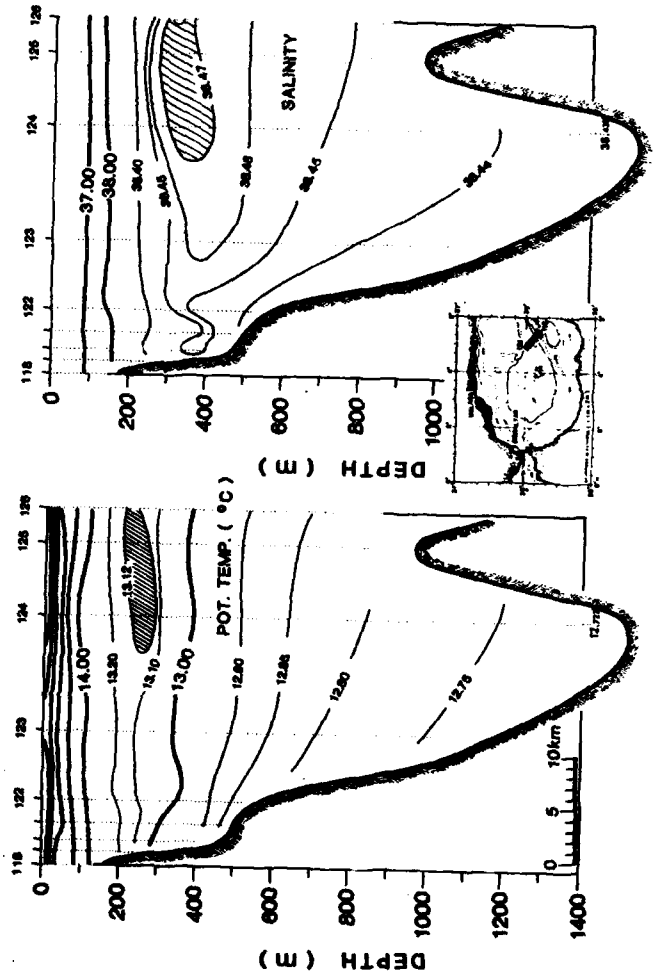
SALINITY
37.00
38.00
38.40
38.45
38.47
38.48
38.46
38.44
DEPTH (m)
POT. TEMP. (°C)
14.00
13.50
13.10
13.00
12.90
12.85
12.80
12.75
10km
DEPTH (m)

Fig. 39. (cont'd.)

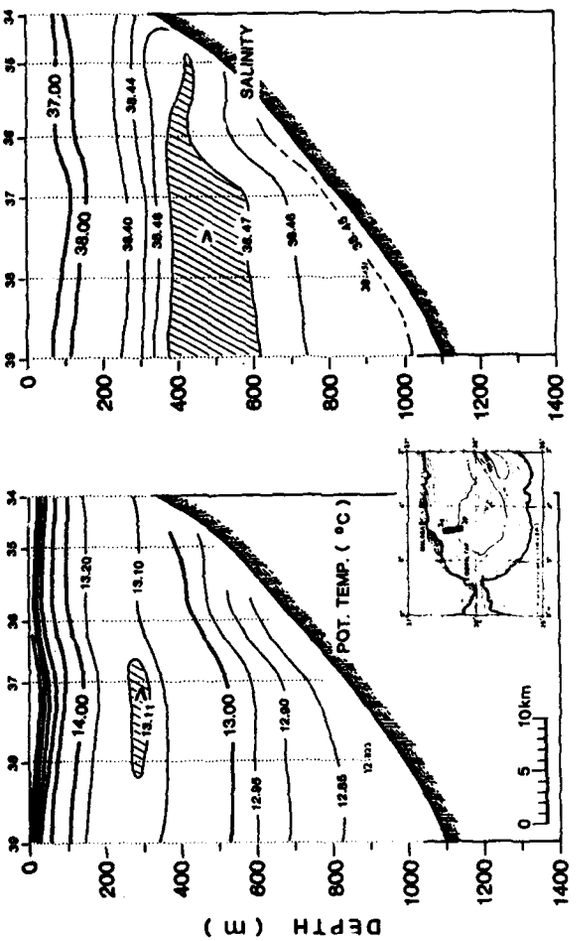
SALINITY
37.00
38.00
38.40
38.44
38.46
38.47
POT. TEMP. (°C)
13.20
13.10
14.00
13.00
12.90
12.85
0 5 10km
DEPTH (m)
0
200
400
600
800
1000
1200
1400
34
35
36
37
38
39

Fig. 39. (cont'd.)

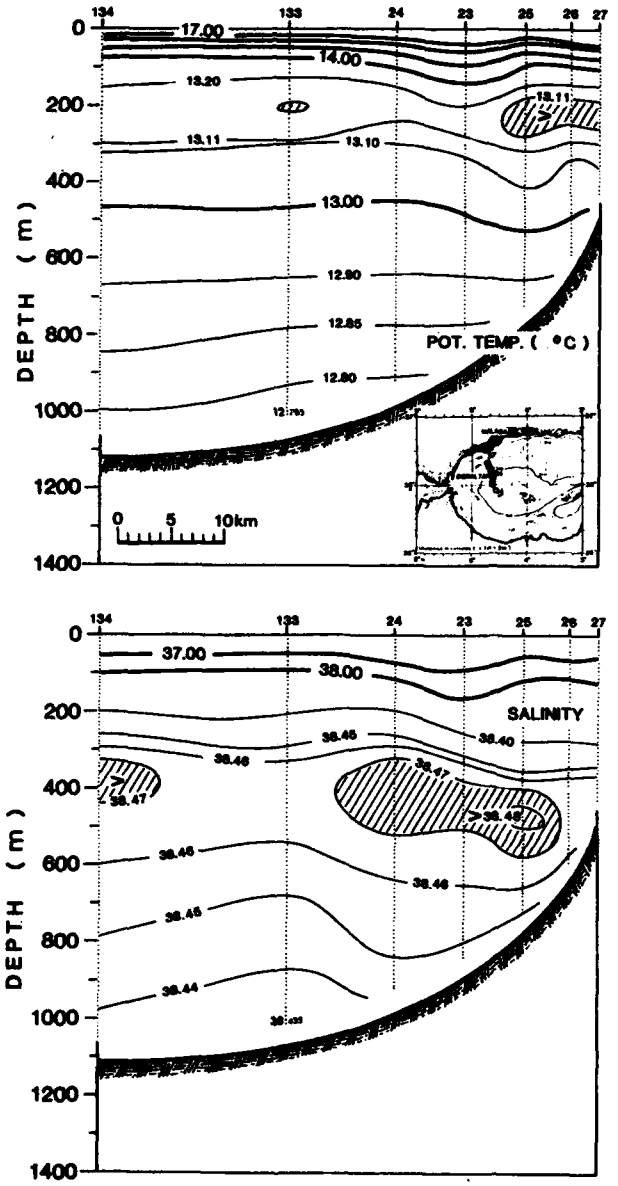
134
133
24
23
25
26
27
0
200
400
600
800
1000
1200
1400
DEPTH (m)
17.00
14.00
13.20
13.11
13.10
13.00
12.90
12.85
12.80
POT. TEMP. (°C)
0 5 10km
37.00
38.00
SALINITY
38.45
38.40
38.46
38.47
38.44

Fig. 39. (cont'd.)

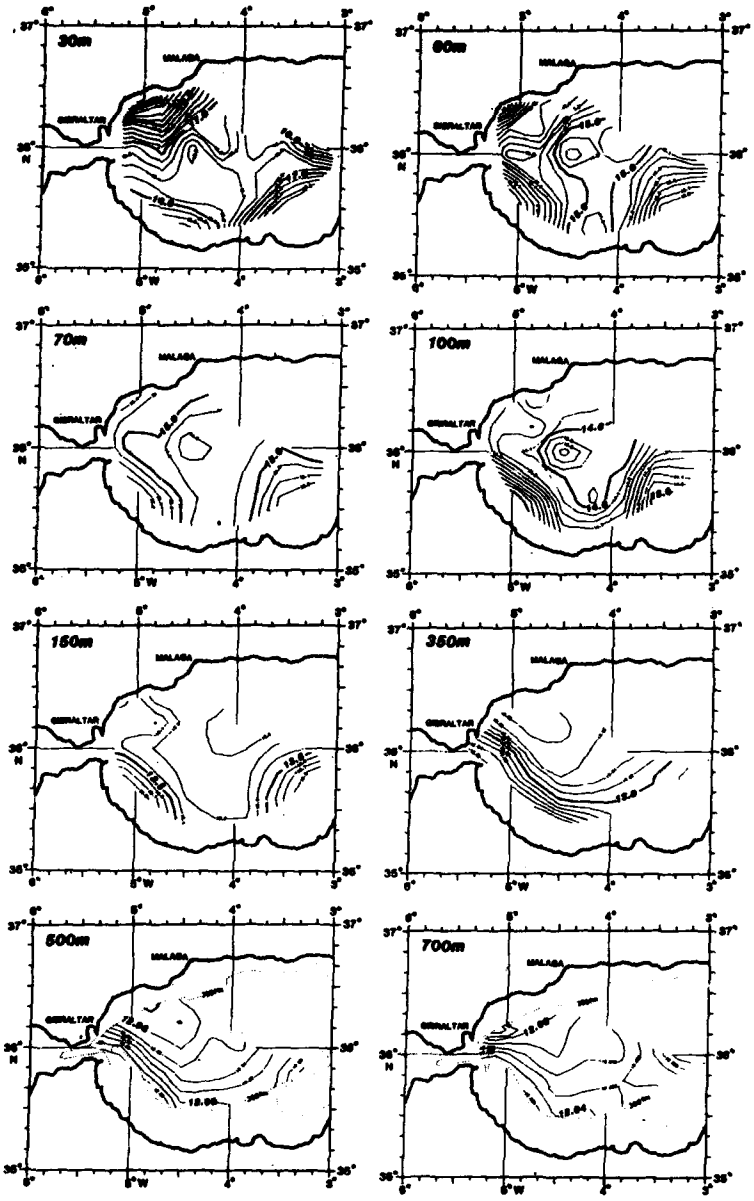

Fig. 40. Contours of potential temperature for the depths of 30, 60, 70, 100, 150, 350, 500 and 700 m. CTD, cruise: Alboran II, October 1983.

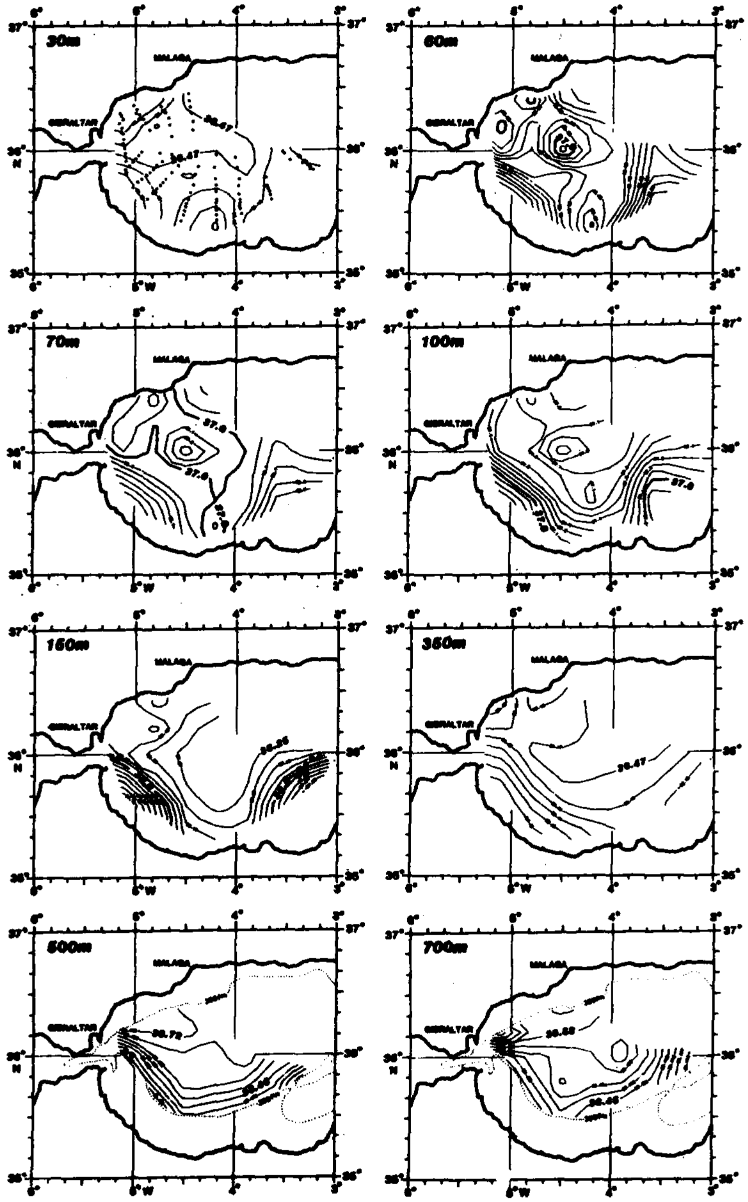

Fig. 41. Contours of salinity for the depths of 30, 60, 70, 100, 150, 350, 500 and 700 m. CTD, cruise: Alboran II, October 1983. Dots signify the positions of CTD casts.

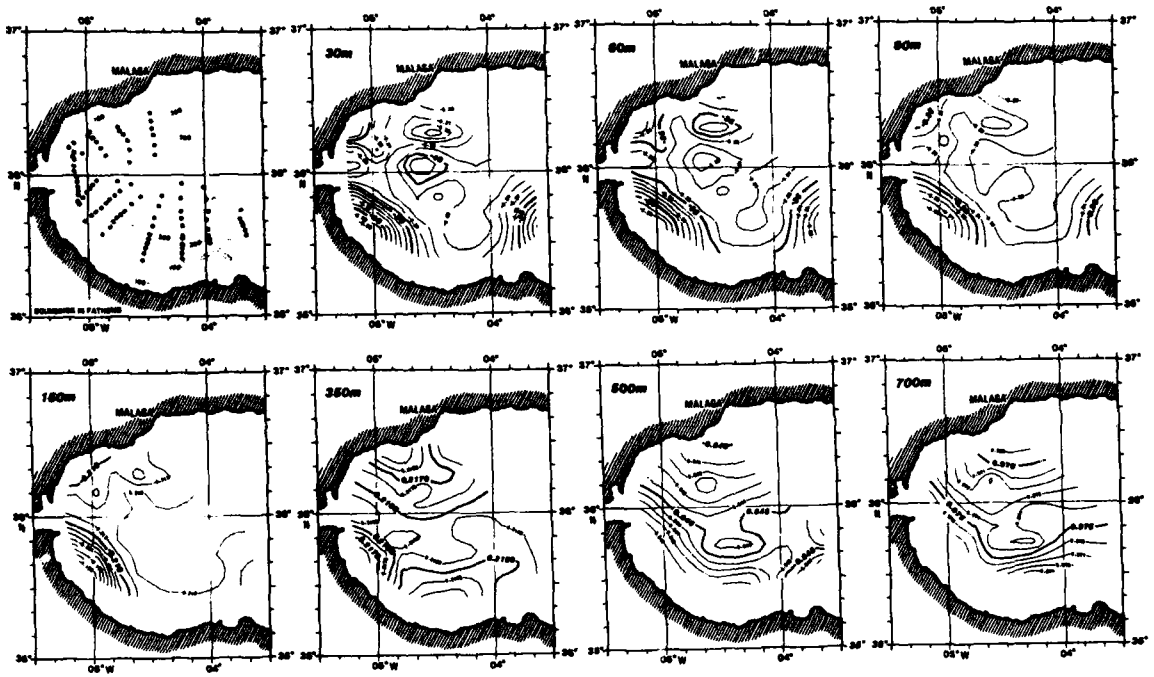

Fig. 42. **Contours of dynamic height anomaly in dynamic meters for the depths of 30, 60, 90, 150, 350, 500 and 700 m (relative to 220 m). CTD, cruise: Alboran II, October 1983. Dots signify the positions of CTD casts.**

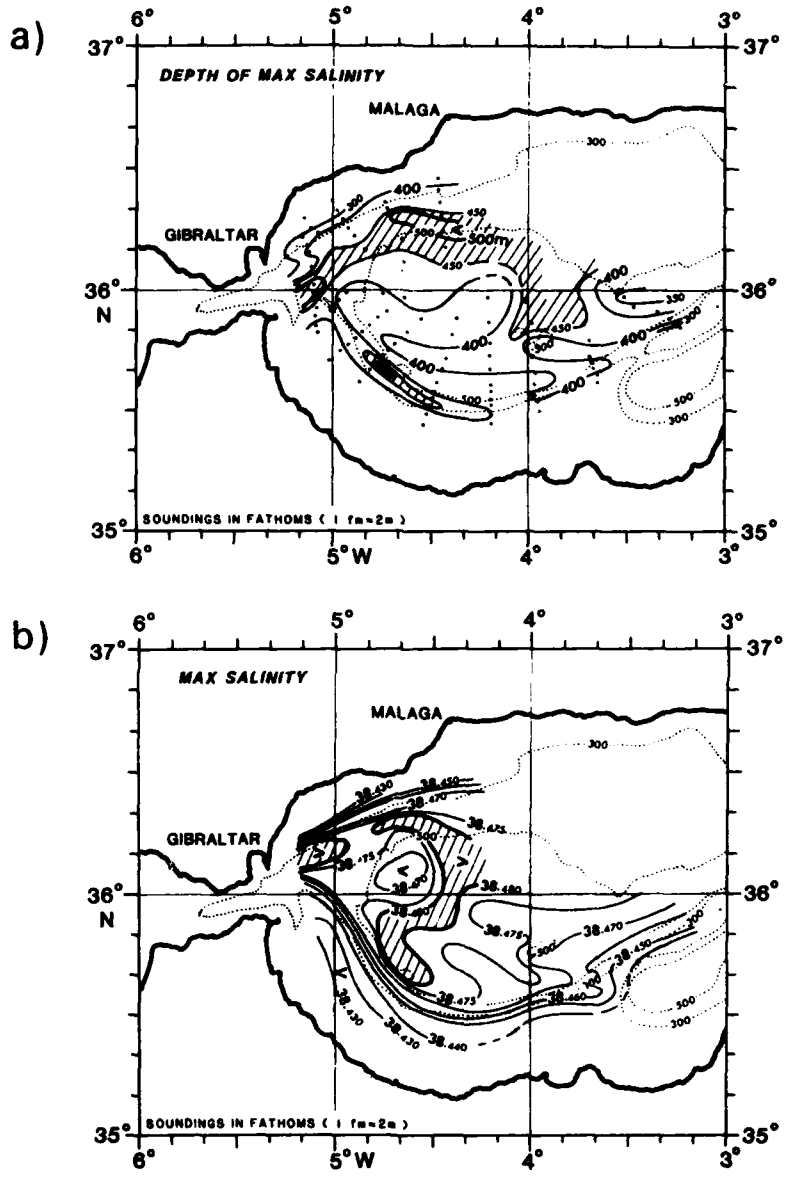

Fig. 43. (a) Contours of depth of maximum salinity; (b) contours of maximum salinity. CTD, cruise: Alboran II, October 1983. Dots signify the positions of CTD casts.

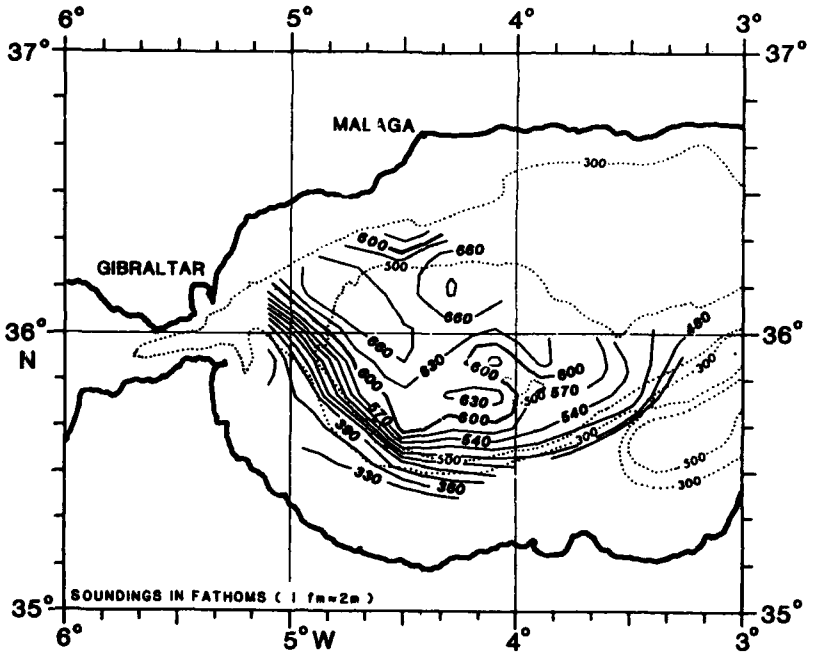

Fig. 44. (a) Contours of depth of 12.9°C potential temperature; CTD, cruise: Alboran II, October 1983.

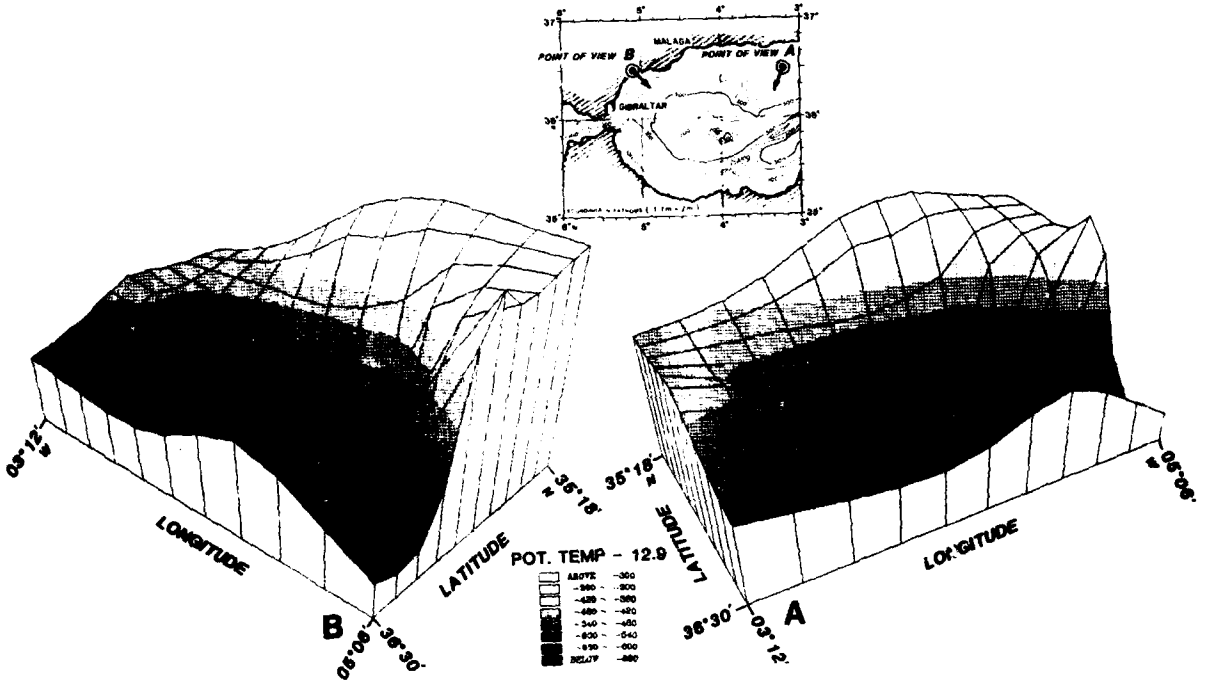

Fig. 44. (b) three-dimensional views of the depth where the potential temperature is 12.9°C.

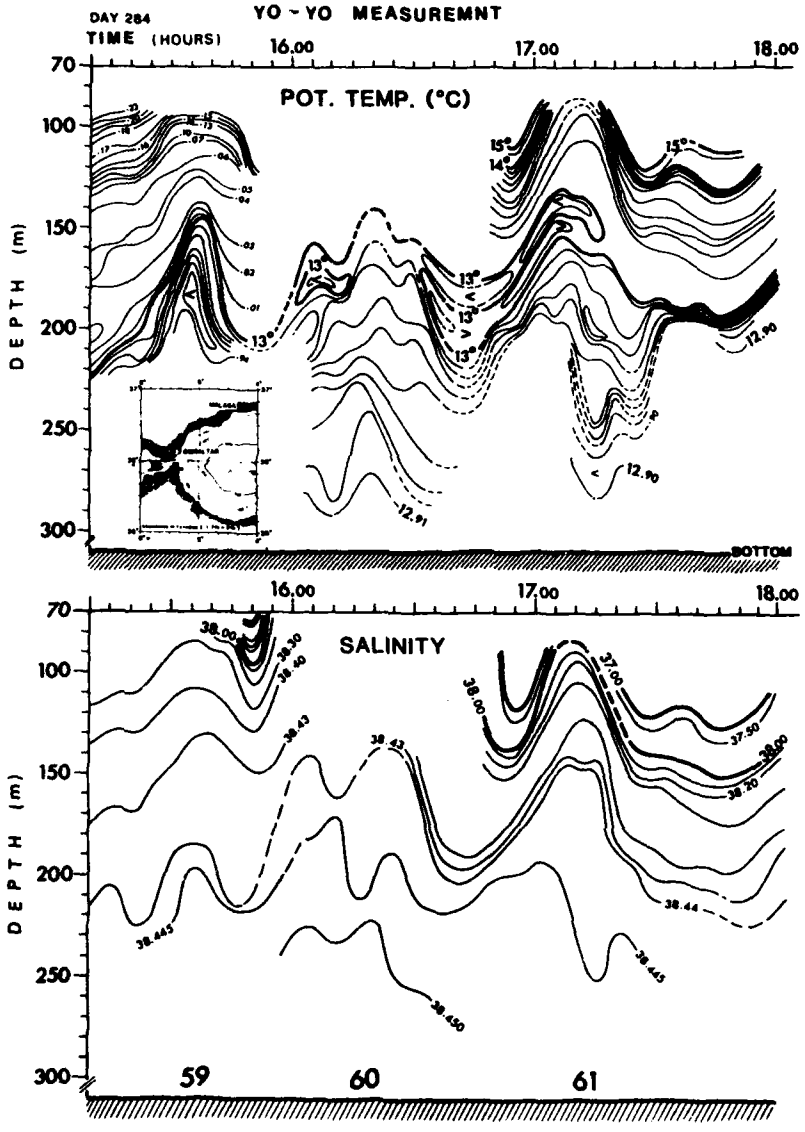

Fig. 45. Time variation of potential temperature and salinity obtained by yo-yo measurement near the sill. Measurement started 2 h before high water in Gibraltar (-2 h HW).

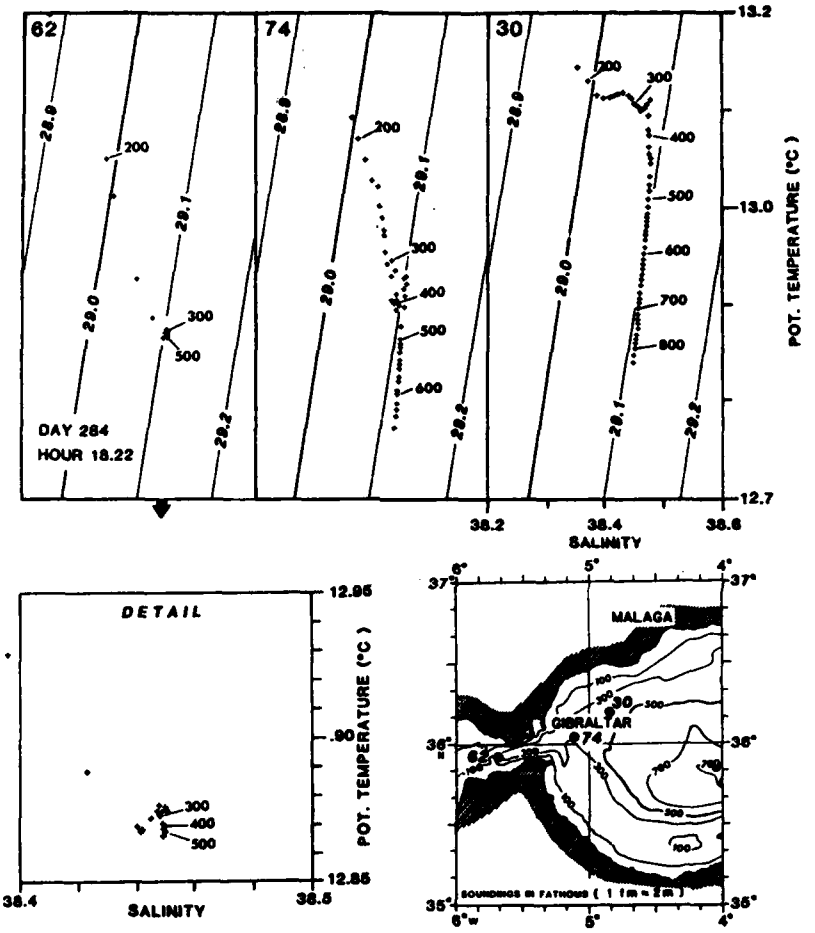

Fig. 46. **Potential temperature/salinity diagrams for CTD casts 6.2, 74 and 30 with potential sigma curves. CTD, cruise: Alboran II, October 1983. Numbers near the crosses signify the depth in m.**

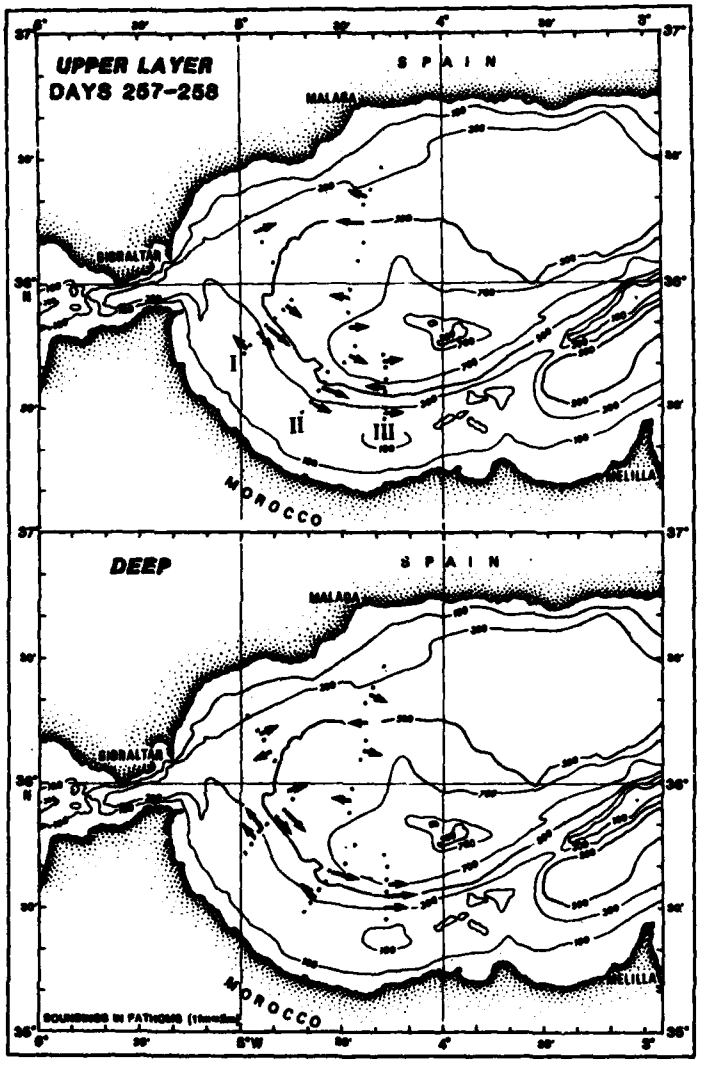

Fig. 47. Schematic results of geostrophic current calculations for the upper and deeper layers. CTD, cruise: Magnaghi, September 1982. Level of no-motion at 250 m. Roman numbers identify the cross-sections used for the calculation.

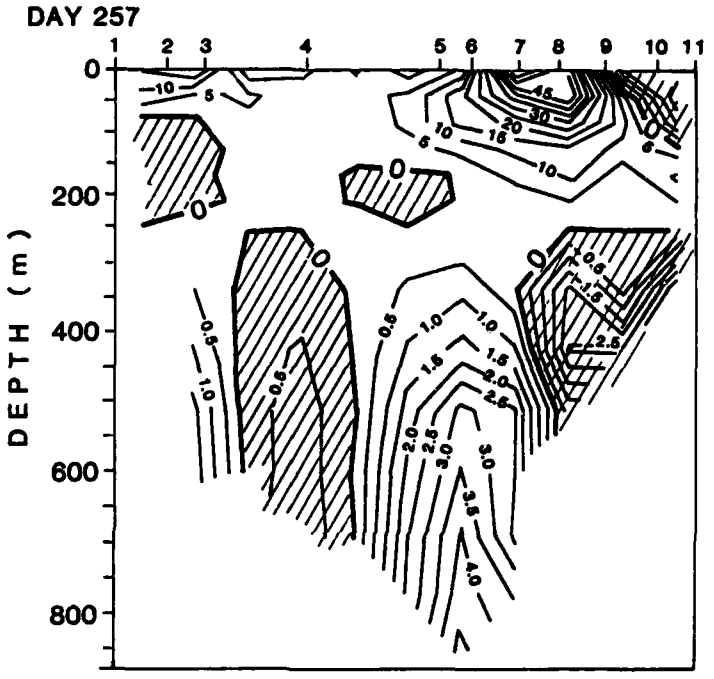

Fig. 48. Cross-sections of computed geostrophic current in cm/s. CTD, cruise: Magnaghi, September 1983. Level of no-motion was 250 m. Days signify the time period when the CTDs involved in cross-section were taken. Positions of cross-sections are shown in Fig. 47.

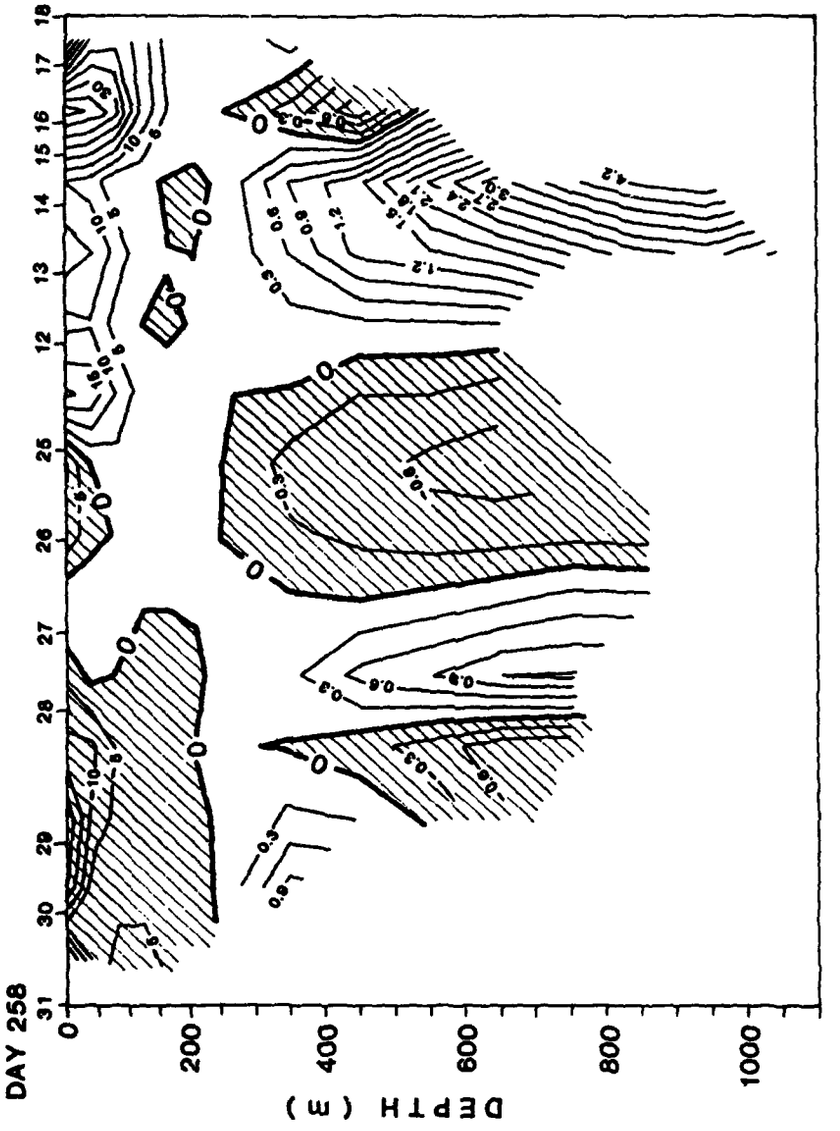
DAY 258
DEPTH (m)
0
200
400
600
800
1000
18
17
16
15
14
13
12
25
26
27
28
29
30
31

Fig. 46. (cont'd.)

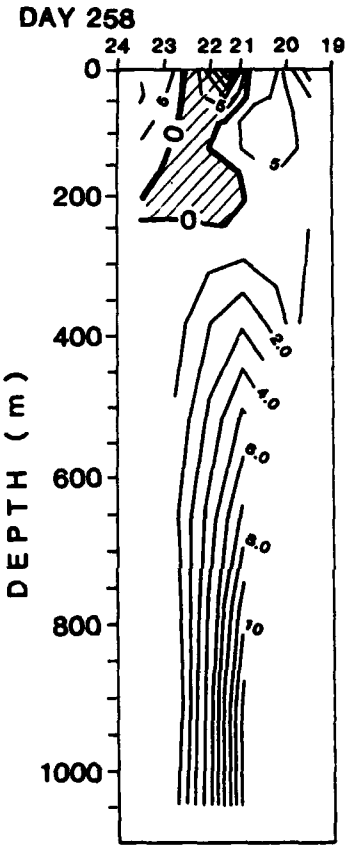
DAY 258
24 23 22 21 20 19
0
200
400
600
800
1000
DEPTH (m)
0
0
5
5
2.0
4.0
6.0
8.0
10

Fig. 48. (cont'd.)

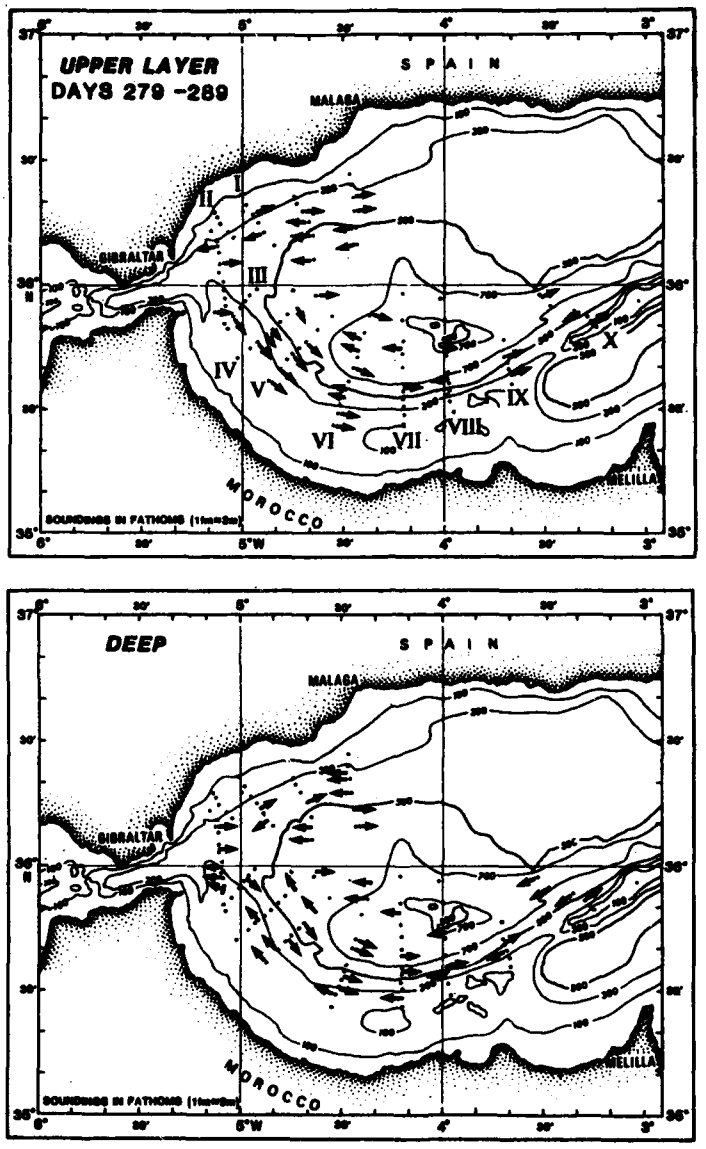

Fig. 49. Schematic results of geostrophic current calculations for the upper and deep layer. CTD, cruise: Alboran II, October 1983. Level of no motion at 250 m. Roman numbers identify the cross-sections used for the calculation.

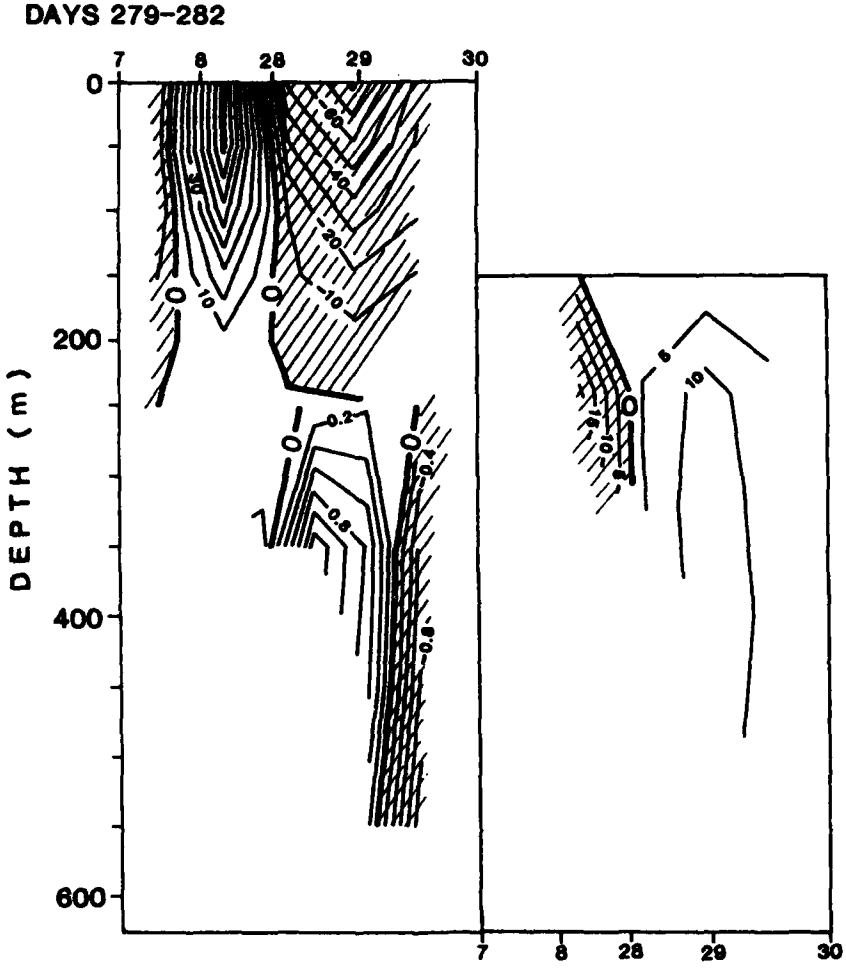

Fig. 50. Cross-sections of computed geostrophic current in cm/s. CTD, cruise: Alboran II, October 1983. Levels of no-motion were chosen at 250 and 150 m for the left and right diagram respectively. Days signify the time period when the CTDs involved in cross-section were taken. Positions of cross- sections are shown in Fig. 49.

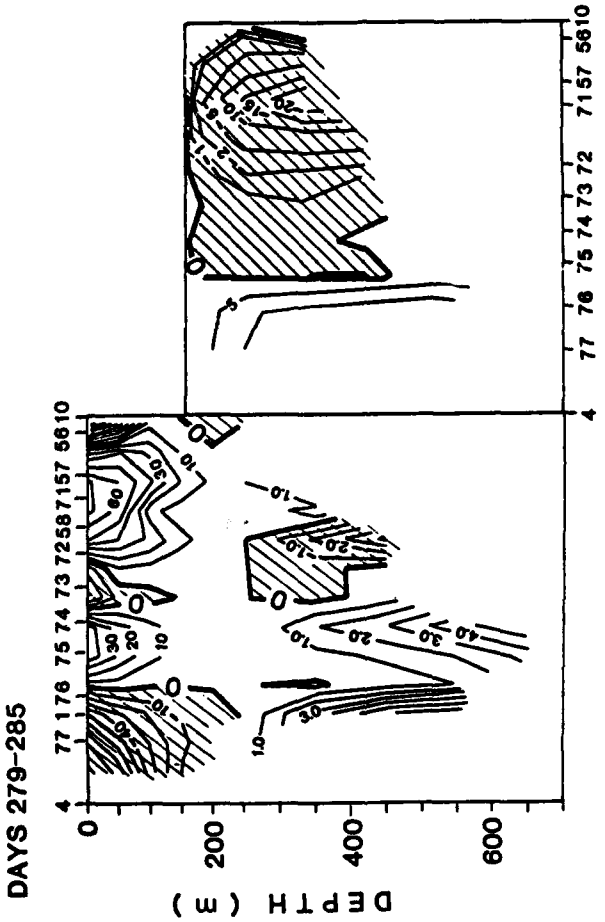
DAYS 279-285
DEPTH (m)
0
200
400
600
4 77 1 76 75 74 73 72 5 8 7 1 5 7 5 8 10
4 77 76 75 74 73 72 7 1 5 7 5 8 10

Fig. 50. (cont'd.)

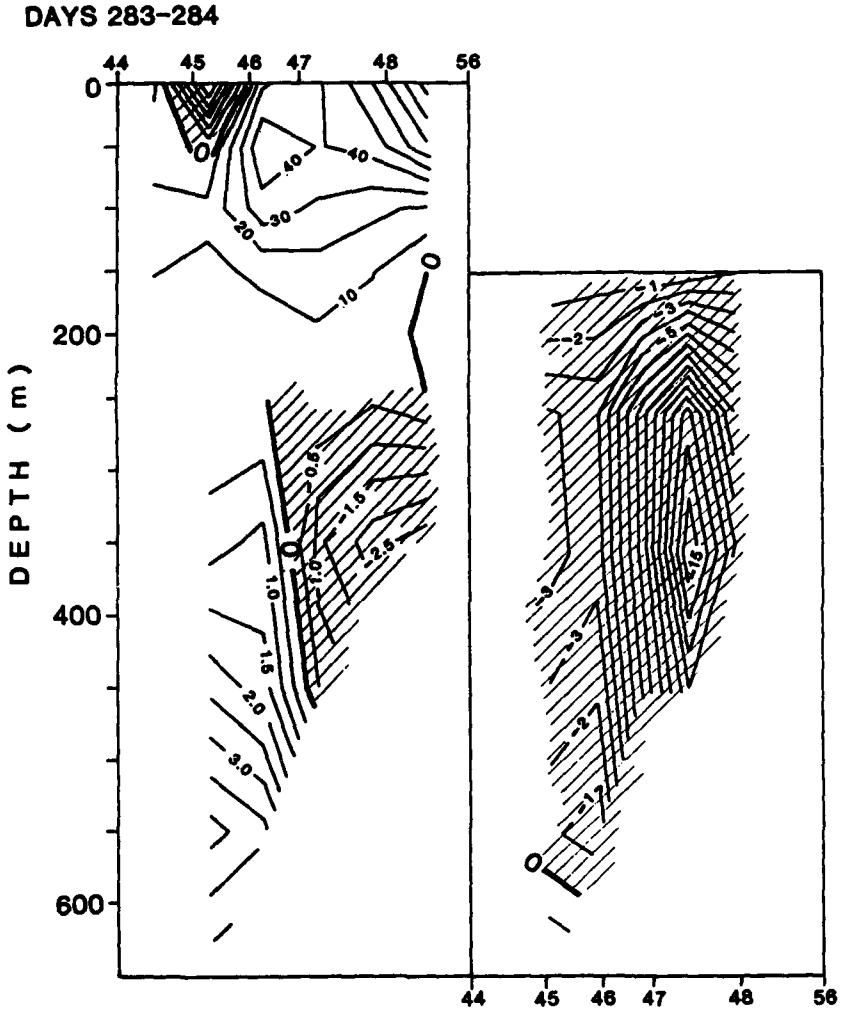
DAYS 283-284
DEPTH (m)
0
200
400
600
44
45
46
47
48
56
40
30
20
10
0
-0.5
-1.5
-2.5
1.0
1.5
2.0
3.0
-1
-2
-3
-5
-10
-15

Fig. 50. (cont'd.)

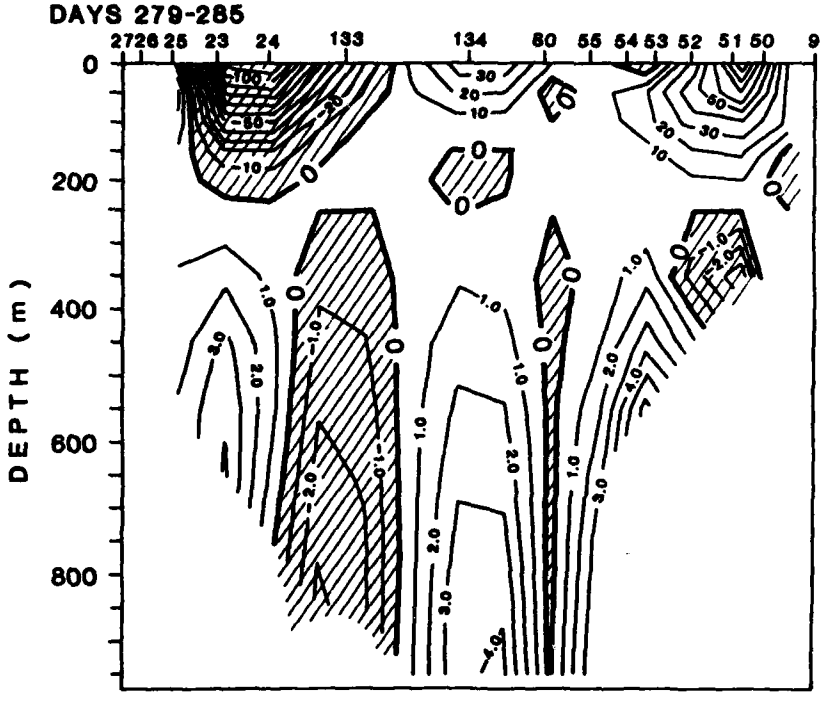
DAYS 279-285
27 26 25 23 24 133 134 80 55 54 53 52 51 50 9
0
200
400
600
800
DEPTH (m)

Fig. 50. (cont'd.)

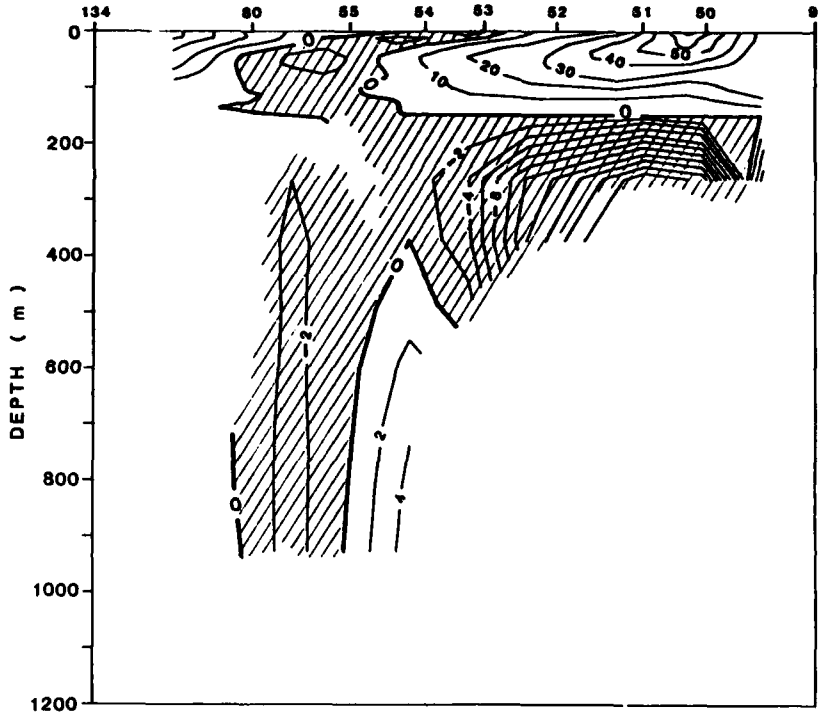
134
80
55
54
53
52
51
50
9
0
200
400
600
800
1000
1200
DEPTH (m)
0
10
20
30
40
50
-2
-4
2
4

Fig. 50. (cont'd.)

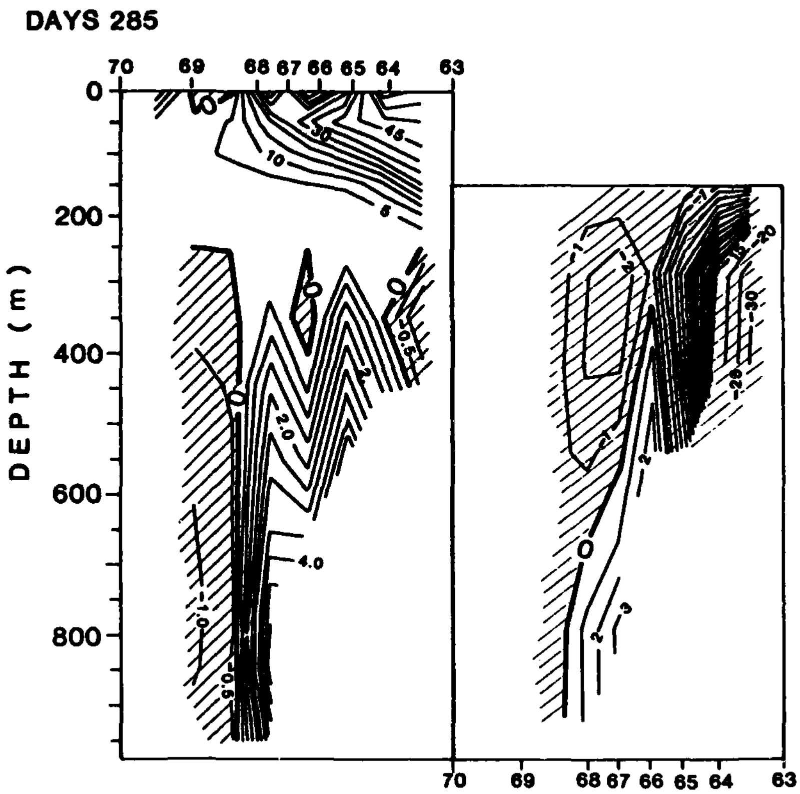
DAYS 285
70
69
68 67 66 65 64
63
0
200
400
600
800
DEPTH (m)
70
69
68 67 66 65 64
63

Fig. 50. (cont'd.)

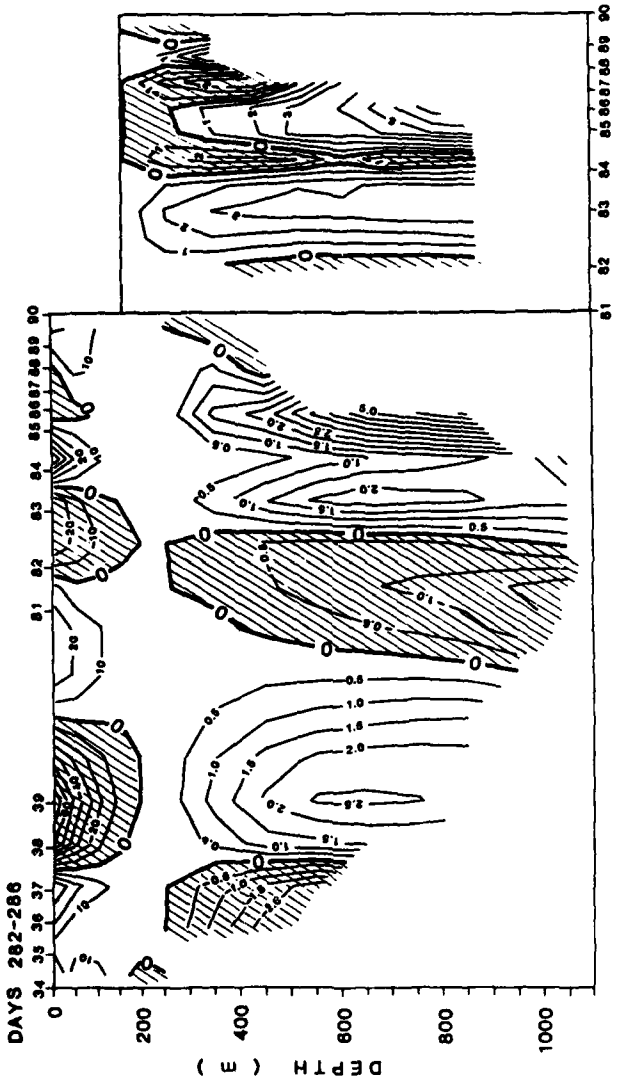

Fig. 50. (cont'd.)

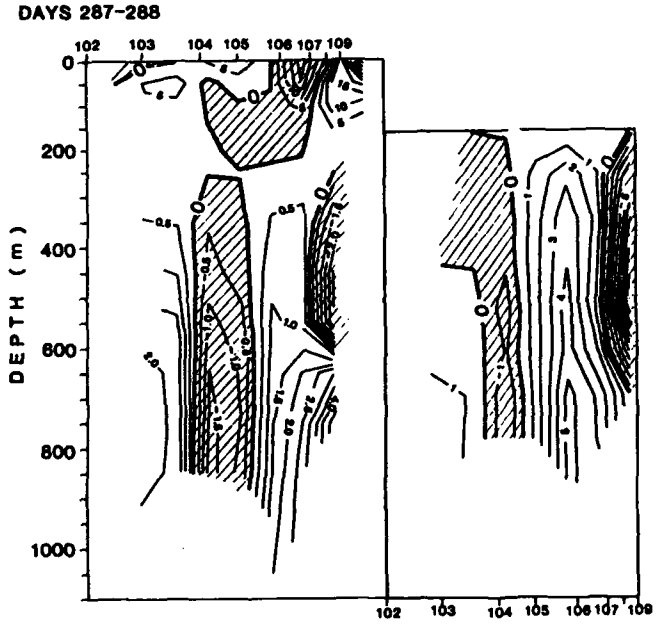
DAYS 287-288
102 103 104 105 106 107 109
0
200
400
600
800
1000
DEPTH (m)
102 103 104 105 106 107 109

Fig. 50. (cont'd.)

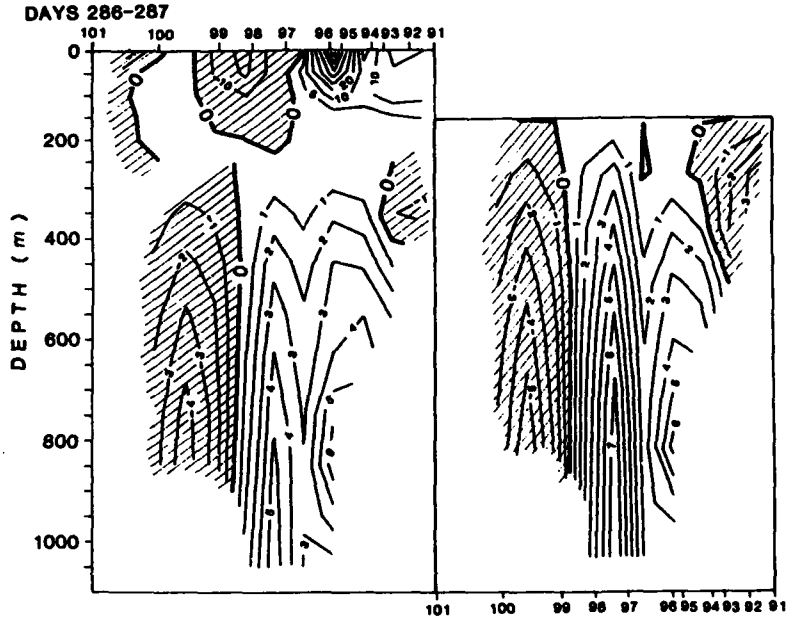
DAYS 286-287
101 100 99 98 97 96 95 94 93 92 91
0
200
400
600
800
1000
DEPTH (m)
101 100 99 98 97 96 95 94 93 92 91

Fig. 50. (cont'd.)

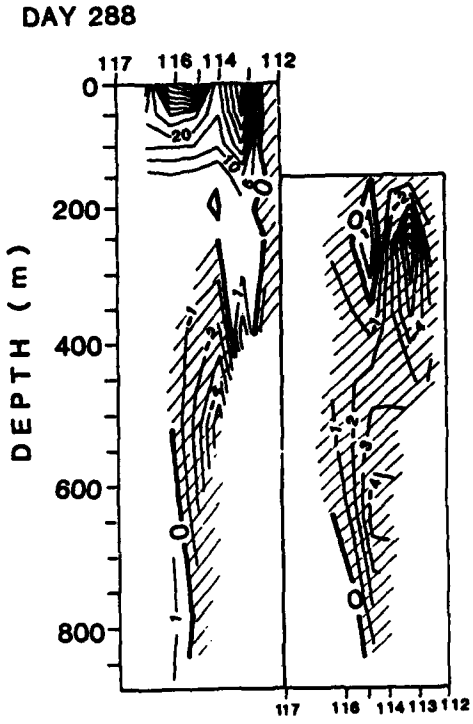
DAY 288
117 116 114 112
0
200
400
600
800
DEPTH (m)
20
117 116 114 113 112

Fig. 50. (cont'd.)

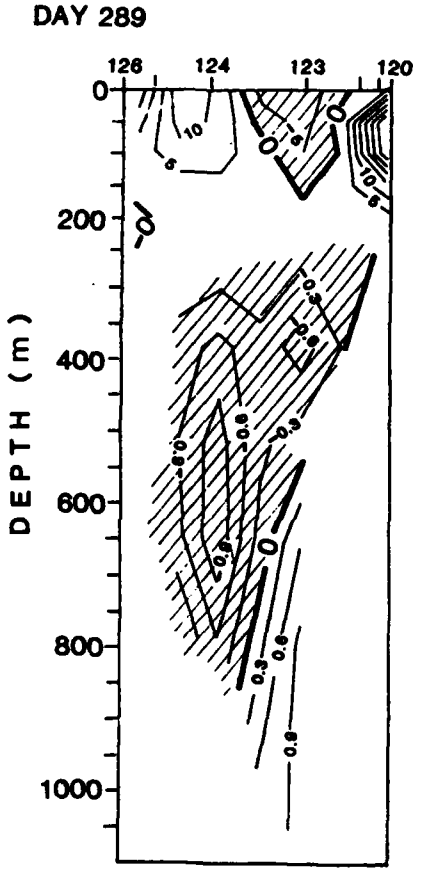

Fig. 50. (cont'd.)

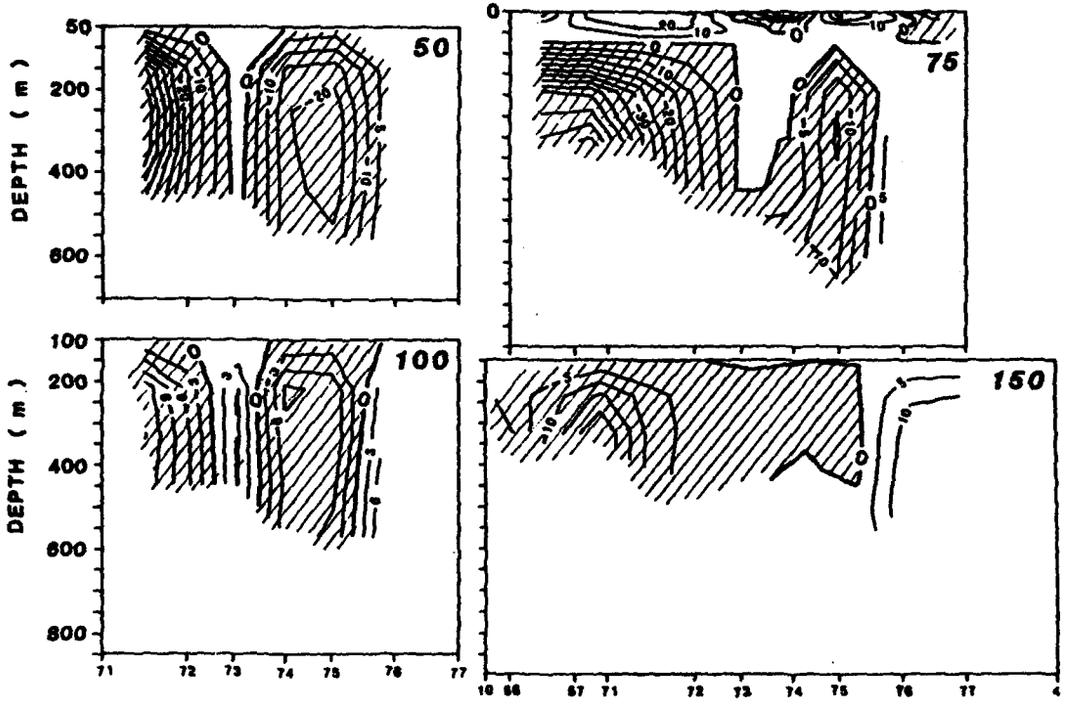

Fig. 51. Cross-sections of geostrophic current near Gibraltar for the level of no-motion at 50, 75 and 100 m in cm/s. Cross-section corresponding to salinity and potential temperature cross-section in Fig. 39 (II).

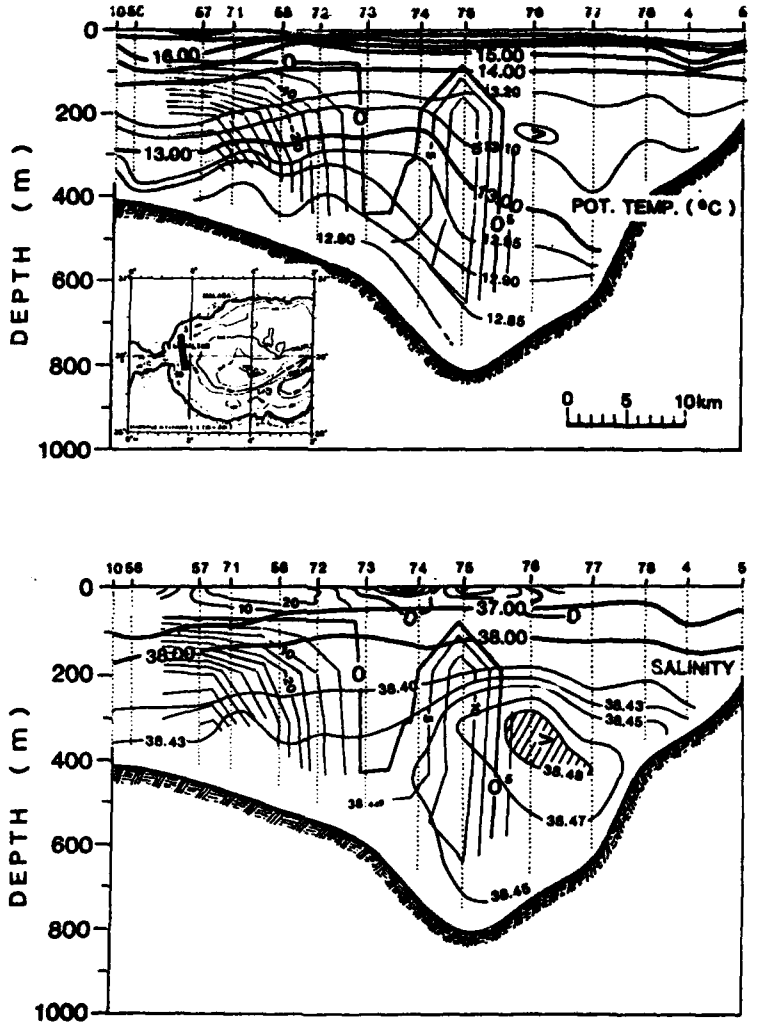

Fig. 52. Geostrophic current cross-section superimposed on salinity and potential temperature structures. Level of no-motion at 75 m. Cross-section corresponds to the one in Fig. 39 (II). Geostrophic current in cm/s.

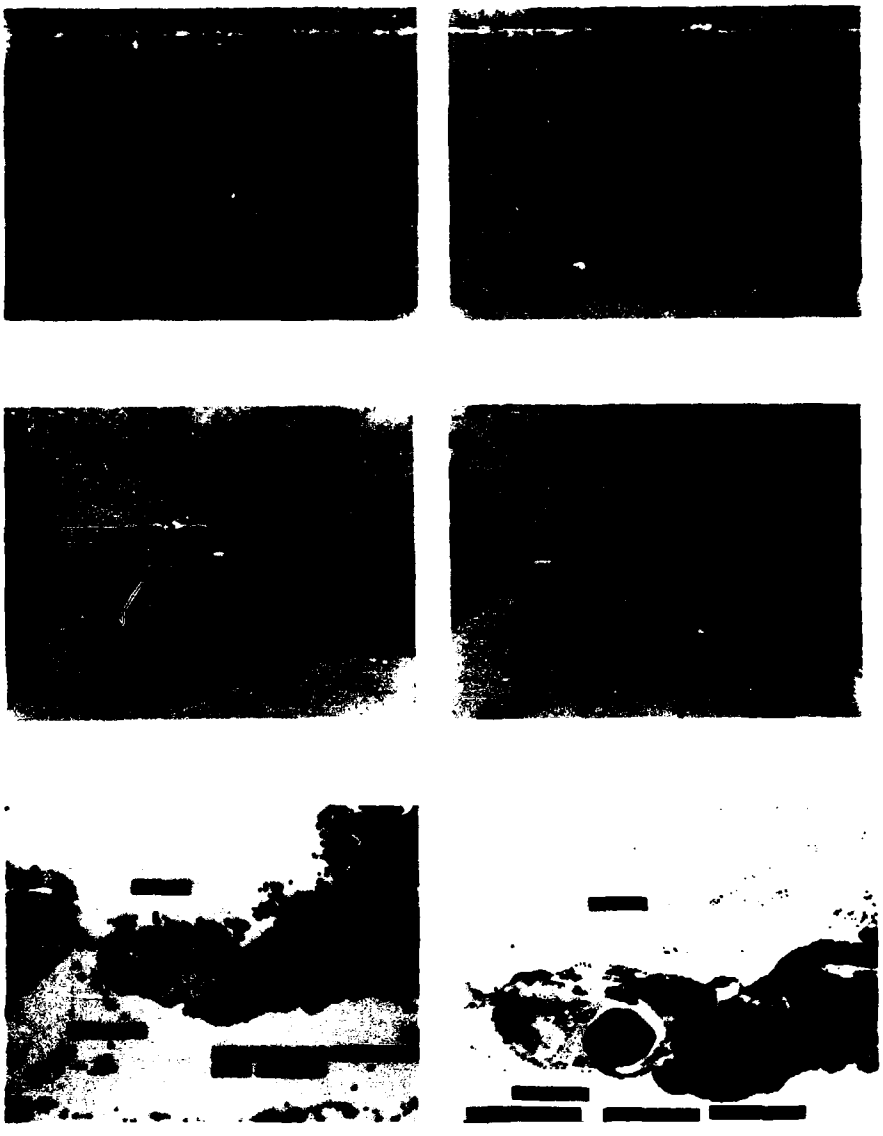

Fig. 53. Satellite infrared images of sea-surface temperature, NOAA-7. Considerable variability is visible; agreement with CTD and floats deployed to 60 m is good. Images were developed at SACLANTCEN.

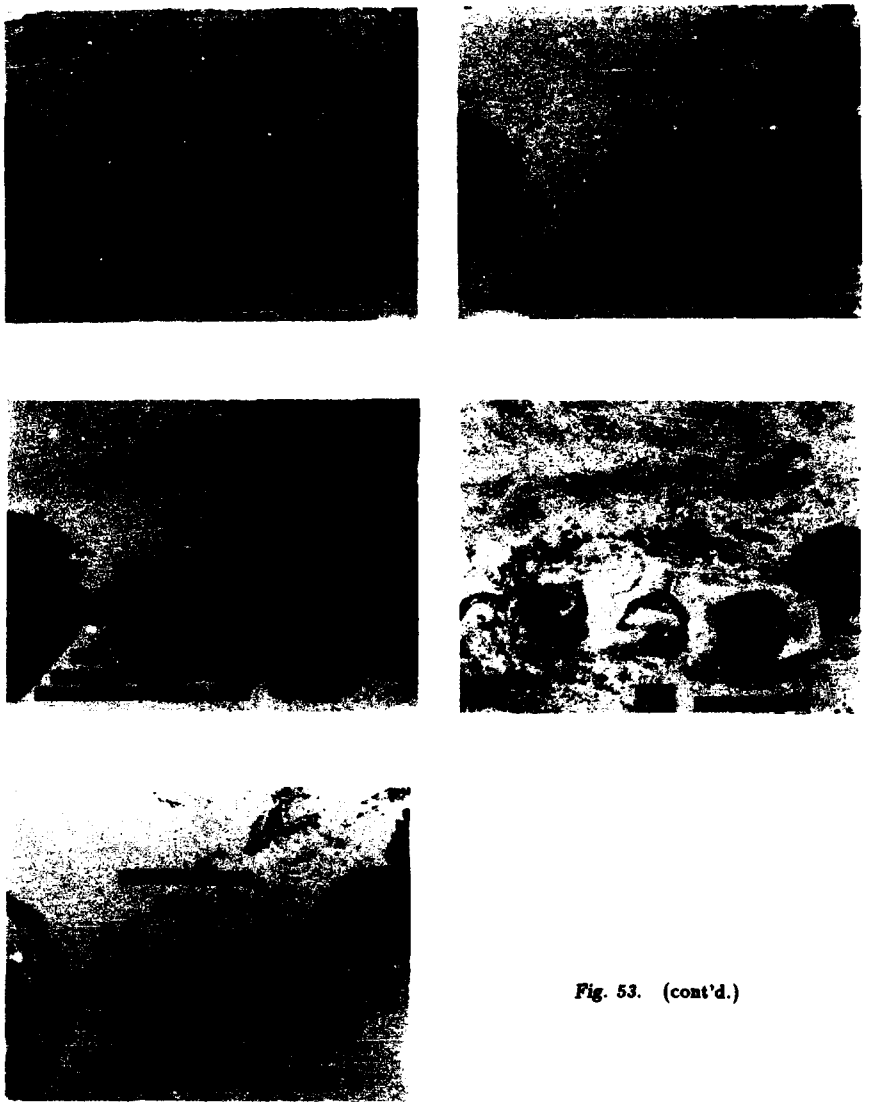

Fig. 53. (cont'd.)

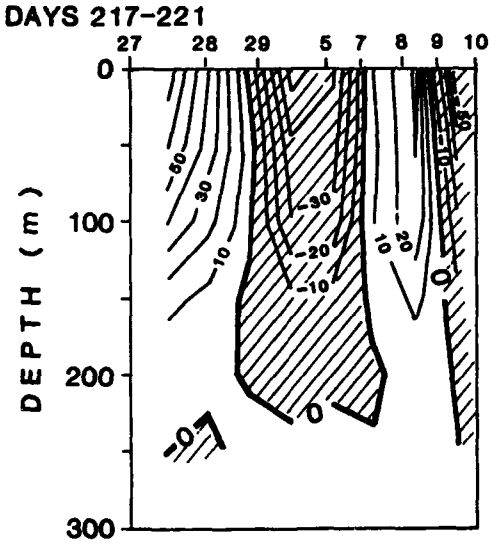

Fig. 54. **Satellite infrared image from the day 220 and geostrophic current computed from CTD cross-section taken at the same period. Agreement is good. Level of no-motion for geostrophic calculation is 200 m. Numbers signify the speed in cm/s.**

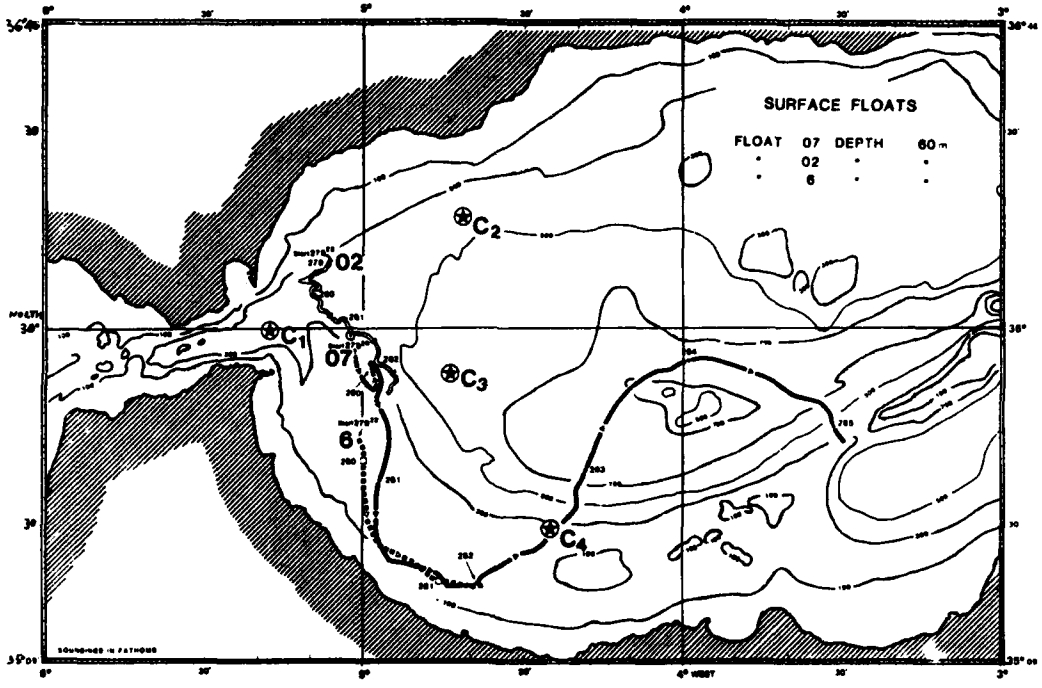

Fig. 55. **Tracks of floats deployed between days 279 to 285 at a depth of 60 m. 'Start' indicates the starting point and numbers near the tracks are Julian days. C1, C2, C3 and C4 are positions of autonomous listening stations; the one at C4 did not work during this period. All floats were destroyed by fishermen.**

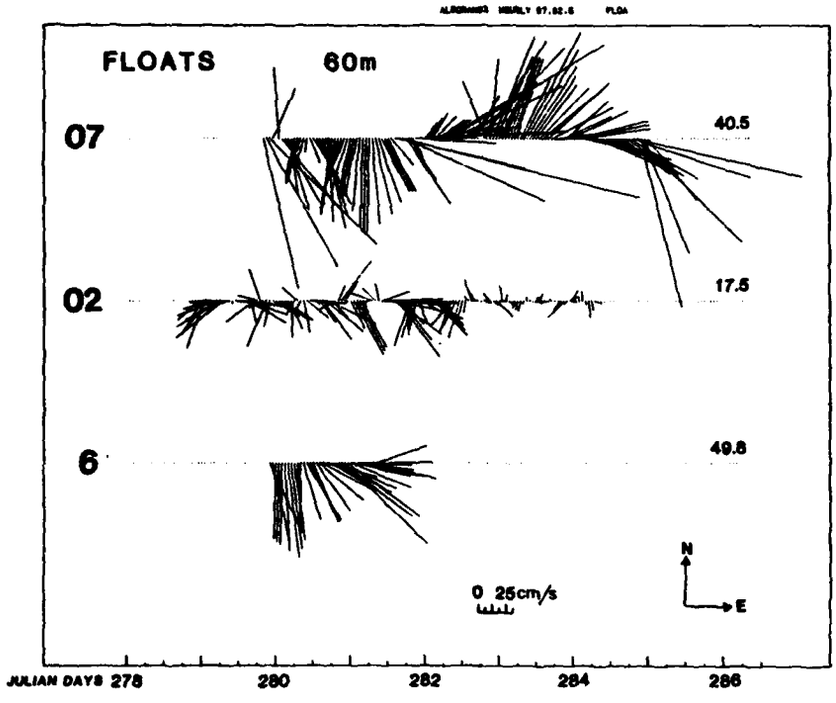

Fig. 56. Time series of 7-hourly velocity vectors for floats deployed at 60 m. Number on the right signifies the float number; number on the right signifies the average velocity amplitude in cm/s.

Fig. 57. Satellite infrared image from day 283 and tracks of floats deployed at 60 m between days 279 to 285.

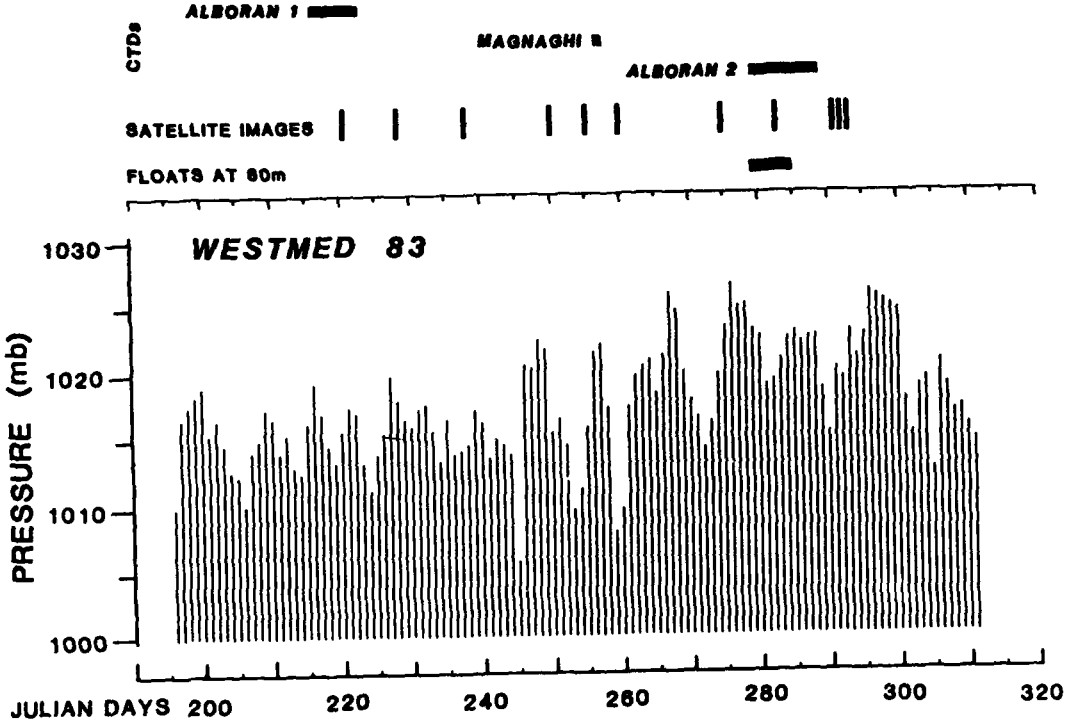

Fig. 58. Time series of average western Mediterranean pressure in mbars. Time series overlaps the period of the 1983 Alboran Sea experiment. Periods of CTD measurements, time of satellite images, and period of float deployment (at 60 m), are shown for comparison.

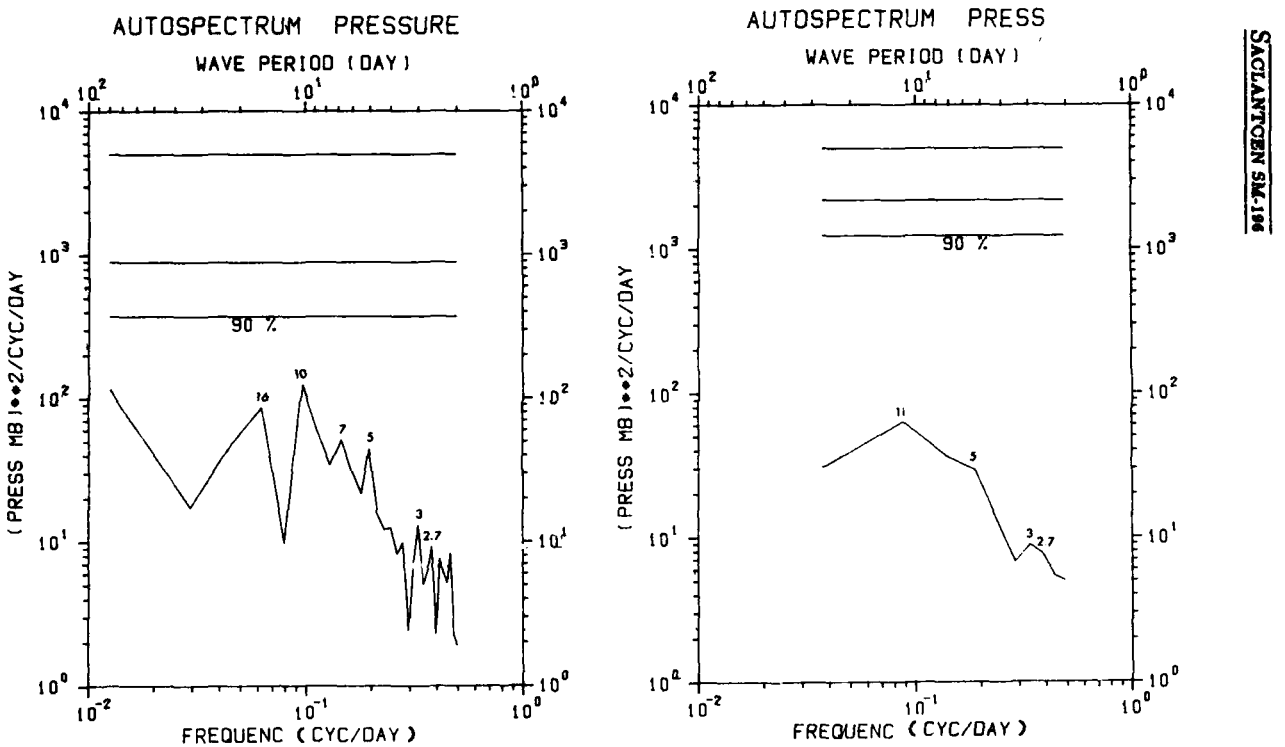

Fig. 59. **Spectra of average western Mediterranean atmospheric pressure. Time series is too short to have a good confidence limit.**

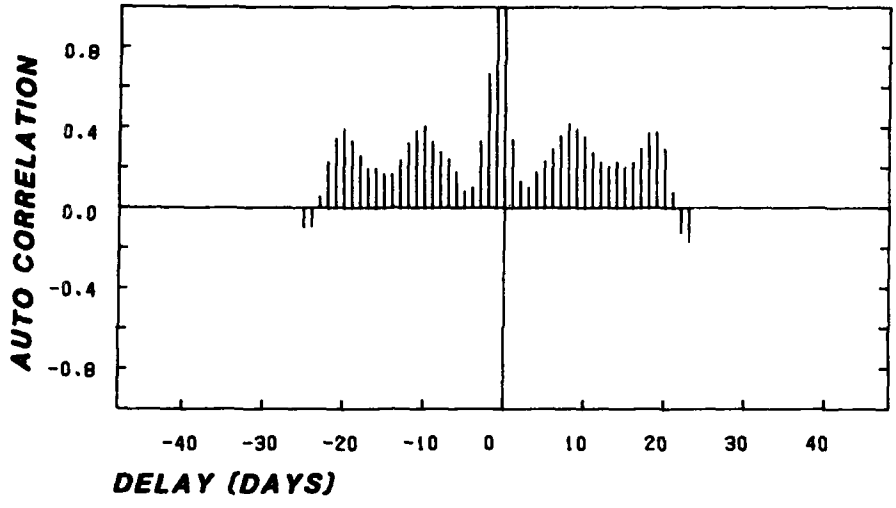

Fig. 60. **Auto-correlation of atmospheric pressure (WESTMED). Repetitive peaks show the low frequency periodicity.**

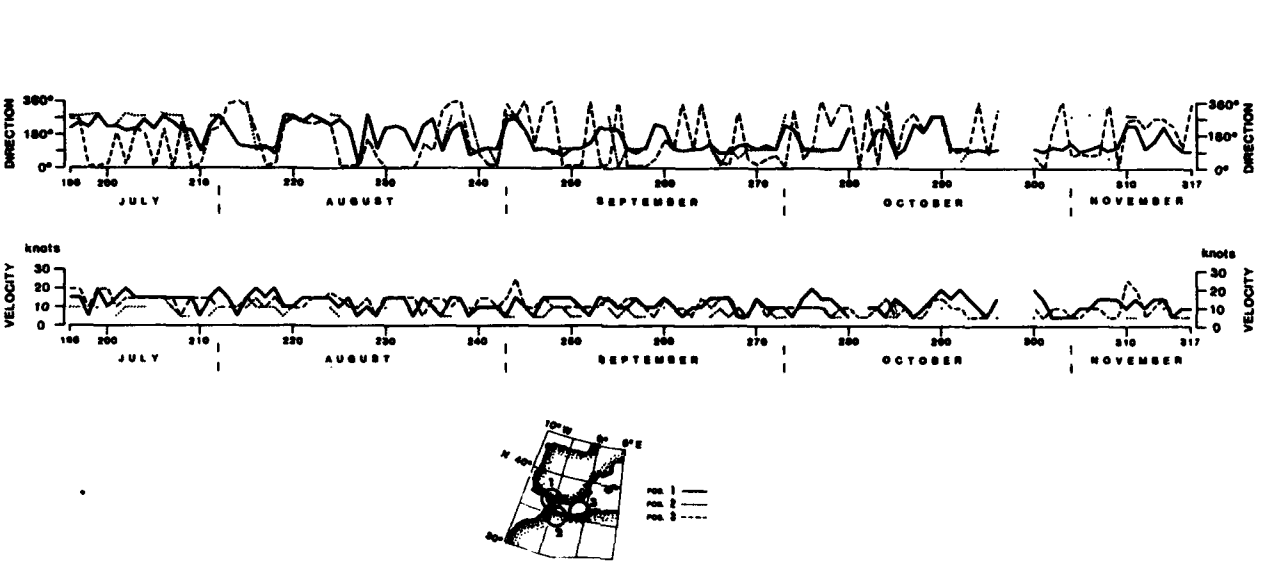

Fig. 61. **Wind amplitude and phase from three stations located near the Alboran Sea.**

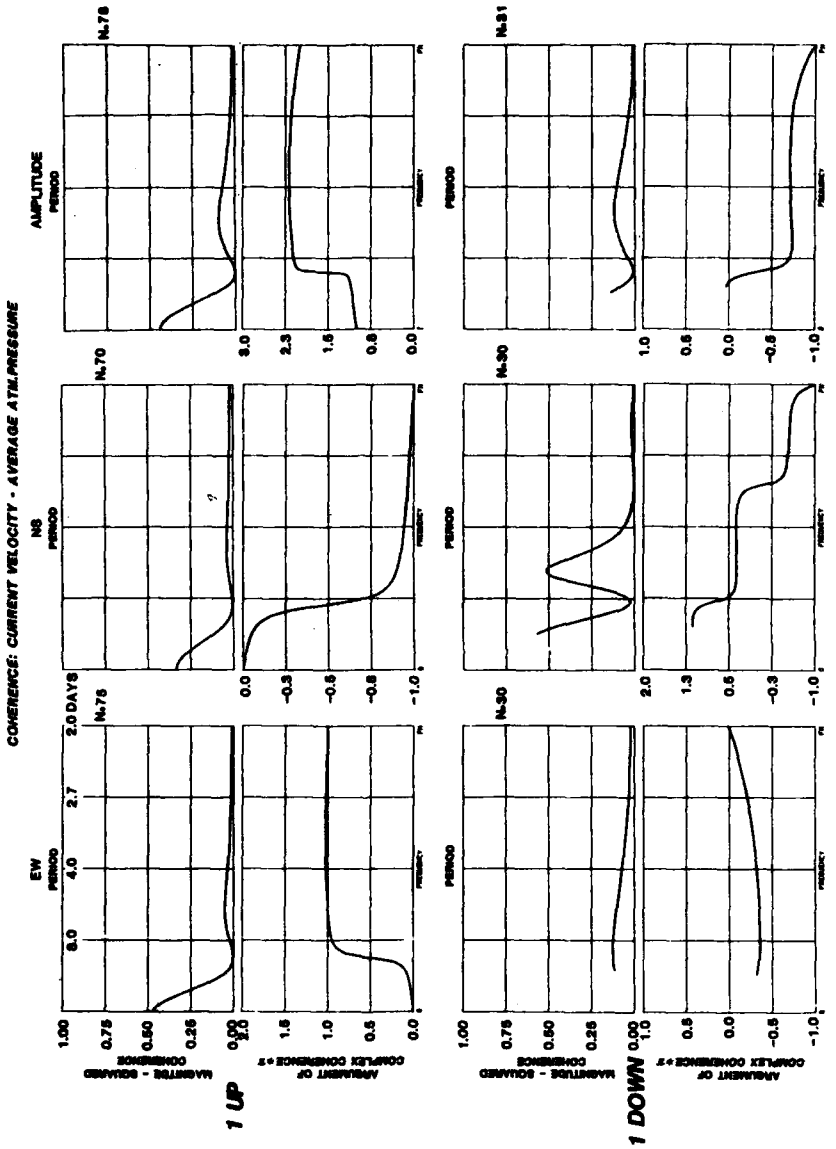

Fig. 62. Coherences between current velocity components or amplitude and average western Mediterranean atmospheric pressure for each current meter. Magnitude-squared coherence and argument of complex coherence are plotted as a function of frequency (period). The scale is linear in frequency. FN is the Nyquist frequency. Numbers signify the upper or lower current meter. Number on the right signifies the number of samples in the time series (days).

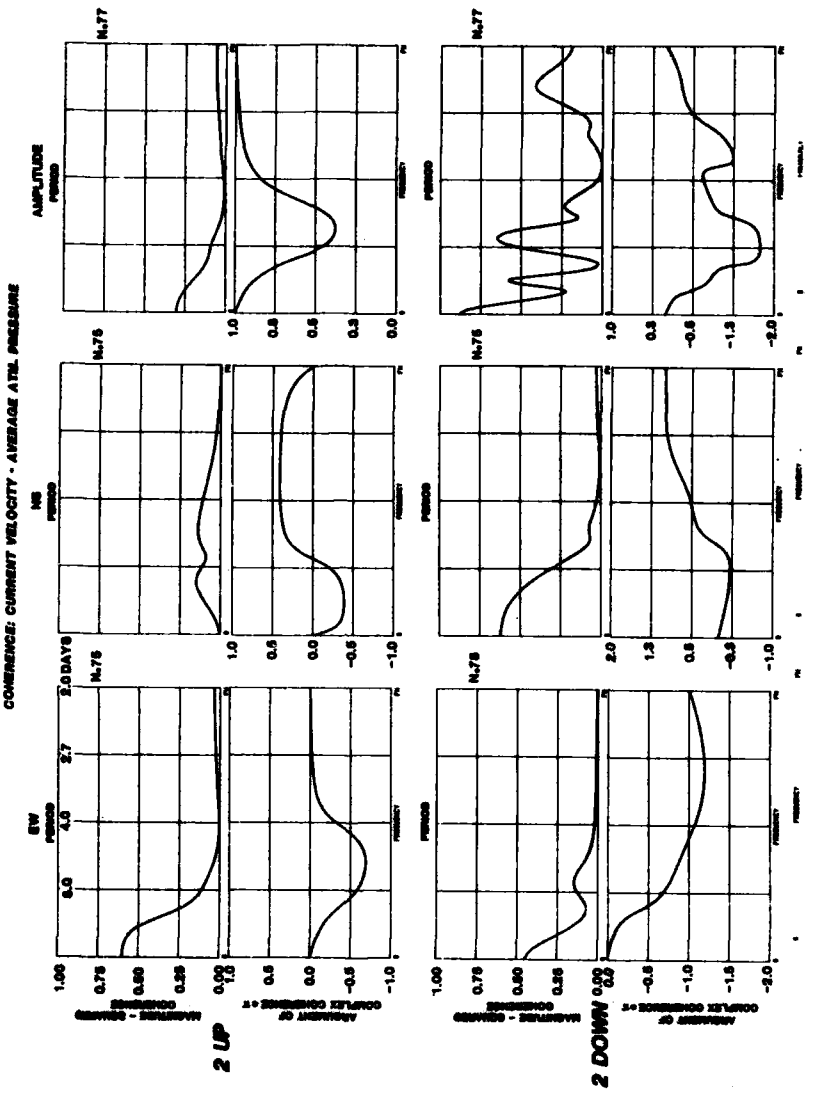
COHERENCE: CURRENT VELOCITY - AVERAGE ATM. PRESSURE
AMPLITUDE
PERIOD
N.77
N.75
NS
EW
2.0 DAYS
2 UP
2 DOWN

Fig. 62. (cont'd.)

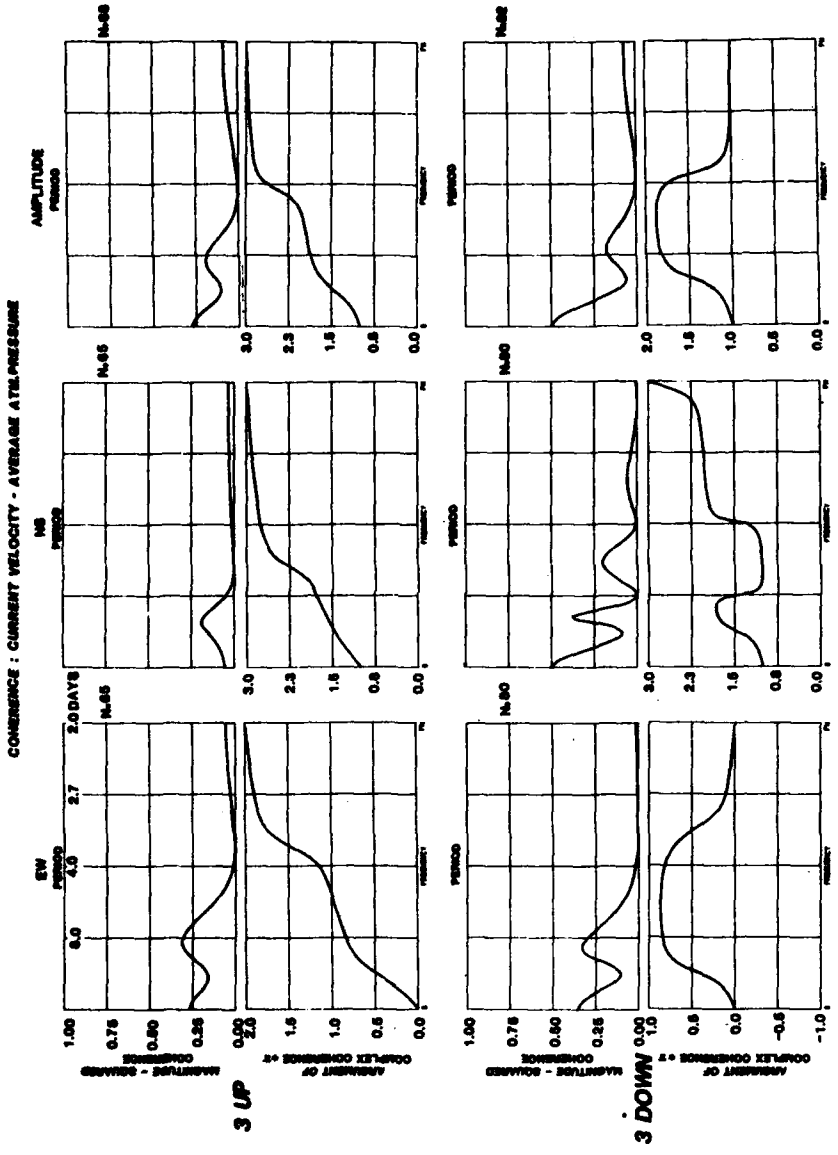
COHERENCE : CURRENT VELOCITY - AVERAGE ATM.PRESSURE
AMPLITUDE
PERIOD
N-68
N-62
N-65
N-60
N-55
N-50
NS
EW
2.0 DAYS
2.7
4.0
6.0
3 UP
3 DOWN

Fig. 62. (cont'd.)

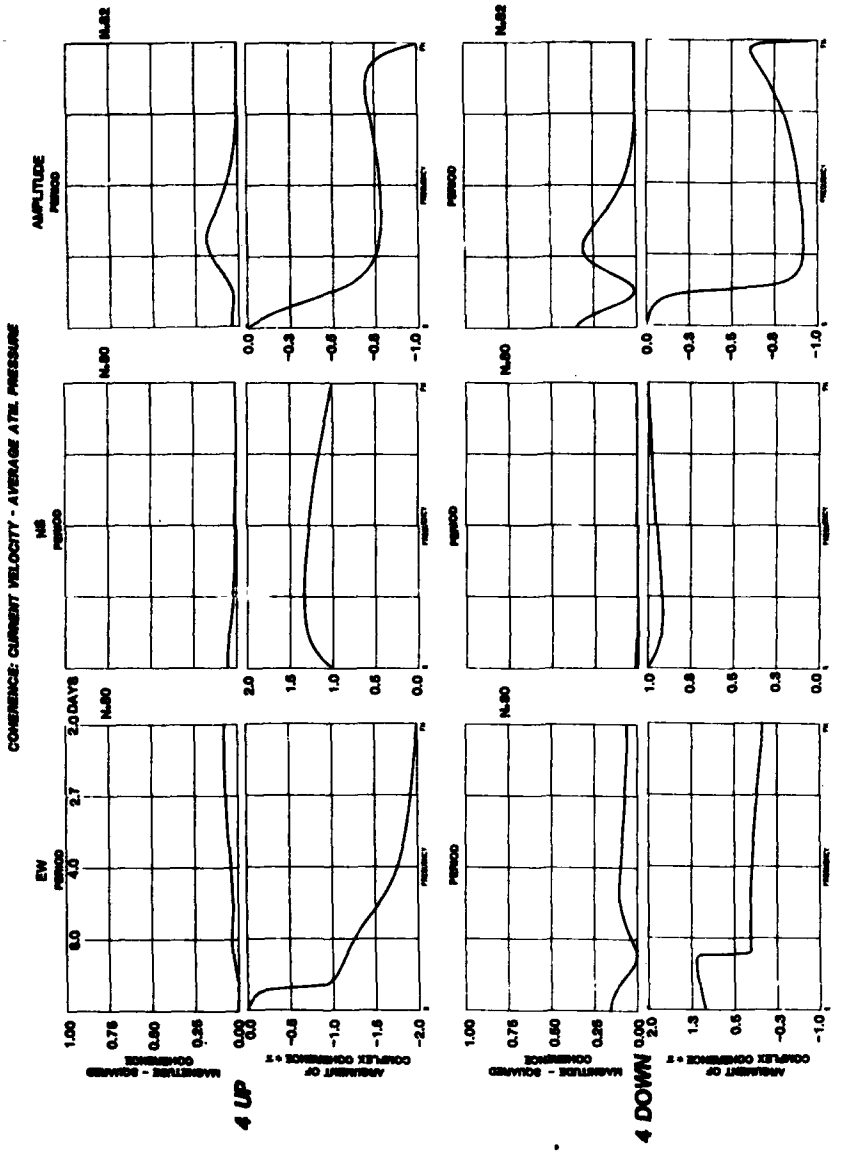
COHERENCE: CURRENT VELOCITY - AVERAGE ATM. PRESSURE
AMPLITUDE
PERIOD
N-S
EW
2.0 DAYS
4 UP
4 DOWN

Fig. 62. (cont'd.)

intentionally blank page

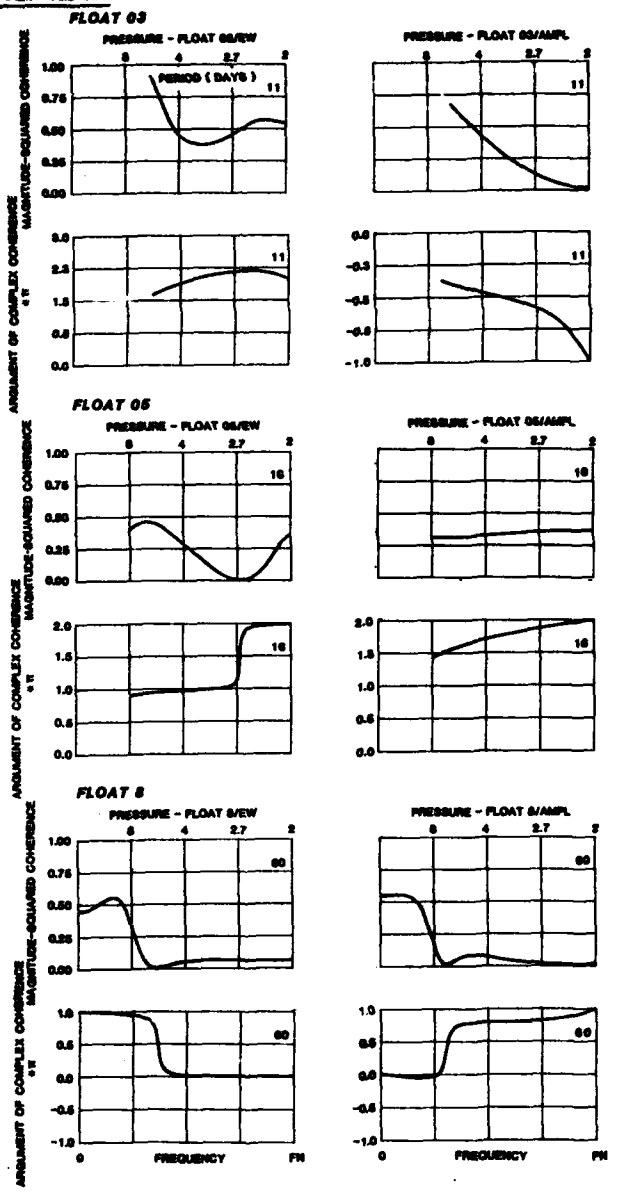

Fig. 63. Coherences between some float velocity components of amplitude and average western Mediterranean atmospheric pressure for floats 03, 05 and 08. Magnitude-squared coherence and argument of complex coherence are plotted as a function of frequency (period). The scale is linear in frequency. FN is the Nyquist frequency. Numbers on the right signify the number of samples in the time series (days).

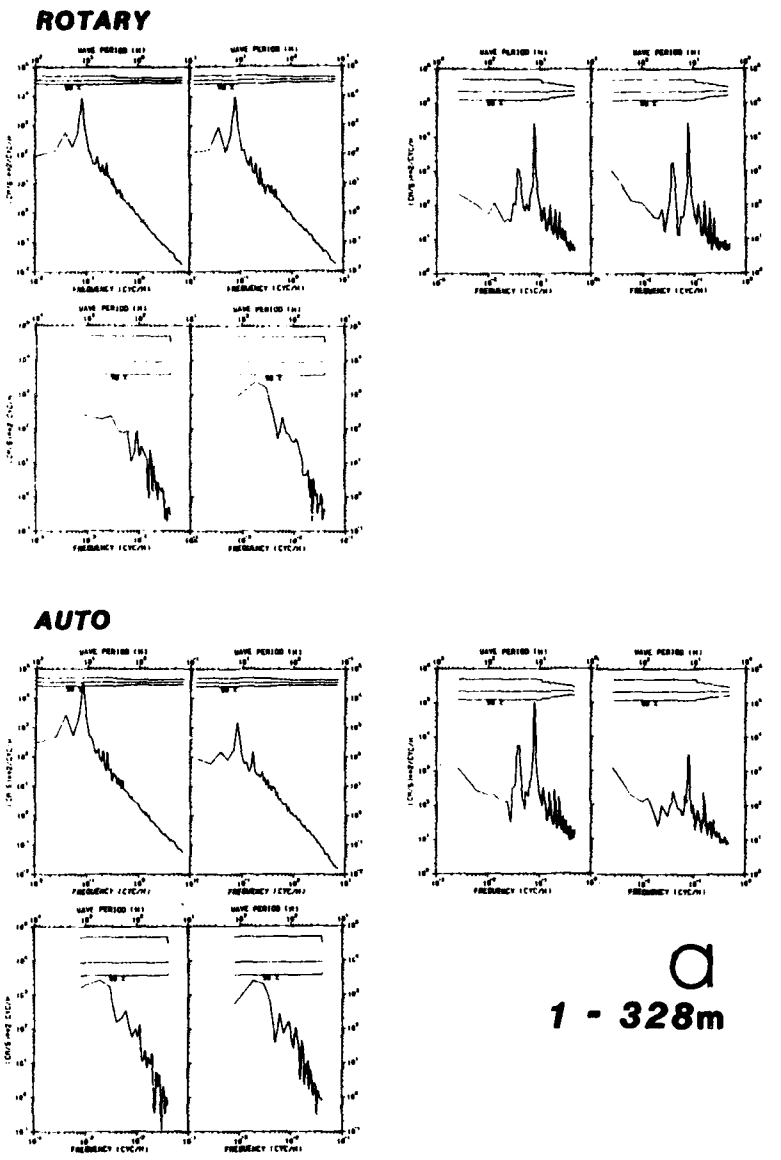

Fig. 64. Rotary and auto spectra of current velocities for each current-meter measurement. Two figures together identify the clockwise and anticlockwise spectra for rotary, and the east-west and north-south velocity component spectra for auto. Data for each range were appropriately filtered. The 90% confidence limit of Gaussian distribution is shown. (a) Mooring 1: depths 328 m and 712 m; (b) Mooring 2: depths 346 m and 731 m; (c) Mooring 3: depths 294 m and 678 m; (d) Mooring 4: depths 298 m and 403 m.

ROTARY

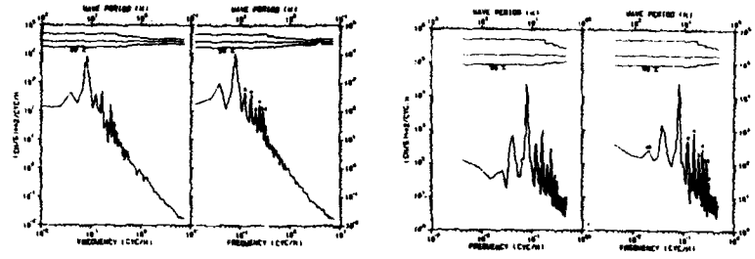

AUTO

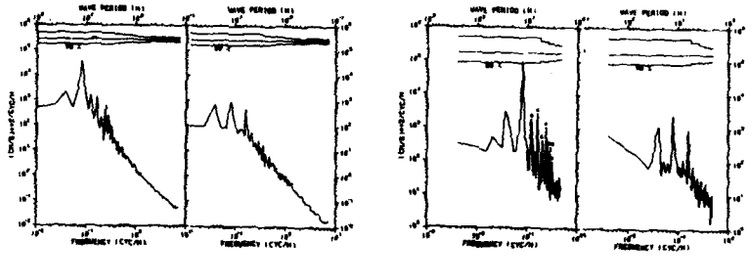

a

1 - 712m

ROTARY

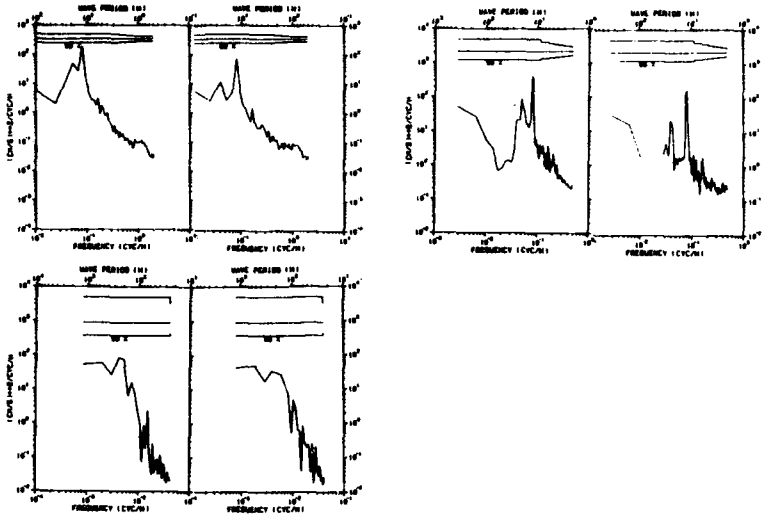

AUTO

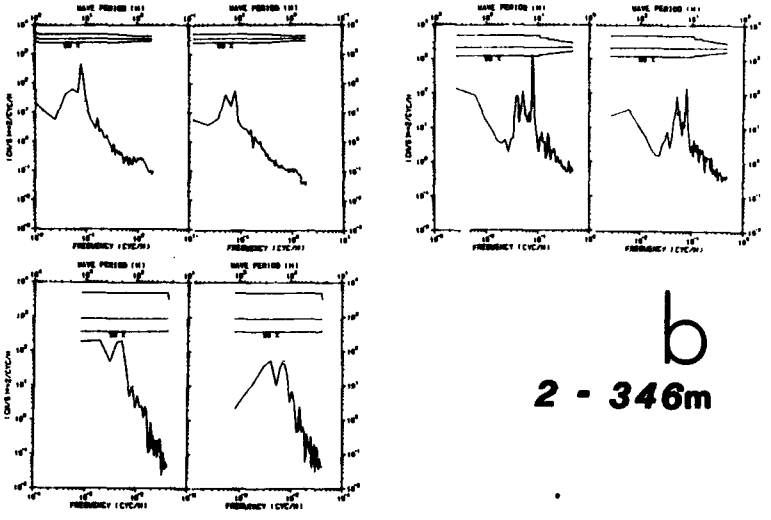

b

2 - 346m

ROTARY

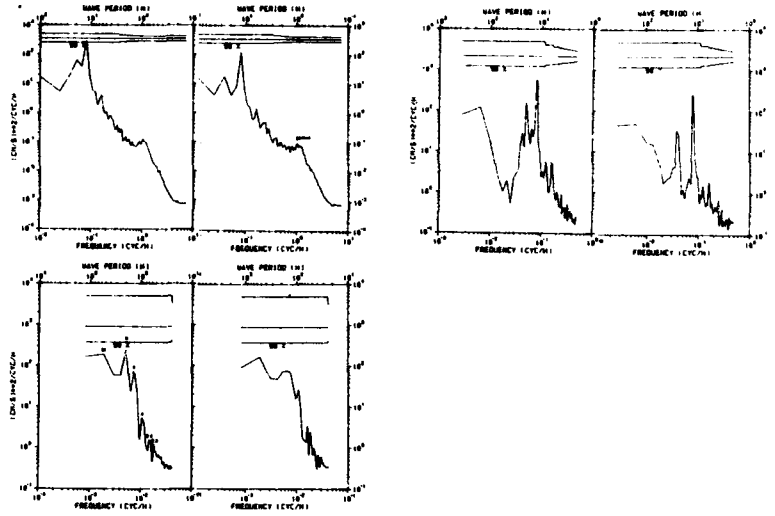

AUTO

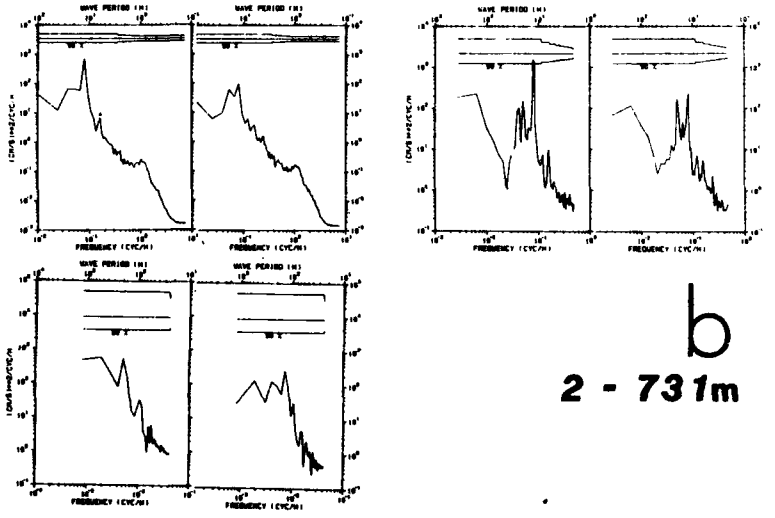

b

2 - 731m

ROTARY

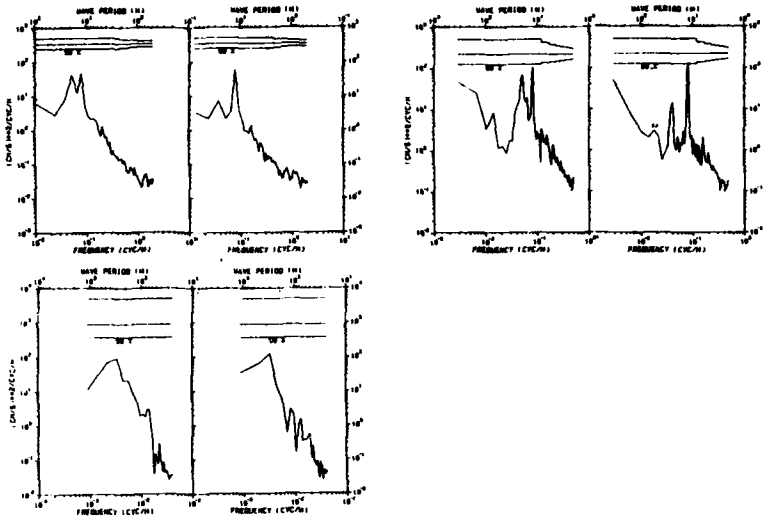

AUTO

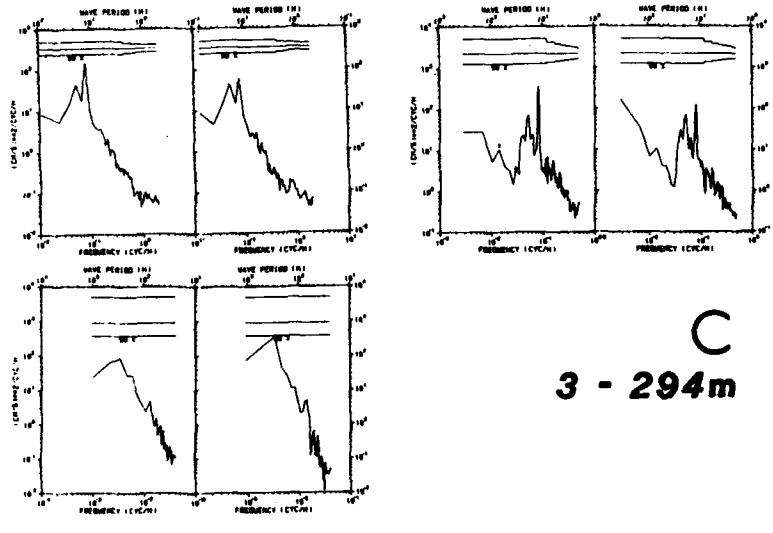

C

3 - 294m

ROTARY

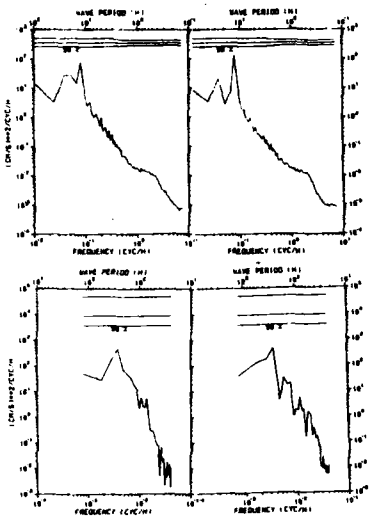

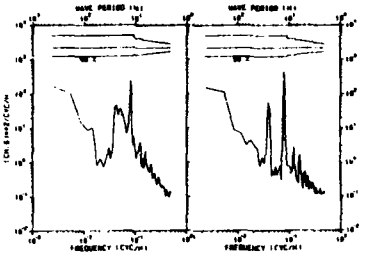

AUTO

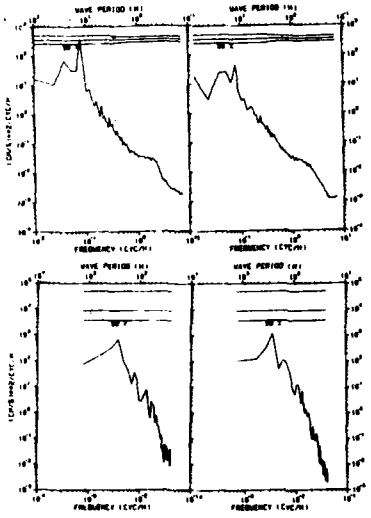

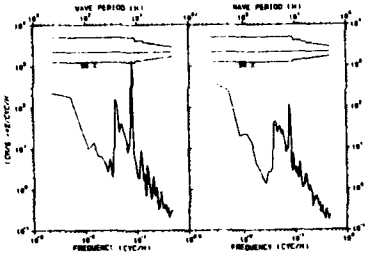

C

3 - 678m

ROTARY

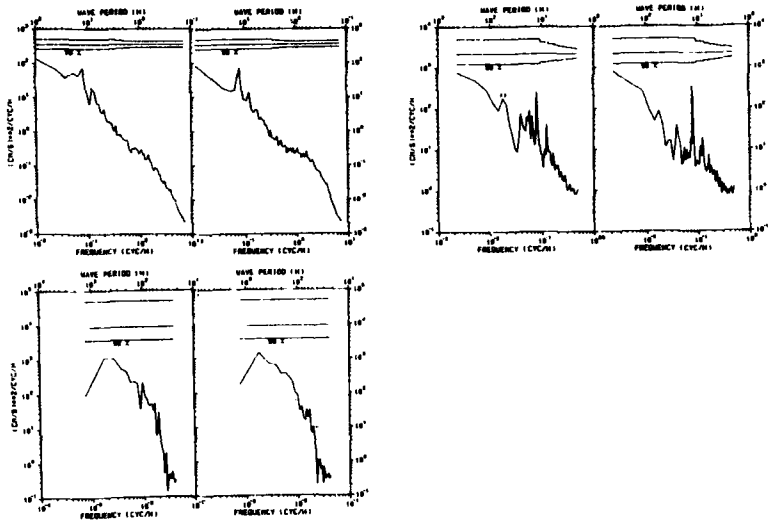

AUTO

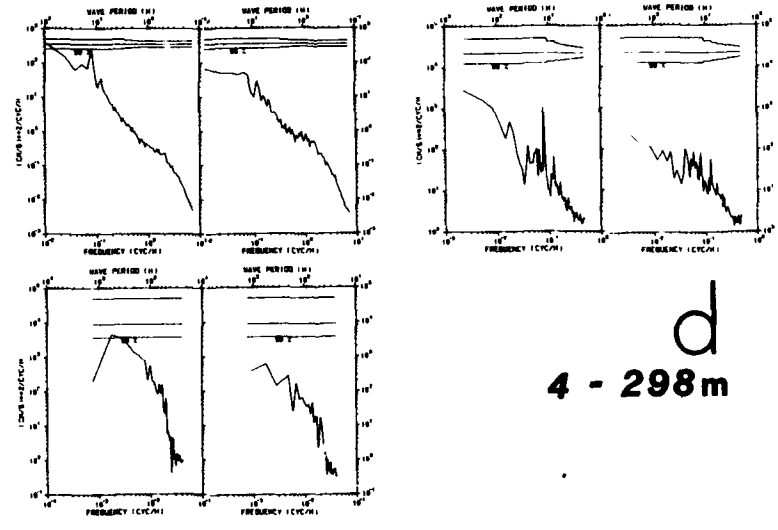

d

4 - 298m

SACLANTCEN SM-196

ROTARY

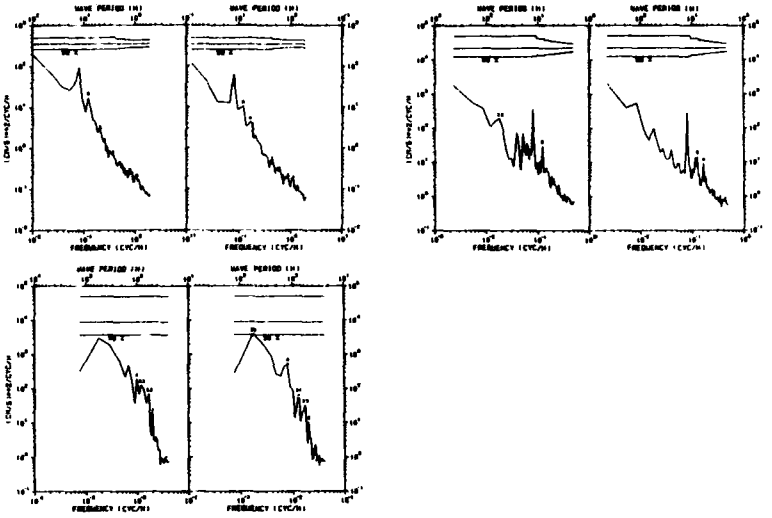

AUTO

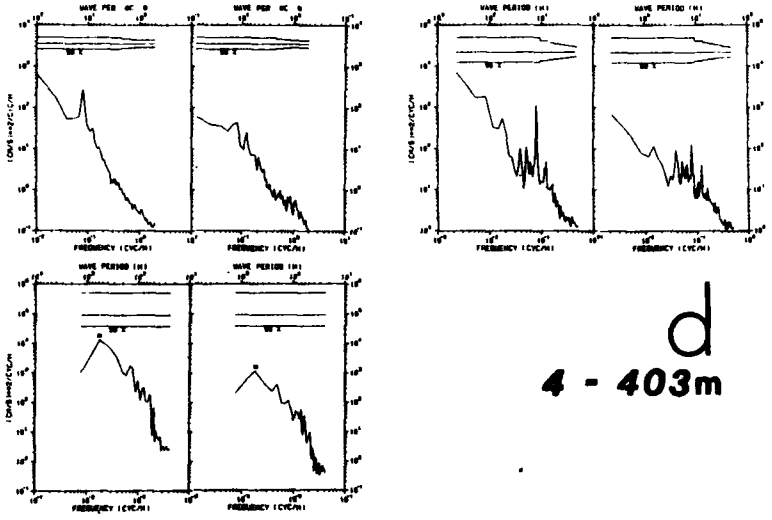

d

4 - 403m

intentionally blank page

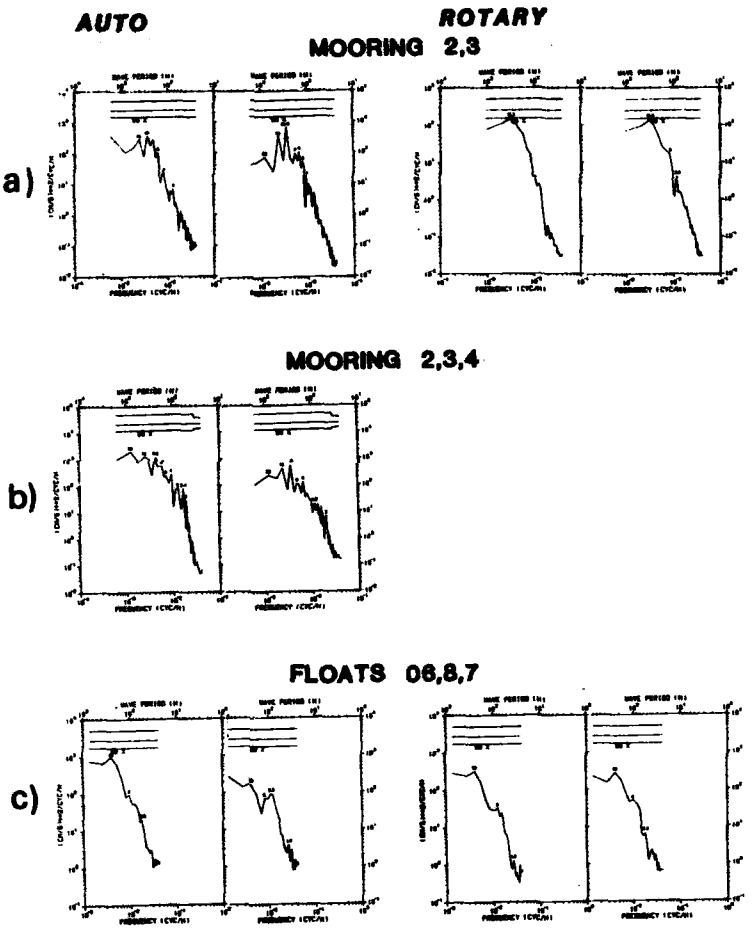

Fig. 65. Averaged low-frequency rotary and auto spectra of current and float velocities: (a) created from 4 current meters deployed on moorings 2 and 3; (b) created from 6 current meters deployed on moorings 2, 3 and 4; (c) created from floats 06, 08, 07.
Two figures together identify the clockwise and anticlockwise spectra for rotary spectra, and east-west and north-south velocity component spectra for auto spectra. The 90% confidence limit of Gaussian distribution is shown.

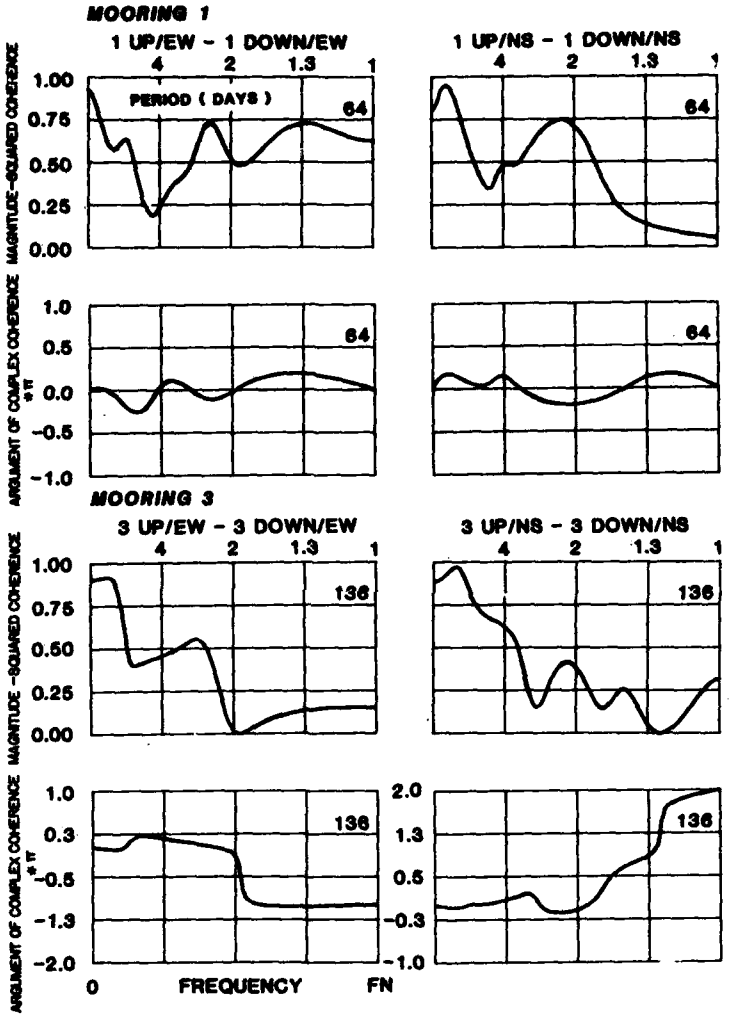

Fig. 66. Magnitude-squared coherence and argument of complex coherence between the current velocity components measured by upper and lower current meters on each mooring. UP and DOWN signify the upper and lower current meters and EW and NS signify the east-west and the north-south current velocity components. Frequency scale is linear, FN marks the Nyquist frequency. Number on the right signifies the number of samples in the time series.

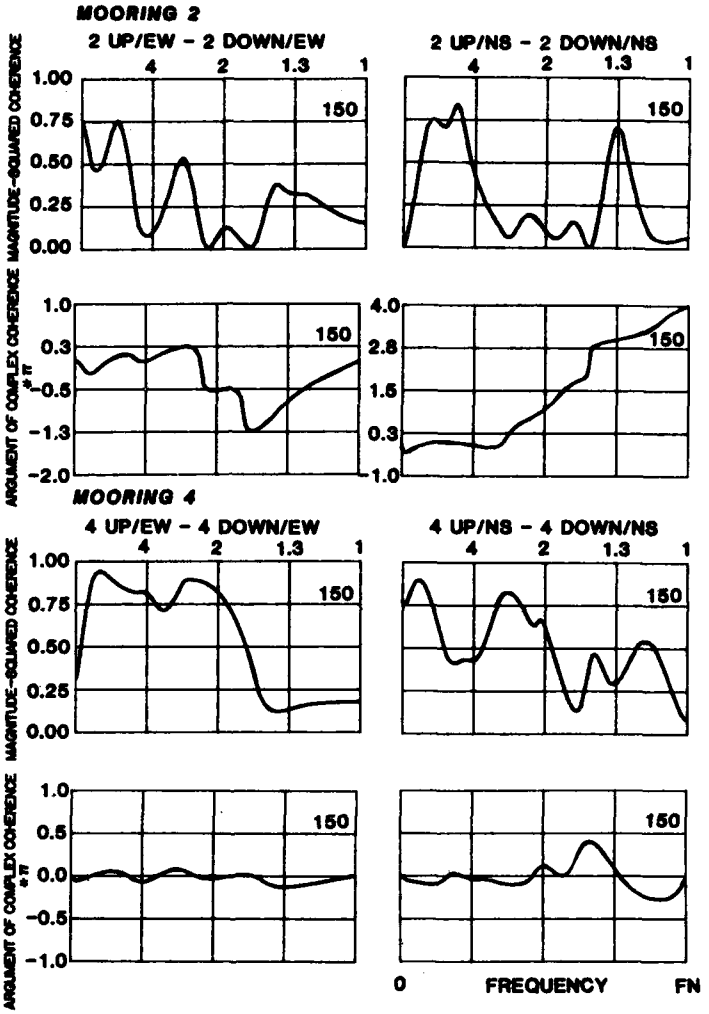
MOORING 2
2 UP/EW - 2 DOWN/EW
2 UP/NS - 2 DOWN/NS
4
2
1.3
1
1.00
0.75
0.50
0.25
0.00
150
MAGNITUDE-SQUARED COHERENCE
1.0
0.3
-0.5
-1.3
-2.0
4.0
2.8
1.5
0.3
-1.0
ARGUMENT OF COMPLEX COHERENCE
±π
MOORING 4
4 UP/EW - 4 DOWN/EW
4 UP/NS - 4 DOWN/NS
0.5
0.0
-0.5
-1.0
0
FREQUENCY
FN

Fig. 66. (cont'd.)

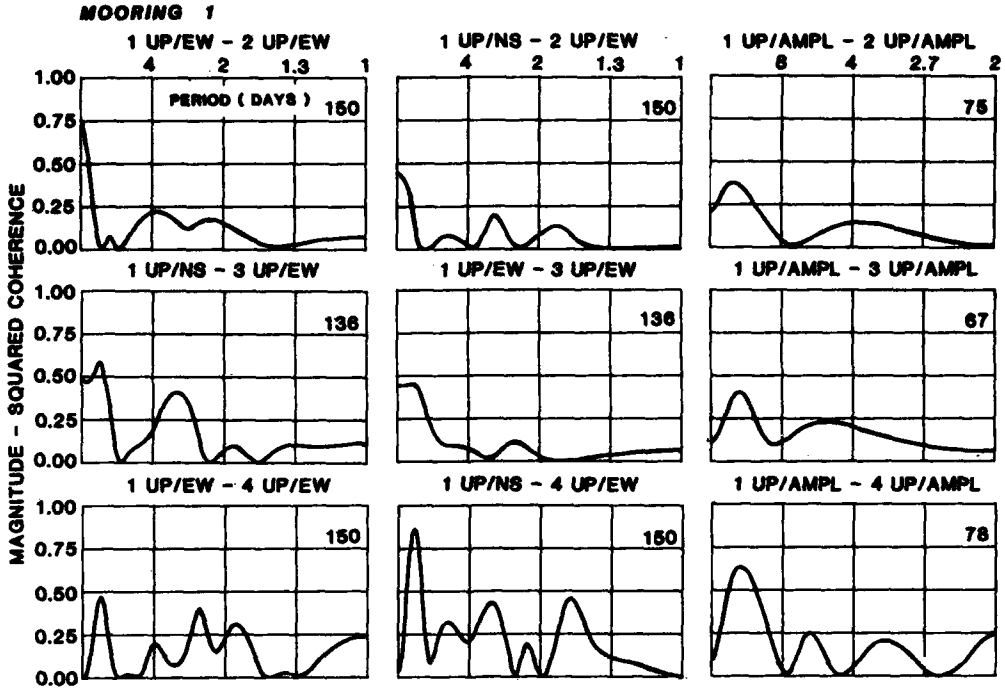

Fig. 67. **Magnitude-squared coherence between some current velocity components on different moorings. UP and DOWN signify the upper and lower current meters and EW and NS signify the east-west and the north-south current velocity components. Number in front of UP or DOWN signifies the moorings 1, 2, 3 or 4. Frequency scale is linear, FN is the Nyquist frequency. Number on the right signifies the number of samples in the time series.**

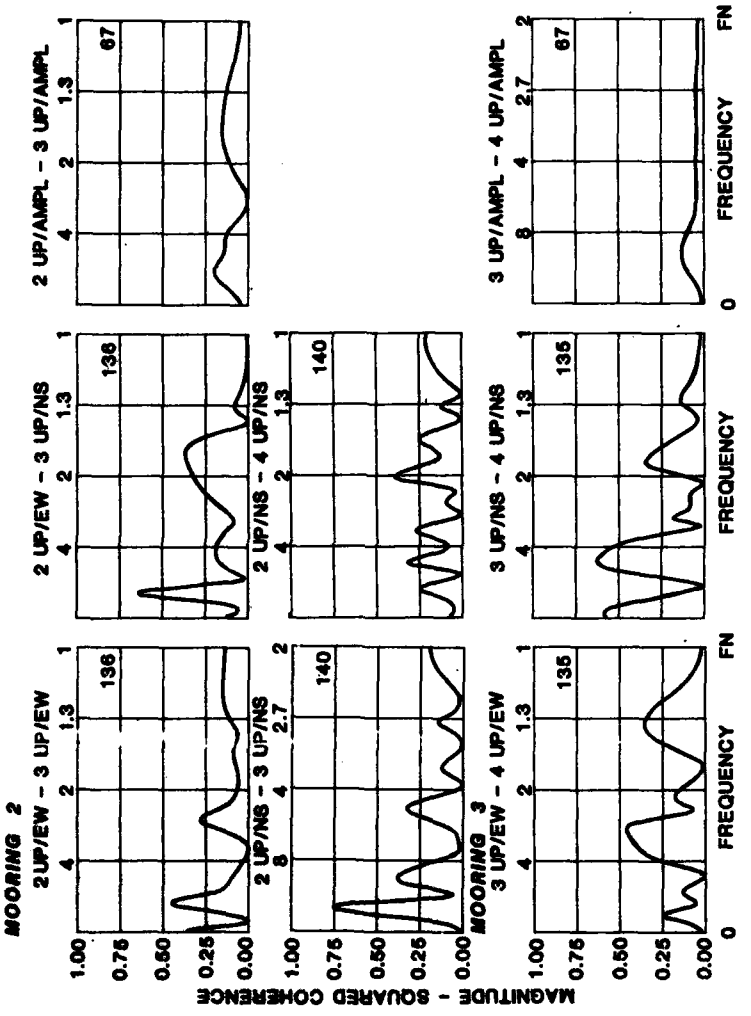
MOORING 2
2UP/EW – 3 UP/EW
2 UP/NS – 3 UP/NS
2 UP/EW – 3 UP/NS
2 UP/NS – 4 UP/NS
2 UP/AMPL – 3 UP/AMPL
MOORING 3
3 UP/EW – 4 UP/EW
3 UP/NS – 4 UP/NS
3 UP/AMPL – 4 UP/AMPL
MAGNITUDE - SQUARED COHERENCE
FREQUENCY
FN

Fig. 67. (cont'd.)

Fig. 68. Magnitude-squared coherence and argument of complex coherence: (a) between float 05 velocity amplitude and some current velocity amplitudes on different moorings; (b) between float 03 velocity amplitude and current velocity amplitude of the upper current meter at mooring 1; (c) between float 06 velocity amplitude and some current velocity amplitudes on different moorings; (d) between float 06 velocity components and some current velocity components on different moorings. UP and DOWN signify the upper and lower current meters and EW and NS signify the east-west and the north-south current velocity components. Number in front of UP or DOWN signifies mooring 1, 2, 3 or 4. Frequency scale is linear, FN is the Nyquist frequency. Number on the right signifies the number of samples in the time series. (e) between the velocity components of different floats. UP and DOWN signify the upper and lower current meters and EW and NS signify the east-west and the north-south current velocity components. Number in front of UP or DOWN signifies mooring 1, 2, 3 or 4. Frequency scale is linear, FN is the Nyquist frequency. Number on the right signifies the number of samples in the time series.

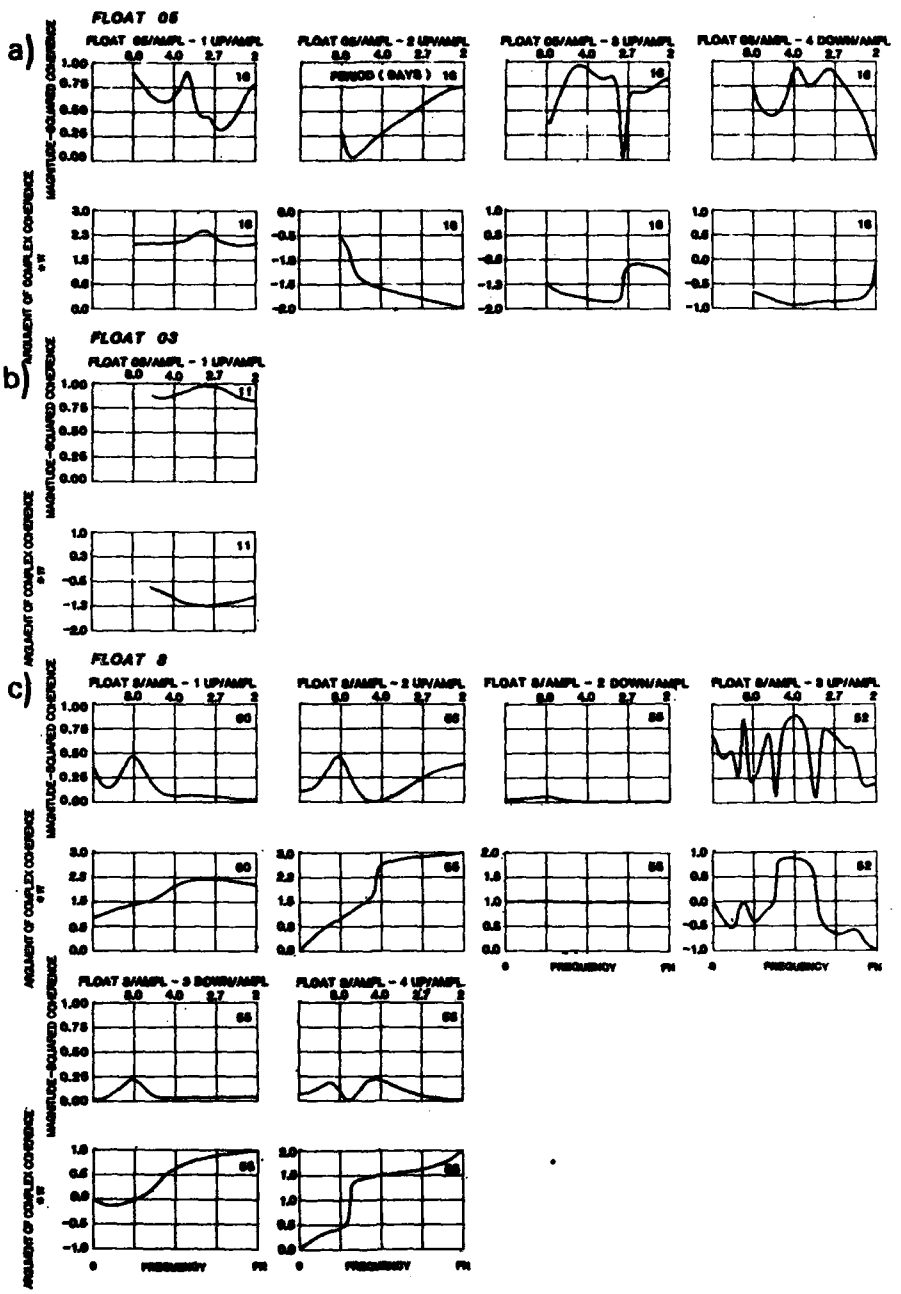
a)
FLOAT 05
FLOAT 05/AMPL - 1 UP/AMPL
FLOAT 05/AMPL - 2 UP/AMPL
FLOAT 05/AMPL - 3 UP/AMPL
FLOAT 05/AMPL - 4 DOWN/AMPL
8.0 4.0 2.7 2
PERIOD (DAYS)
MAGNITUDE-SQUARED COHERENCE
ARGUMENT OF COMPLEX COHERENCE
b)
FLOAT 03
FLOAT 03/AMPL - 1 UP/AMPL
c)
FLOAT 8
FLOAT 8/AMPL - 1 UP/AMPL
FLOAT 8/AMPL - 2 UP/AMPL
FLOAT 8/AMPL - 2 DOWN/AMPL
FLOAT 8/AMPL - 3 UP/AMPL
FLOAT 8/AMPL - 3 DOWN/AMPL
FLOAT 8/AMPL - 4 UP/AMPL
FREQUENCY

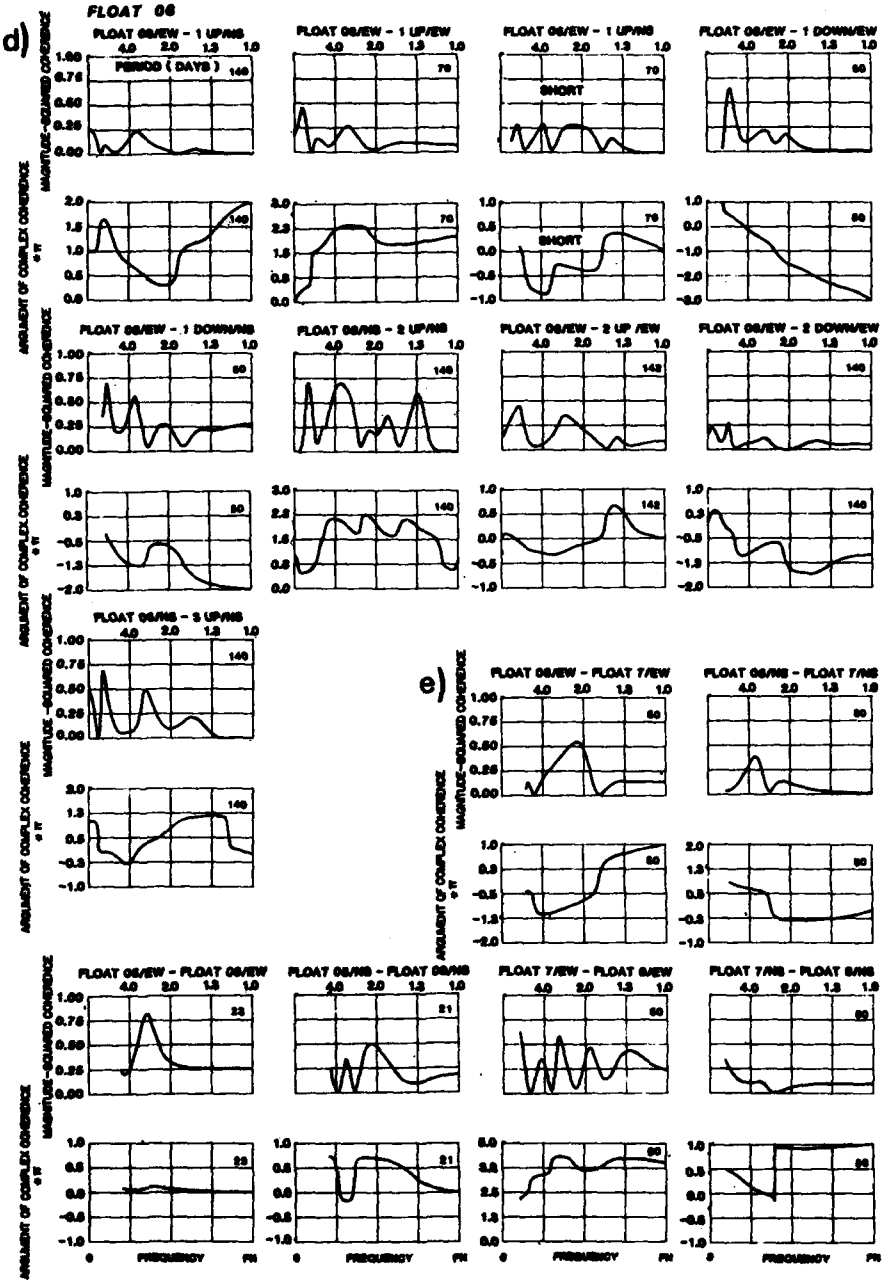
d)
FLOAT 06
FLOAT 06/EW - 1 UP/NS
FLOAT 06/EW - 1 UP/EW
FLOAT 06/EW - 1 UP/NS
FLOAT 06/EW - 1 DOWN/EW
FLOAT 06/EW - 1 DOWN/NS
FLOAT 06/NS - 2 UP/NS
FLOAT 06/EW - 2 UP /EW
FLOAT 06/EW - 2 DOWN/EW
FLOAT 06/NS - 2 UP/NS
PERIOD (DAYS)
SHORT
MAGNITUDE-SQUARED COHERENCE
ARGUMENT OF COMPLEX COHERENCE
e)
FLOAT 06/EW - FLOAT 7/EW
FLOAT 06/NS - FLOAT 7/NS
FLOAT 06/EW - FLOAT 06/EW
FLOAT 06/NS - FLOAT 06/NS
FLOAT 7/EW - FLOAT 8/EW
FLOAT 7/NS - FLOAT 8/NS
FREQUENCY
FN

END

DATE

FILMED

8 8-